Fluorous membrane-based separations and reactions

by

Yanhong Yang

BS, Peking University, 1999

MS, Peking University, 2002

Submitted to the Graduate Faculty of

Arts and Sciences in partial fulfillment

of the requirements for the degree of

Doctor of Philosophy

University of Pittsburgh

2011

UNIVERSITY OF PITTSBURGH

GRADUATE ARTS AND SCIENCES

This dissertation was presented

by

Yanhong Yang

It was defended on

February 22nd, 2011

and approved by

Dr. Shigeru Amemiya, Associate Professor, Department of Chemistry

Dr. Kazunori Koide, Associate Professor, Department of Chemistry

Dr. Robert M. Enick, Professor, Department of Chemical and Petroleum Engineering

Dissertation Advisor: Dr. Stephen G. Weber, Professor, Department of Chemistry

FLUOROUS MEMBRANE-BASED SEPARATIONS AND REACTIONS

Yanhong Yang, PhD

University of Pittsburgh, 2011

Porous alumina membranes were rendered compatible with fluorous liquids by surface modification with a carboxylic acid terminated perfluoropolyether (Krytox 157FSH). FTIR and contact angle measurements demonstrate the success of the modification.

Fluorous liquids are readily imbibed by modified alumina membranes, resulting in fluorous supported liquid membranes. Fluorine-containing organic solutes are selectively transported through the fluorous supported liquid membranes. Selectivity is defined as the permeability of a fluorous tagged solute over an analogous organic compound. The membrane modification conditions (reagents, concentrations, reaction time) were optimized to maximize the selectivity. The membrane pore size affects the solute permeabilities and selectivities.

Two series of homologous esters of perfluoroalkanoic acids with different organic moieties were studied. Permeability increased for both series as the perfluoroalkyl chain was lengthened. This shows that the difference in permeabilities is dominated by partitioning rather than diffusion. We further measured the partition coefficients of the homologs. The free energy of transfer of a $–CF_2–$ group (ethanol to perfluorinated solvents) is -1.1 kJ/mol. The experimental values of the partition coefficients are well correlated with the ‘mobile order and disorder’ theory. This provides an easy way to estimate partition coefficients in any biphasic system, even for solvents that are fluorous mixtures. Diffusion coefficients were determined from permeabilities and partition coefficients based on the solution-diffusion model of permeability.

Measured values are satisfactorily related to the Stokes-Einstein equation, especially for higher homologs. This investigation enables the prediction of transport properties of the fluorous supported alumina membranes.

Krytox 157FSH, which is virtually insoluble in any but fluorous solvents, was deposited on the fluorous-modified alumina membranes. FTIR shows the presence of the H-bond-based carboxylic acid dimers for these adsorbed Krytox 157FSH molecules. The carboxylate groups of Krytox 157FSH extract cations from aqueous solutions.

TABLE OF CONTENTS

LIST OF TABLES

LIST OF FIGURES

LIST OF SCHEMES

LIST OF EQUATIONS

PREFACE

First and foremost, I owe my sincerest gratitude to my advisor and mentor, Prof. Stephen G. Weber for his encouragement, guidance, patience and support throughout my graduate study in the United States. His broad knowledge and remarkable insight motivated my research a lot and helped me to grow into a better scientist. I am also really grateful to the members of my comprehensive, proposal and dissertation committees: Prof. Shigeru Amemiya, Prof. Billy Day, Prof. Robert M. Enick, Prof. Kazunori Koide, Prof. Adrian Michael and Prof. Megan Spence.

I would like to thank the members of the Weber research group (past and present). I feel lucky to have so many great labmates. We are together like a family rather than a research group. My special thanks go to Hong Zhang for her encouragement during my frustrating time and helpful discussion at my confusing moment.

I would like to show my gratitude to all the administrative and technical staff at our department. Tom Gasmire made the holders for FTIR measurements and modification experiments. Chuck Fleishaker helped me to fix my laptops so that I can finish my proposal and dissertation writing smoothly. Thanks for their expertise and generous help during my graduate study.

I would like to thank Pingping Gou from the Star research group. She taught me the synthetic skill of the last chapter. I also thank Drs. Phil Yeske and MarvinYu from FTI for providing the fluorous solutes for my research.

I want to thank the National Science Foundation for financial support through Grant CHE0615952.

Finally, I am indebted to my parents and family for their unconditional support, love and encouragement throughout my study over the years.

1.0 INTRODUCTION

1.1 MEMBRANE-BASED TECHNIQUES

Over the past few decades, membrane-based technologies have been widely applied in gas separations[1-4], wastewater treatments[5-8], removal of environmental pollutants[9-12], performance improvements for batteries[13-15] and reactors[16-19], drug delivery[20-24] and surgical/ medical interests[25, 26]. These applications motivated the production of membranes with diverse structures and surface functionalities.

Porous inorganic membranes (alumina, silica, titania and zirconia) and polymeric organic membranes (Nylon, Teflon, polypropylene and so on) have been developed, derivatized and investigated. Polymeric organic membranes selectively transport/capture targets over interfering species. Sulfone modified polyvinylidene fluoride (PVDF) membranes efficiently separated SO_2 from a binary mixture of SO_2 and N_2[27, 28]. However, the tortuous path decreases permeability and makes it difficult to predict membrane performance. In addition, the thermal/chemical stability is also a concern for organic membranes. An example is the biofouling that occurs when polymeric membranes interact with biological environments[29, 30]. Porous inorganic membranes have controllable pore size, shape and distribution, and hence large permeabilities and good

correlation to theoretical modeling. However, selectivity is achieved by the pore size and thus the solute size and shape. Surface modifications on inorganic membranes have been emerging to improve the membrane selectivity and open up the new scopes for porous inorganic membranes[31-34]. Porous alumina membranes are well represented in several of those properties.

1.1.1 Porous alumina membrane fabrication

Among the various alumina membranes, porous anodic alumina membranes (PAAMs) are produced by anodization of an Al sheet in an electrolytic cell. The morphology and growth mechanism have been intensively investigated[35-38]. Pore density and size were demonstrated to be controlled by the anodizing voltage and electrolyte used, while thickness is subject to the amount of charge passing through the aluminum foil. Figure 1-1 shows the influence of voltages on the membrane morphology. The upper and lower row represent the front and back view of membranes anodized under 40 V (left), 80 V (middle) and 150 V (right), respectively. Such fabrication method results in the PAAMs with narrow pore distribution, high pore density and parallel, non-intersecting pores.

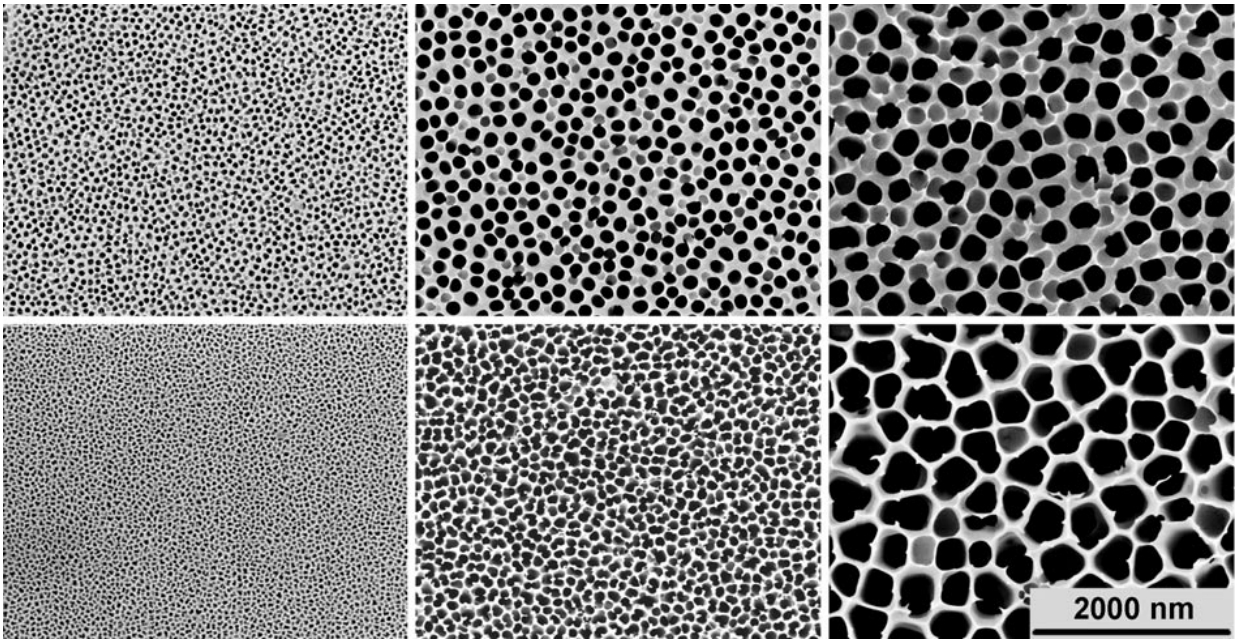

Figure 1-1. Reproduced with permission from Thormann *et al*.,[39] SEM images for porous anodic alumina membranes anodized under 40 V (left), 80 V (middle) and 150 V (right).

1.1.2 Porous alumina membrane applications

Due to the well-defined pore properties and large surface area, porous alumina membranes have been employed for gas phase[40, 41] and liquid phase separations[40] (ultrafiltration and reverse osmosis). The narrow pore size distribution provides accurate cut-off molecular weight. Sano *et al.* successfully separated a DNA mixture based on size-exclusion using PAAMs as separation matrix in a bio-chip[42]. Ma and Yeung utilized the unique pore structure of PAAMs as the model surface for chromatographic retention to observe the motion of single DNA molecules and nanoparticles, which provide valuable insights for the separation mechanisms in traditional/size-exclusion chromatography[43]. Besides the size-dependent separations, electrostatic interactions

with the rich content of hydroxyl groups on alumina membranes also facilitate the selective transport through the PAAMs[44-46]. Bluhm *et al.* systematically investigated the transport of monovalent, divalent and trivalent ions through the porous alumina membranes. Trivalent cations show slower transport rate than mono/divalent cations due to the enhanced electrostatic interactions between the porous alumina membranes and the most highly charged cations[47, 48]. An interesting example is the fabrication of stacked PAAMs as a stationary phase into a fluid chip for the separation of adenine, adenosine-5'-monophosphate (AMP) and adenosine-5'-triphosphate (ATP)[49]. The solute retention depends on the number of phosphate functional groups and the pH value of the mobile phase, which influence the interactions of solutes with the membrane surface.

Alumina membranes may also include a modification layer. Such membranes provide great robustness, reliability, diversity and high selectivity. The modification layer can be made of organosilicon[50]/silicon oil[51]/silica[52-57]/silane[58-61], metals[62-68], metal oxides/hydroxides[69-71], carbon[72], organic acids[73] and polymers[74-79]. Vlassiouk *et al.* demonstrated the separation of ss-DNA by the covalently linked DNA through a glutaraldehyde linker attaching to the terminal amino group of aminosilane modified PAAMs[80]. Moreover, porous alumina membranes are able to imbibe liquids, forming supported liquid membranes[81-83]. Odom *et al.* investigated the influence of the incorporated liquid on the transport performance through octadecyltrimethoxysilane (ODS) modified porous alumina membranes[58]. Poor selectivity for homogeneous phenol analogues was achieved for ODS modified membranes without any liquid in the pores. Significant improvement in selectivity was observed when the membranes imbibed mineral oil. Supported liquid membranes based on porous anodic alumina membranes are attractive and promising platforms for separations and purifications.

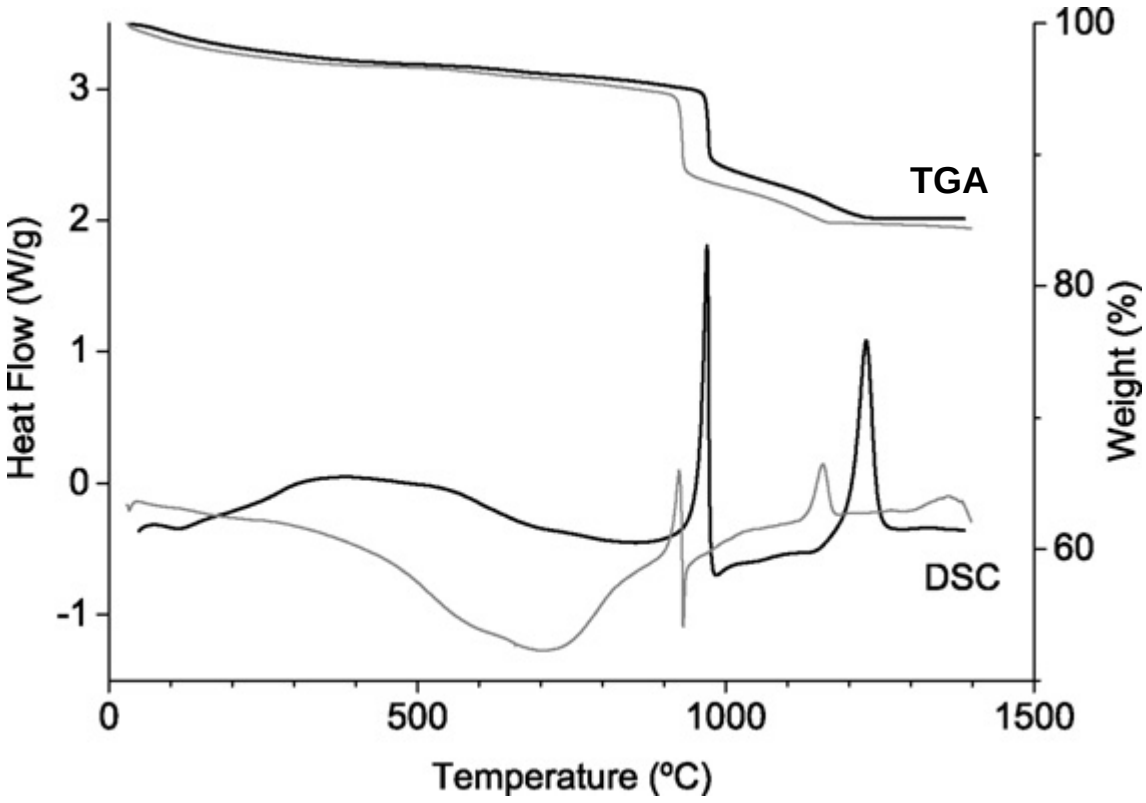

Figure 1-2. Reproduced with permission from Kirchner *et al.*[84] DSC (*left*) and TGA (*right*) of PAA up to 1400 ˚C. Black line: scanning rate 20 K/min, grey line: scanning rate 2 K/min. The DSC signal of the latter is shown 2.5× for clarity.

Porous anodic alumina membranes are stable at high temperature since they are ceramic oxides[84-86]. Figure 1-2 shows the typical thermal analysis results (differential scanning calorimetry (DSC) as well as thermal gravimetric analysis (TGA)) for the porous anodic alumina membranes anodized in sulfuric acid[84]. Four weight-loss sections were similar in the TGA curves

at two different heating rates. The membrane weight initially decreased because water was gradually lost. A sharp weight loss happened at ~970 °C, which is linked to the crystallization of the membrane from amorphous phase to γ-Al_2O_3 caused by the decomposition of sulfate anions. A corresponding exothermic peak was observed at the same temperature from the DSC curves. The sulfate anions decomposed up to about 1200 °C. The membrane experienced second phase transition to the stable α-Al_2O_3 (corundum) above 1200 °C, coincident with the second exothermic peak in the DSC curves. The membrane weight remained constant after the phase transition. The preservation of pore structure is another concern for high-temperature applications. The pore architecture was studied by scanning electron microscope (SEM) after heat treatments, as shown in Figure 1-3. Virtually no pore decomposition and cracking were observed below 800 °C. Special attention should be paid to the commercially available Anodiscs™ manufactured by Whatman Ltd. Such membranes stand for lower temperature (~700 °C) compared to the membranes used in Figure 1-2 and 1-3 because of the slightly different anodization process. The Anodiscs™ membranes are fabricated in a phosphate solution. The phosphates go into the pores and form a gradient distribution along the pore direction. However, the membranes used in Figure 1-2 and 1-3 are produced in a sulfate electrolyte. The sulfates homogenously distribute in the pores. The unevenly distributed phosphates in the Anodiscs™ membranes lead to higher mechanical tension and make them buckle or crack at low temperature[73]. Porous anodic alumina membranes have been applied as chemical reactors. Increased conversion and better selectivity are achieved due to confined porous structure[87]. An interesting example is the hydrogenation of 1,3-butadiene and oxidation of carbon monoxide catalyzed by palladium and ruthenium nanoparticles in porous alumina membranes. High catalytic activities were observed because of the well-defined pore structure and large surface

area, compared to traditional supports[88]. Omata *et al.* applied porous anodic alumina membranes as reaction supports for screening catalysts for methane reformation aided by artificial neural network[89].

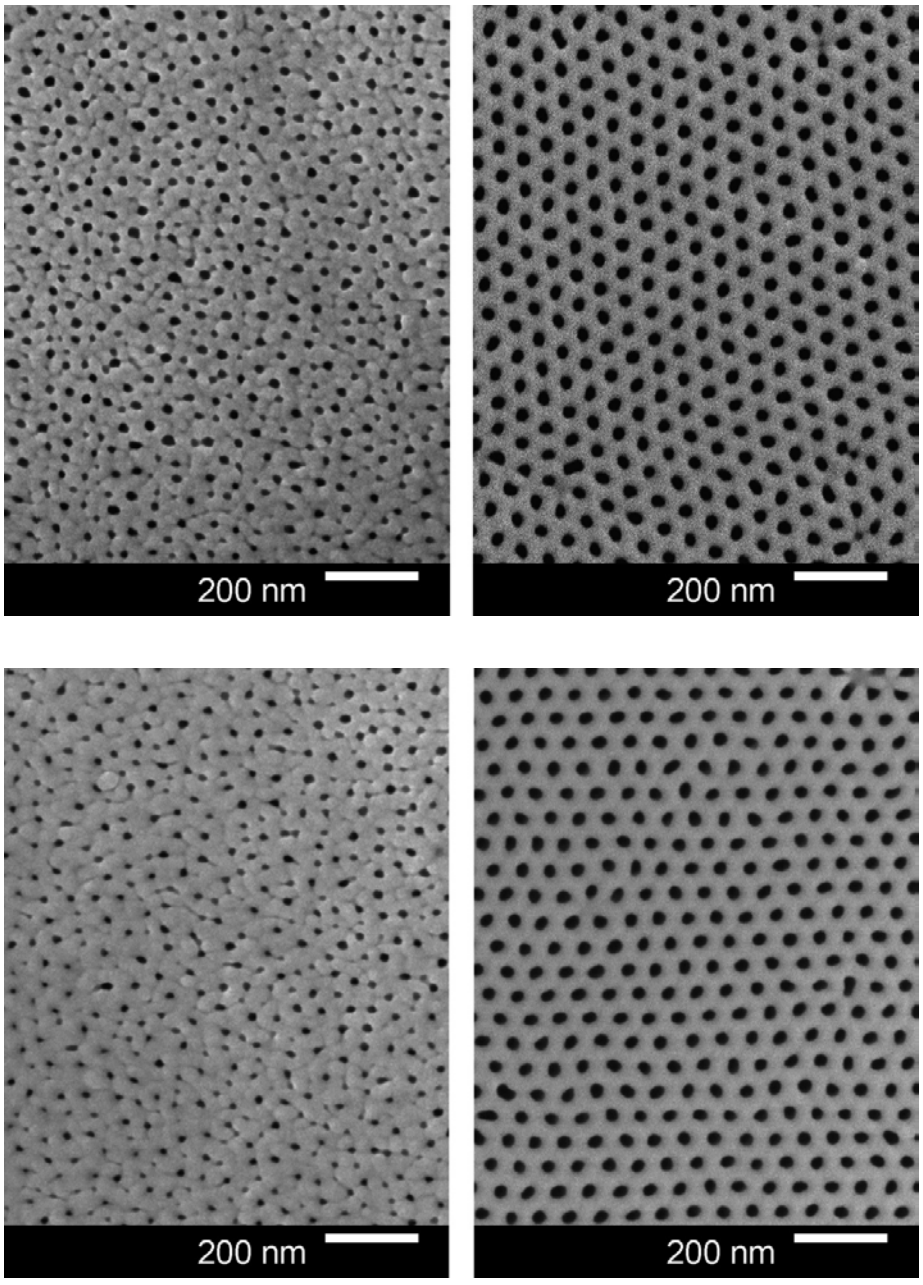

Figure 1-3. Reproduced with permission from Kirchner *et al.*[84] SEM images of the active (left) and support side (right) of an as-prepared porous alumina membrane (upper) and after heating to 800 °C (lower).

Besides those applications, porous anodic alumina membranes have been widely used as the template for the productions of various nanoarrays with different shape, size and materials. Precursors are filled into the confined pores of PAAMs by vapor infiltration, sputtering, electrochemical deposition, sol-gel and sublimation. Alumina membrane template is easily etched away by acids or bases on demand. This fabrication method has successfully produced metal/metal oxide fibers, rods, particles, pillar and wires[90-97], chalcogenide nanowires (Bi_2S_3, Bi_2Se_3, Bi_2Te_3, Sb_2S_3, Sb_2Se_3, Sb_2Te_3)[98], silica and boron nitride nanotubes[99] and polymeric nanowires[100-106]. An example is the CeO_2 nanotubes grown inside the PAAMs which show 400 times higher catalytic activity for CO oxidation reactions than powdered CeO_2[107]. Liu *et al.* fabricated a potential supercapacitor based on poly(3,4-ethylenedioxythiophene) (PEDOT) nanotubes synthesized in the porous alumina membranes[108]. Tao *et al.* produced bovine serum albumin/hemoglobin lyophilized bovine erythrocytes hybrid protein nanotubes with variable diameters and wall thickness by simple and versatile layer-by-layer deposition for potential in vivo applications[109].

1.2 FLUOROUS MEDIA

Fluorous media are notoriously poor solvents for non-polar organic compounds and water at room temperature. Their poor solubility can be simply accounted for by a large difference of the solubility parameter, δ, which is defined as the square root of the energy of vaporization of a pure component over its molar volume at temperature T[110]. For example, perfluorohexane is observed to phase separated from hexane since the solubility parameter for perfluorohexane (δ_f = 12.3 $MP_a^{1/2}$) is smaller than that for hexane (δ_o = 14.9 $MP_a^{1/2}$). In contrast, perfluorohexane is

soluble in supercritical carbon dioxide (δ = 12.1 $MP_a^{1/2}$)[111]. The weaker van der Waals interactions result in decreased solubility parameters for F-containing compounds because of the replacement/addition of electrophilic fluorine[112]. Therefore, an F-containing solute is expected to preferentially partition to fluorous solvent from organic solvent, which is literally termed as "fluorophilicity" even though it should be recognized as "oleophobicity"[113]. Typically, organic solutes are rendered F-containing by covalently attaching a perfluoroalkyl chain $–(CF_2)_nCF_3$[114]. The partitioning of solutes can be adjusted by the number of $–CF_2–$ groups (n). Figure 1-4A shows the typical trend for partition coefficients of F-containing solutes. More incorporated $–CF_2–$ group results in smaller solubility parameter, and hence larger partition coefficient to fluorous solvent. However, an abnormal partition trend would be expected as shown in Figure 1-4B. Lengthening perfluoroalkyl chain leads to reduced partition coefficient until the solubility parameter of solute reaches that of the organic solvent[115]. Nevertheless, this interesting trend is difficult to observe in reality since the solute is possibly a surfactant with a very polar organic part and a very non-polar perfluoroalkyl chain, which is insoluble in both fluorous and organic solvents[113]. In addition, the weak solvent-solvent interactions of fluorous media can maximize the interactions between solutes and receptors incorporated into the fluorous media. Therefore, the poor solvation properties encourage the applications of fluorous media in selective extraction/transport with or without the aid of receptors.

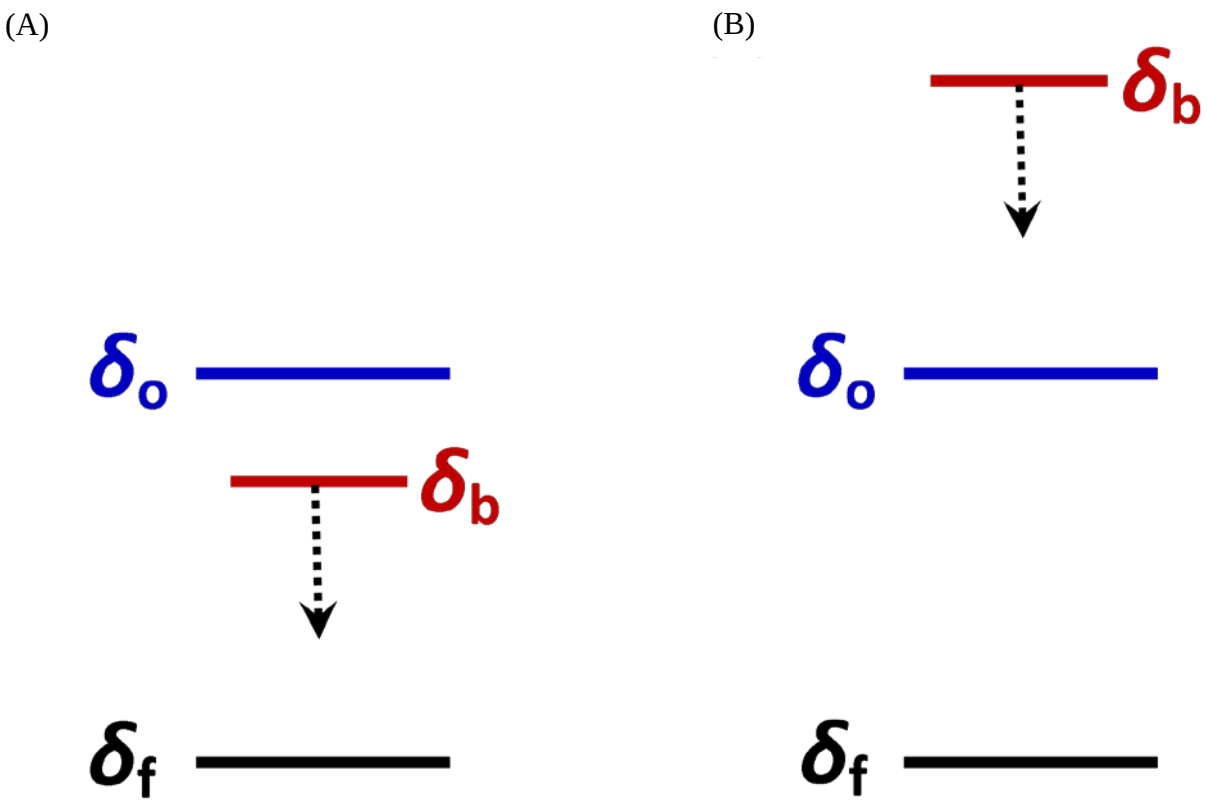

Figure 1-4. Reproduced with permission from O'Neal *et al.*,[113] Schematic diagram showing the effect of adding –CF_2– groups to an organic molecule. The solubility parameter of the organic solvent is indicated as δ_o. The solubility parameter of the fluorous solvent is given as δ_f. The latter is smaller than the former. (A) The solubility parameter of the solute, δ_b, is between those of the two solvents. It partitions between the solvents. As more –CF_2– groups are added (arrow) the solute's solubility parameter becomes closer to δ_f and the partitioning favors the fluorous phase more. (B) If the organic moiety is more polar, its solubility parameter is larger than in the previous case. In this case, adding –CF_2– groups makes the solute more similar to the organic solvent, leading to the prediction that the effect of adding –CF_2– groups in this case is to make the partition coefficient favor the organic phase more.

1.2.1 Fluorous separations

Horváth and Rabai exploited biphasic catalytic recycling utilizing the unique properties of fluorous media[114] that have been demonstrated by Hildebrand and Scott[116]. An F-containing catalyst dissolves in fluorous solvent, which is immiscible with organic solvent at room temperature. One phase forms when heated. The catalyst contacts reagents and initiates or accelerates a chemical reaction. After cooling, the catalyst precipitates out of the reaction mixture. The easy purification coupled with the reactions leads to the interests in the field of organic synthesis[117-120]. In addition, the use of fluorous media extended to petrochemical processes[121], protein/drug design[122, 123], chemical biology[124] and intervention/control of biological process[125].

Our group has done a great deal of work on selective extraction by noncovalent association with a receptor in fluorous media[113]. A study of liquid-liquid extraction based on H-bonding interactions in perfluorohexanes (fluorinert FC-72)/chloroform was performed by O'Neal[126-128]. This work provides fundamental understanding of noncovalent associations in poor solvents. Fluorous polymeric carboxylic acid (Krytox 157FSH, MW = 5840 g/mol) was employed as the receptor to selectively extract structurally related polar solutes, because of its poor solubility in organic solvents and superior H-bonding capacities from the carboxylic acid terminal.

$$CF_3 - CF_2 - CF_2 - O - \left[CF\left(CF_3\right)CF_2 - O - \right]_n CF\left(CF_3\right)COOH$$

Scheme 1-1. Krytox 157FSH (**1**), $n \approx 33$

Improved extraction was achieved for most studied N-heterocyclic bases. Proton transfer occurs from Krytox 157FSH to pyridine (Figure 1-5A). The free energy of the complex formation was quantified in FC-72 at room temperature, as shown in Figure 1-5B. A further study took a closer look at molecular and ionic complex formation in fluorous solvents (chiefly FC-72)[127]. Excess Krytox 157FSH (1 base: 3 acid) is necessary to facilitate ionic complex formation in fluorous solvent, while the complex with 1:2 (base: acid) is supported in non-polar organic solvents and 1:1 (base: acid) in polar solvents. O'Neal further extended the extraction system from small molecule (pyridines) to large molecules, porphyrins[128]. Two protons were observed to transfer to 5, 10, 15, 20-tetra(4-phenyl)porphyrin (TPhP), forming porphyrin dication in FC-72. For 5, 10, 15, 20-tetra(4-pyridyl)porphyrin (TPyP), the protonation occurred on the outside pyridyl nitrogen, followed by the central pyrrole ring with excess Krytox 157FSH. Zinc salt of Krytox 157FSH (Zn$\mathbf{1}_2$) metalated the TPyP and formed ZnTPyP and **1**. The interactions between the liberated **1** and the pyridyl groups of ZnTPyP stabilize the complex in FC-72. Similar extraction showed no TPhP partitioning to FC-72 by zinc salt of Krytox 157FSH. O'Neal's work has been nicely reviewed by Vincent[129]. Other noncovalent associations in fluorous media are included, such as ion-pairing, halogen bonding and gelation.

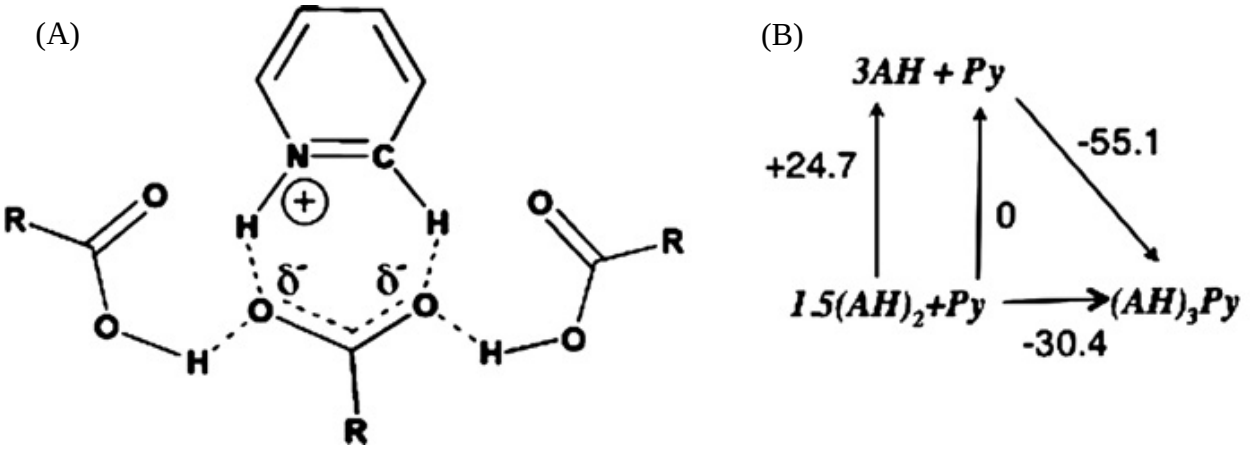

Figure 1-5. Reproduced with permission from O'Neal *et al.*,[126] (A) Proposed structure for the complex between pyridine and Krytox 157 FSH which includes proton transfer. (B) Thermodynamics of complex formation. Numbers are Gibbs free energies in kJ/mol.

Hobbs *et al.* utilized Krytox 157FSL (L indicates MW = 2500 g/mol)) to solubilize enzymes in fluorous solvent through hydrophobic ion-pairing[130] interactions. Up to 20 mg cytochrome c per mL could be extracted by Krytox 157FSL to perfluoromethylcyclohexane (PFMC). KDP 4606 (a Krytox ammonium salt with MW = 1400 g/mol) readily ion paired with cytochrome c, α-chymotrypsin and lipase, forming transparent solutions in PFMC[130-132]. Dynamic Light Scattering (DSL) measurements showed that the enzyme was surrounded by KDP 4606. Improved catalytic efficiency was observed for the enzymes[130].

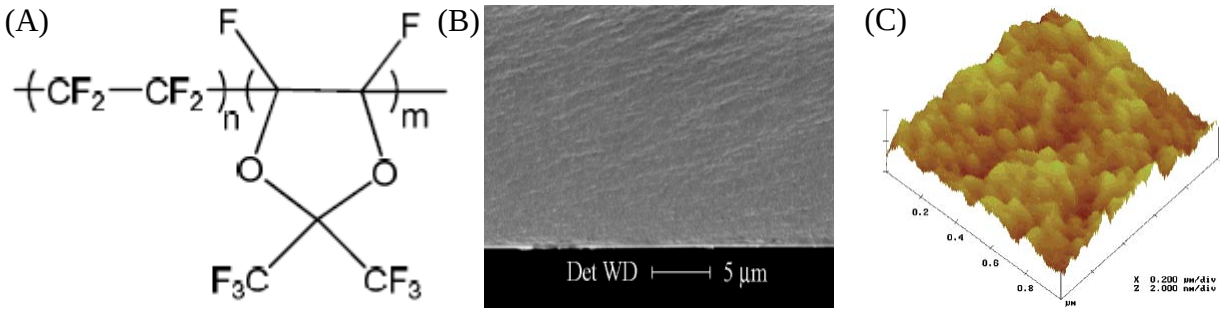

Figure 1-6. Reproduced with permission from Zhao *et al.*,[133] Structure of Teflon AF 2400 (A), SEM (B) and TEM (C) images of Teflon 2400 membranes.

Our group is interested in selective transport of F-containing solutes through fluorous membranes. Teflon AF 2400 is a commercially available perfluoropolymer with a high fractional free volume (FFV), which is of special interests as the matrix for gas transport[134-136], pervaporation[137-139] and gas sensor[140]. Zhao from our group initiated the investigation of Teflon AF 2400 as the matrix for liquid phase transport[133, 141]. Figure 1-6 show the structure of Teflon AF 2400 and SEM as well as atomic force microscopy (AFM) images of Teflon AF 2400 membranes. A smooth and homogeneous membrane was achieved by the simple casting method. Selective transport of F-containing solute (α,α,α,-trifluorotoluene) over H-containing toluene was observed. However, the selectivity is not as expected because of the organic solvent uptake (chloroform) in Teflon AF 2400 membranes. Zhang successfully doped perfluorotripentylamine (fluorinert FC-70) into Teflon AF 2400 membranes[142]. Chloroform uptake significantly decreased for 27 wt% FC-70 doped membranes, compared to the pure Teflon AF 2400 membranes. The physical and chemical properties of FC-70 doped Teflon AF 2400 membranes are summarized in Table 1-1. Improved selectivity for octafluorotoluene/toluene and pentafluoronitrobenzene/nitrobenzene was achieved while increasing FC-70 contents in Teflon AF 2400 membranes.

Table 1-1. Reproduced with permission from Zhang *et al.*,[142] Summary of the physical and chemical properties of FC-70-doped Teflon AF membranes at 20.0 °C

property	Teflon AF 2400 doped with FC-70	
	0-12 wt % FC-70 content	>12 wt % FC-70 content
free volume	decreasing, FC-70 fills the free volume of Teflon AF 2400	increasing, FC-70 dilutes Teflon AF 2400
storage modulus	increasing	decreasing
sorption of $CHCl_3$	decreasing and approaching the solubility of $CHCl_3$ in FC-70	
permeability coefficients	decreasing	increasing
diffusion coefficients	decreasing	increasing
partition coefficients	decreasing trend in general	
partitioning selectivity (8F/8H, 5F/5H)[a]	increasing trend in general	
partitioning selectivity (3F/3H)[a]	no increase	

[a] Partition coefficient of a fluorous compound with the stated number of F atoms divided by the partition coefficient of the analogous hydrogen-containing compound.

In the case of fluorous membrane based separation, Teflon is widely used because it is the most permeable among fluorous polymers due to large free volume. However, the average radii of each volume element is a few angstroms[143], which is only suitable for the transport of gases or small size solutes. In addition, Teflon membranes uptake organic solvents when

contacted, which makes Teflon membrane less “fluorous”. The selectivity of F-containing solutes over H-containing solutes is decreased. Hence, more “fluorous” membranes should be produced and systematically investigated to achieve high selectivity. Fluorous bulk liquid membranes are possibly the most “fluorous”. They selectively transport F-containing solutes over organic controls due to the weaker Van der Waals interactions even though no receptors are employed. The Curran group introduced a fluorous triphasic reaction based on bulk liquid membrane in which a separation is directly coupled with a chemical reaction to produce a pure product from impure starting material[144]. Fluorous media are naturally nontoxic, but they are persistent in the environment due to their excellent chemical stability[113]. Many perfluorocarbons are believed to deplete the ozone layer and are classified as potential greenhouse gases[145]. On the other hand, the cost of fluorous media leads to another concern if they are used in large quantities. Hence, fluorous supported liquid membranes are promising and attractive from an environmental and economic point of view. Therefore, work need to be done to develop and investigate fluorous supported liquid membranes.

1.3 OBJECTIVE AND RESEARCH PLAN

Porous alumina membranes have high pore density and narrow pore size distribution, which is suitable as the matrix of supported liquid membranes. Moreover, they are chemically stable in organic solvents and aqueous solutions. Therefore, we decided to develop fluorous supported liquid membranes based on porous alumina membranes for selective transport. The fluorous inorganic membranes are expected to combine the good pore structure of alumina membranes and the unique properties of fluorous liquids. To our knowledge, there is no previous report to

systematically investigate the fluorous supported liquid membranes based on porous alumina membranes.

In Chapter 2, we render porous alumina membranes fluorophilic by surface modification with the perfluoropolyether Krytox 157FSH. The importance of filling fluorous liquids in membranes is demonstrated. Membrane preparation conditions (reagents, concentrations and time) are evaluated based on the selectivity of perfluoroalkyl tagged solutes over organic control. Optimized selectivity is achieved by the supported liquid membranes that are refluxed in 3 mM Krytox 157FSH/HFE 7100 solution for 3 hours. The influence of membrane pore size is investigated for a series of analogues with different length of perfluoroalkyl chain. Chapter 3 further studies the transport properties of the fluorous supported alumina membranes. Increased transport rates for larger solutes show that the difference in permeabilities is dominated by the difference in partitioning rather than diffusion. Independent partition coefficients to fluorous liquids were measured. A group contribution method with 'mobile order and disorder' theory is used to estimate the partition coefficients. Regardless of the fact that the fluorous liquids are mixtures, the calculated partition coefficients well correlate to the experimental values. Diffusion coefficients determined by the solution-diffusion model satisfactorily relate to the Stoke-Einstein equation. Chapter 4 utilizes the fluorous alumina membrane as a solid matrix to attach another Krytox 157FSH layer. The fluorous-fluorous interactions ensure the immobilization of Krytox 157FSH under variable organic solvents. However, perfluorohexanes (FC-72) readily remove adsorbed Krytox 157FSH without destroying the modification layer. This property provides a new opportunity for the fluorous alumina membrane as solid support for reactions coupled with easy separation and purification. Adsorbed Krytox 157FSH can be easily transferred to ionic form when contacting water. Therefore, we have applied the fluorous membranes with Krytox

157FSH as ion exchange membranes for $Ru(bpy)_3^{2+}$ ions. Preliminary study shows all Krytox 157FSH are available to react.

2.0 PREPARATION AND ASSESSMENT OF FLUOROUS SUPPORTED LIQUID MEMBRANES BASED ON POROUS ALUMINA

Reprinted from ***Journal of Membrane Science***, *345,* Yanhong Yang, Lei Hong, Nithya Vaidyanathan, Stephen G Weber*, Preparation and assessment of fluorous supported liquid membranes based on porous alumina, 170-176, Copyright (2009), with permission from Elsevier.

2.1 ABSTRACT

Fluorous media have gained a foothold in the synthetic and analytical communities. There is a need for membranes or films that have good selectivity for transport of molecules with fluorous tags. We show here that supported liquid membranes (SLMs) based on modified porous alumina have the desired properties. Hydrophobic alumina membranes were prepared by surface modification with perfluoroalkanoic acids. The initial contact angles of modified alumina membranes exceed 130^{o}. FTIR shows the loss of –OH stretching modes and the gain of carboxylate carbonyl stretch as well as C-F stretching modes indicative of the surface modification. SEM shows no gross changes in the membrane morphology resulting from the modification. The resulting modified membranes readily imbibe and hold fluorous solvents forming SLMs. Cinnamyl alcohol (**2**) and its ester with 2H,2H,3H,3H-perfluorononanoic acid

(HOOC-$(CH_2)_2$-$(CF_2)_5CF_3$) (**3c**) were employed as solutes in transport experiments with the membranes. Transport selectivity (ratio of permeabilities of **3c** to **2**) was used as a measure of effectiveness in the optimization of modification conditions. Conditions for the surface modification leading to maximum selectivity for transport of **3c** over **2** by the resulting SLM were to reflux membranes in 3 mM Krytox 157FSH/HFE 7100 solution for 3 hours. Finally, the influence of membrane pore size on transport rate and selectivity was investigated for cinnamyl alcohol and its esters with fluorous carboxylic acids HOOC-$(CH_2)_2$-$(CF_2)_{n-1}CF_3$, n=2, 4, 6, 8. The transport rate for the smallest pore size (20 nm) and largest solute (n=8) is anomalously high. This may be due to solute being transported in the modification layer as well as solvent.

2.2 INTRODUCTION

Fluorous separations have gained a foothold in synthetic organic chemistry[146]. Fluorous tags, which contain a moiety rich in carbon-fluorine bonds[147], have been developed. Such tags are affixed to a target species, functioning as a "phase label" directing the target to a fluorous phase resulting in separation from the organic matrix[117]. Techniques suitable for separating fluorous species from mixtures include fluorous liquid-liquid extraction[148-150], fluorous solid phase extraction[151-154], fluorous flash chromatography[155, 156], fluorous HPLC[119, 157] and fluorous membranes[158-160].

Fluorous materials and liquids have also been recognized by the analytical community in sensors and extraction-based separation techniques[161-164]. The poor solubility of most solutes in fluorous liquids makes them good solvents for biphasic extraction-based separation techniques based on molecular receptors or hosts. Several groups[129] including ours[126] are making progress

in the preferential extraction of target species into fluorous liquids. Generally, a fluorous-soluble molecular receptor is introduced into the fluorous liquid to solubilize the target species[129]. High extraction efficiency has been achieved based on a variety of receptors.

Supported liquid membranes (SLMs) are recognized as a promising technology for separations. A supported liquid membrane usually consists of an organic liquid in a compatible matrix. The interactions between the organic liquid and the supporting matrix must be favorable. Hence, highly hydrophobic supporting matrices are desirable for a successful organic SLM. For example, porous alumina membranes functionalized by octadecyltrimethoxysilane with mineral oil as the membrane liquid demonstrated about 10 times higher selectivity for 2,4,6-trimethyl phenol over phenol than that for the same membranes without the membrane liquid[58]. In the few published reports on fluorous supported liquid membranes, polymeric membranes such as Teflon AF or poly(tetrafluoroethylene) (PTFE) are used as the support matrix for SLMs[163-165]. We are attracted to the high porosity of porous alumina membranes, and wondered if they would be suitable supports for a fluorous SLM.

Porous alumina membranes are characterized by their well-ordered, nearly cylindrical pore structure, high pore density, and good thermal stability[166, 167]. Besides these features, the rich content of hydroxyl groups on the membrane surface facilitates the production of hydrophobic alumina membranes by silanization[168], esterification[58, 73]or other methods. Such membranes with modified surfaces open up new applications to which unmodified membranes cannot be applied. Examples are biochemically modified alumina membranes used for selective separation of drug enatiomers[169] and DNA oligomers[170]. The Suen group has utilized *n*-alkanoic acid modified membranes for protein adsorption[73]. The Belleville group has successfully rendered porous alumina membranes hydrophobic with a fluoroalkylsilane surface modification

and applied them to osmotic evaporation[171]. The Pashley group has investigated in detail the production of highly hydrophobic alumina surfaces (planar surfaces, not porous alumina) based on esterification of the surface hydroxyl groups with alkanoic and perfluoroalkanoic aids. They found that surfaces modified by perfluoralkanoic acids[172] have larger contact angles than those modified with organic carboxylic acids, and the longer perfluoroalkanoic acids produce alumina membranes with higher contact angles.[173] There is to date one report, a spectroscopic study, on the modification of porous alumina membranes with fluorous carboxylic acids[174], and no investigation of fluorous SLMs based on them.

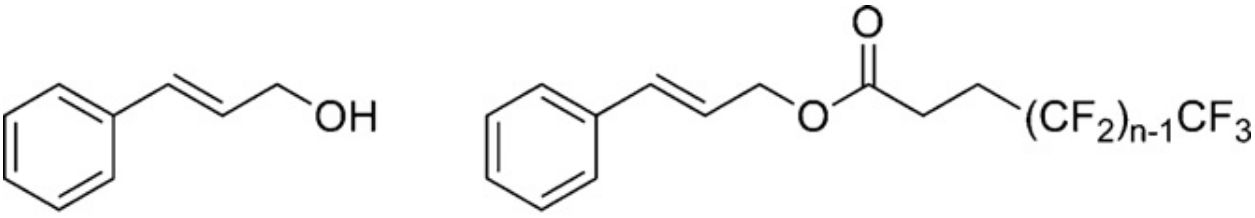

2

3

3a (n = 2)

3b (n = 4)

3c (n = 6)

3d (n = 8)

Scheme 2-1.

In this article, we report the development and optimization of supported fluorous alumina membranes. The selectivity based on the permeabilities of **3c** over **2** was used to judge the performance of the membranes. Several factors were investigated to improve the selectivity of

alumina-based fluorous SLMs, such as the modification reagent, reaction time, reagent concentration and membrane pore size. A companion paper describes transport properties of SLMs created from several fluorous solvents[175].

2.3 EXPERIMENTAL SECTION

2.3.1 Materials

All the chemicals, unless specified otherwise, were obtained from Aldrich (Milwaukee, WI) or Sigma (St. Louis, MO). Krytox 157FSH (**1**) with a carboxylic acid end group was obtained from Miller-Stephenson Chemical Co. (Morton Grove, IL). Perfluorooctadecanoic acid (**4**) was obtained from Alfa Aesar (Ward Hill, MA). Fluorous-tagged solutes were gifts from FTI (Pittsburgh, PA). Alumina Membranes (20, 100 and 200 nm pore size, 13 mm diameter and 60 μm thickness) were purchased from Whatman (Florham Park, NJ). Hydrofluoroether-7100 (HFE-7100) (a mixture of methyl nonafluorobutyl and nonafluoroisobutyl ethers) was obtained from 3M (Minneapolis, MN). FC-3283 Fluoroinert Electronic Liquid (a mixture of perfluorononanes) and PF-5080 Performance Fluid (a mixture of perfluorooctanes) were purchased from 3M (Minneapolis, MN). Sodium ethoxide (21% in ethanol) was purchased from Cole-Parmer (Vernon, IL).

2.3.2 Membrane modification

All membranes were cleaned by sonicating them in 30% H_2O_2 for 30 min, followed by H_2O for 15 min and absolute ethanol for 30 min. The cleaned membranes were transferred to a piece of aluminum foil and then dried at ~100 °C for 30 min in an econotherm laboratory oven (Precision, Winchester, VA). Clean alumina membranes were vertically mounted into a homemade Teflon rack with forceps and refluxed in HFE-7100 solution with defined concentrations of **1** or **4** for various times. The modified membranes were thoroughly rinsed with HFE-7100, absolute ethanol and dried at 80 °C for 45 min.

2.3.3 Membrane characterization

Water contact angles for modified membranes were measured with a VCA 2000 Video Contact Angle System (Billerica, MA). FTIR (Excalibur FTS 3000, Varian, Randolph, MA) was used to analyze the modified membranes with the spectrum of the unmodified membrane as reference. The membranes were imaged using a Philips XL30 FEG scanning electron microscope (Hillsboro, OR). For the base stability, the receiving phase was made 9 mM in sodium ethoxide after transport (see below) had reached steady state. The absorbance was monitored following the addition of base. For determining the pressure, a piece of membrane was sandwiched between the arms of a homemade U-tube setup. Four mL of water were initially placed on each side of the tube. Excess water was added to one side of the tube until flow was observed. The difference in the height of the water on each side of the membrane was converted to a pressure.

2.3.4 Transport experiments

The modified membrane was dipped in a fluorous solvent and then mounted between two quartz cuvettes with holes in them[176]. Viton gaskets between the membrane and cuvette prevented leaking. The transport area (0.196 cm^2) was defined by the holes in the cuvettes. A modified eight-position cuvette holder (Agilent) held four transport experiments in a rack. Each of the eight cuvettes was stirred magnetically with the same stirring speed controlled by a locally built stirring module. Typically, the four transport units were used for duplicate transport experiments conducted for two related solutes simultaneously. The source phase was filled with 3 mL of 1 mM solute in ethanol saturated with the fluorous solvent used in the SLM, while the receiving phase contained 3 mL of fluorous-solvent-saturated ethanol. Solute transport was monitored by observing the rate of increase of the UV absorbance at 250 nm in the receiving phase (Hewlett-Packard 8452A UV-Vis diode array spectrophotometer (Palo Alto, CA)). Calibration curves were used to convert the UV absorbance to concentration for each solute. The steady state flux, J, of a solute is given by Eq. 2-1:

$$J = \left(\frac{dC_r}{dt}\right)\left(\frac{V}{A}\right)(\text{mol} \bullet \text{s}^{-1} \bullet \text{cm}^{-2})$$

Equation 2-1

where A is the effective area of the membrane for transport, V is the volume of the receiving phase and dC_r/dt is the steady state accumulating rate of the solute in the receiving phase. The permeability, P, can be calculated from the flux using the following Eq. 2-2.

$$P = \frac{J \cdot l}{(C_s - C_r)} \approx \frac{J \cdot l}{C_{s_0}} (\mathrm{cm}^2 \bullet \mathrm{s}^{-1})$$

Equation 2-2

l is the thickness of the membrane and C_s and C_r are the concentrations of the solute in the source phase and the receiving phase, respectively. C_s - C_r is close to C_{so}, the initial concentration of the solute in the source phase, since C_r is negligible at the beginning of the experiment. Selectivity is defined as the permeability ratio of the fluorous solute, i, over an analogous organic control (**2**).

$$S_i = \frac{P_i}{P_1}$$

Equation 2-3

2.4 RESULTS AND DISCUSSION

2.4.1 Modified membrane characterization

SEM is a convenient way to investigate the influence of modification on the morphology of membranes. Figure 2-1 shows the micrographs taken before and after modification. The membranes have different morphologies on the two sides[177, 178]. The 'active' side (Figure 1A and D) shows a porous network corresponding to the pore size stated by the manufacturer, while the support side (Figure 1B and E) contains larger, more circular pores about 200 nm in diameter. Furthermore, the "active" layer is just about ~1 µm thick, while the rest of the membrane has the

straight channels with 200 nm diameter as shown in the cross-section of Figure 2-1C and F. It is interesting to note that modification does not alter the structure of the membranes. The support side and the cross-section are just slightly coarser as a result of the modification. Clearly, the modification occurs on the pore walls without significantly changing the membrane area for transport.

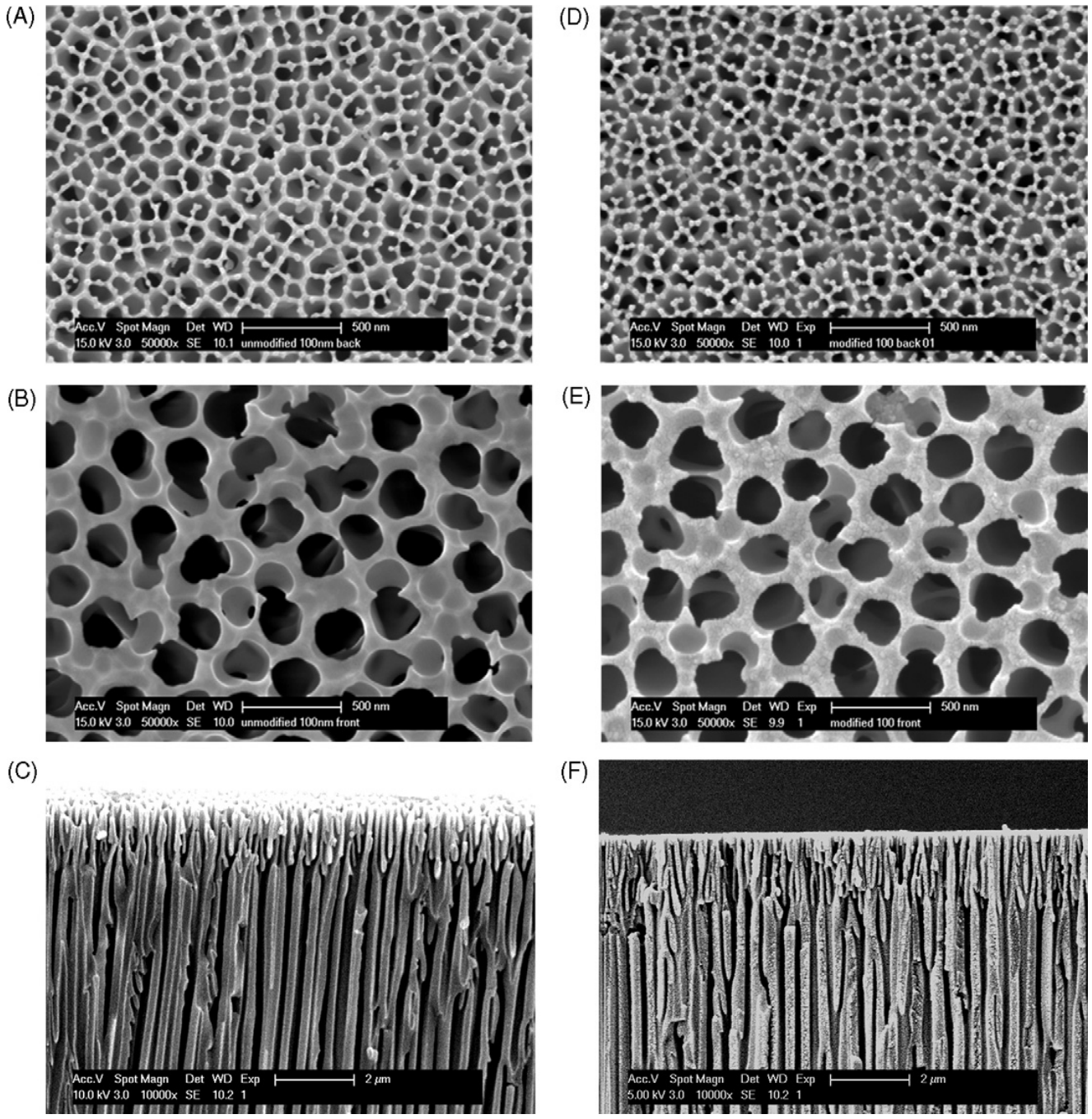

Figure 2-1. SEM micrographs of the original ((A), (B) and (C)) and modified ((D), (E) and (F)) nanoporous alumina membranes with a nominal 100nm pore size.

Following the surface modification reaction, FTIR can be used to demonstrate the success of the modification. Figure 2-2A shows representative spectra after separate modifications with two carboxylic acids. One is the long and flexible polymeric fluorous carboxylic acid, Krytox 157FSH (**1**). The other reagent is the short and stiff perfluorooctadecanoic acid (**4**).

1 **4**

Negative peaks were obtained for both acids in the range of 3000~3600 cm^{-1}. This demonstrates the loss of hydroxyl groups from the alumina membranes because of the modification reaction. The vibration centered at 1678 cm^{-1} shows the characteristic stretch mode for the carboxylate carbonyl[174, 179]. This demonstrates the presence of carboxylates on the membrane surface. Meanwhile, the vibrations in the range of 1100 ~ 1400 cm^{-1} indicate the presence of C-F bonds (stretch) from the modification reagents. Compared to the **1**-modified membrane, the **4**-modified membrane demonstrates a slightly larger peak at 1678 cm^{-1} and a more negative peak at 3000~3600 cm^{-1}. This indicates that the surface coverage of **4** is somewhat higher than for **1** because of the relatively smaller molecular size of **4**. The significantly lower absorbance from C-F bonds in the membrane modified with **4** reflects its lower molecular weight.

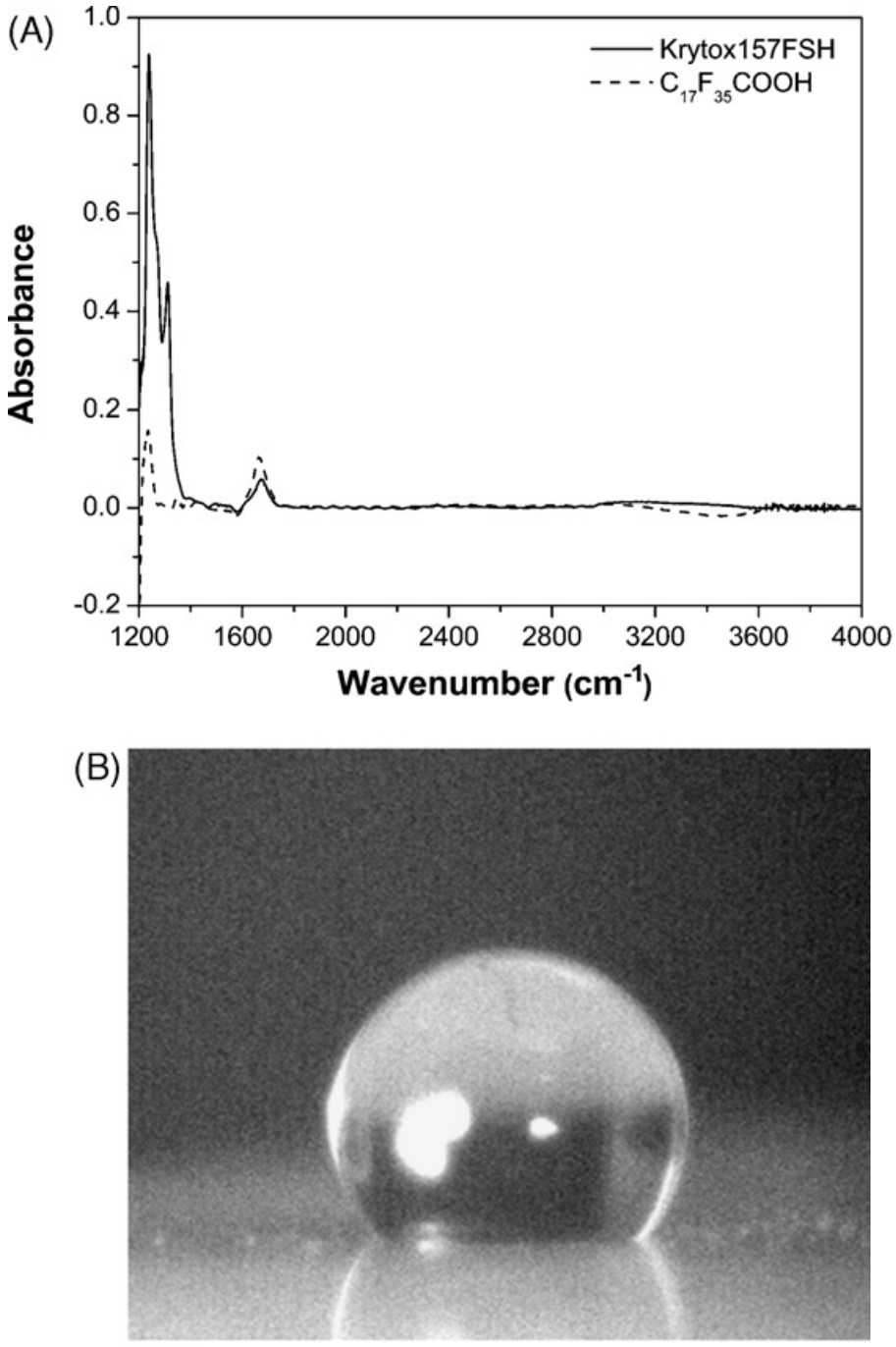

Figure 2-2. (A) Representative FTIR spectrum for **1** (—) and 4 (- - -) modified 100nm alumina membranes. The unmodified 100nm alumina membranes were used as reference. (B) Representative contact angle image for the active side of a **1**-modified 100nm membrane. The membranes were refluxed in HFE-7100 solution containing 3mM modification reagent for 3 h.

Water contact angle (θ) measurements were used to determine quantitatively the material's hydropobicity, as shown in Figure 2-2B. Generally, surfaces with $\theta < 90°$ are considered hydrophilic, while surfaces with $\theta > 90°$ are considered hydrophobic. Higher contact angles correspond to lower surface tension. The initial contact angles for our modified membranes are 134 ± 6° for **4**-modified membranes and 130 ± 2° for **1**-modified ones. For comparison, we attempted to measure contact angles for unmodified membranes. However, water droplets simply pass through the porous, hydrophilic structure. Similar contact angles have been reported for *n*-alkanoic acid[73] or perfluorodecyltriethoxysilane-modified[171] alumina membranes. Nanostructured surfaces can exhibit the superhydrophobic effect because of the nanoscale porous surface topography[180]. Water contacts the modified alumina on the surface while air remains inside the pores of the membranes. Hence, the measured contact angle (θ) is related to the fraction of the surface that is solid (φ_s) and the contact angles of a smooth flat surface of the same material (θ_e) and air (θ_a) by Eq. 2-4[181].

$$\cos\theta = \varphi_s(\cos\theta_e) + (1-\varphi_s)(\cos\theta_a)$$

Equation 2-4

For our 100 nm membranes, the air fraction roughly equals the membrane porosity (28%), since the surface structure did not change due to the modification as shown in Figure 2-1. Using the observed contact angle, we can determine that the contact angle of a smooth flat surface of **1**-modified alumina would be 120 ° according to Eq. 2-4. This value is close to the maximum observable water-contact angle on a fluorous flat surface (~120° for PTFE) [182, 183].

Hence, we conclude that modification produces a porous and hydrophobic surface from the original hydrophilic membrane.

2.4.2 Transport of solutes by SLMs

The permeabilities and selectivities of the resulting membranes for organic and fluorinated solutes **2** and **3d** are shown in Table 2-1. Table 2-1 includes data for unmodified, 100 nm pore-size membranes, membranes that have been modified by **1** but not filled with fluorous solvents, and SLMs. SLMs were created by dipping **1**-modified membranes in FC-3283, a mixture of perfluorononanes.

Table 2-1. Permeability and selectivity of solutes through different alumina membranes[a]

Transport condition	Solute	P /10^{-7} cm^2s^{-1}	S
Unmodified membrane	**2**	11.45 ± 0.091	0.68 ± 0.01
	3d	7.81 ± 0.050	
1-modified membrane	**2**	11.03 ± 1.27	1.00 ± 0.15
	3d	11.02 ± 1.12	
SLM[b]	**2**	0.017 ± 0.002	94.7 ± 3.5
	3d	1.61 ± 0.06	

[a] The transport was carried out through 100 nm membranes at room temperature.

[b] **1**-modified membranes containing FC-3283 (a mixture of perfluorononanes).

As can be seen from Table 2-1 and as expected, no significant selectivity was observed for unmodified and modified membranes without membrane solvent. Selectivity (**3d**/**2)** is 0.68 which is very close to the diffusion coefficient ratio calculated from the Stokes-Einstein equation (0.69). This indicates that, as expected, the difference in diffusion coefficients dominates the transport and hence selectivity for unmodified membranes. Modified, but unfilled membranes show changes in the permeabilities of the two solutes. For organic compound **2**, modification results in a slight decrease in permeability, on the order of 4%. Thus, the ratio of the porosities (modified/unmodified) is 0.96. This corresponds to an approximately 2% decrease in pore radius. As the nominal pore size is 100 nm, the 2% change in radius is equivalent to an approximately 1 nm thick layer resulting from the modification. For fluorous compound **3d**, the permeability was significantly increased due to the modification. Recall that the permeability is the product of a diffusion coefficient and a distribution coefficient. In the modified membrane, the distribution of solute between the source phase and the membrane will reflect the average concentration of solute in the membrane. The small, approximately 4%, volume of fluorous material increased the permeability by increasing the observed distribution coefficient of the fluorous compound into the membrane. The small volume of fluorous material had a substantial effect on the permeability because the distribution coefficient of the solute into the fluorous phase is significant. If we make a reasonable assumption, we can obtain an approximate value of the partition coefficient between the ethanol and the surface layer of **1**. The assumption is that diffusion through the pore takes place solely in the central, ethanol-filled pore space. It can be shown that the observed value of the distribution constant for the modified membrane, K_m, (outside the membrane to inside the membrane) is related to the fraction of the pore volume that

is ethanol, ε′, the complementary fraction that is the modification, and the partition coefficient of the solute going from ethanol to the fluorous modification, K_f, as shown in Eq. 2-5.

$$K_m = \varepsilon' + (1 - \varepsilon')K_f = 0.96 + 0.04K_f$$

Equation 2-5

Further, the value of K_f can be determined from the permeabilities (m=modified, u=unmodified) as shown in Eq. 2-6.

$$K_f = \frac{\frac{P_m}{P_u} - \varepsilon'}{1 - \varepsilon'}$$

Equation 2-6

Based on our data, we find that K_f is approximately 1×10^1. This is a large partition coefficient in comparison to partition coefficients for this solute from ethanol to other fluorous liquids[175], which are less than unity.

The selectivity increased significantly while the permeabilities decreased substantially when membrane solvent FC-3283 was used to form an SLM. The results demonstrate that the membrane modification allows the membrane to imbibe a fluorous liquid. This in turn results in selective membranes. We turn now to the influence of modification factors, such as modification reagent, concentration, and reaction time on the selectivity and permeability.

2.4.3 Influence of modification on the selectivity and permeability

In this set of experiments, the SLMs contained the fluorous solvent PF-5080, unless specified otherwise. The selectivities are summarized in Table 2-2. The permeabilities are also listed along with the selectivities. A word about experimental design is in order. The 'change one variable at a time' approach is of limited value in finding maximum performance when the variables interact[184]. In this case, we did not anticipate strong interactions based on our experience. As Table 2-2 shows, under a variety of conditions, we found the same maximum selectivity. Thus, the experimental design seems adequate.

From an inspection of Table 2-2, the selectivity for the **1**-modified membranes is nearly twice that for the **4**-modified membranes (other conditions the same). The difference results from the higher permeability of the organic control (**2**) through the **4**-modified membranes than for the **1**-modified membranes, as the permeability does not change significantly for the target **3c**. Compared to the small and stiff reagent **4**, modification from reagent **1** brings about a thicker layer. Although the contact angle for the **4**-modified membrane is higher than for the **1**-modified membrane, clearly the **1**-modified membrane performs better.

Table 2-2. Influence of membrane modifications on the selectivity and permeability.

Conditions		$P/10^{-7}$ cm^{2}s^{-1}[a]		S
		2	**3c**	
Reagent[c]	**1**	0.025 ± 0.003	1.33 ± 0.03[f]	53 ± 6
	4	0.06[b]	1.58 ± 0.15	26 ± 3
Concentration[d]	1 mM	0.17 ± 0.02	1.90 ± 0.24	11 ± 2
	3 mM	0.025 ± 0.003	1.33 ± 0.03[f]	53 ± 6
	10 mM	0.026 ± 0.002	1.41 ± 0.02	54 ± 4
Reaction times[e]	1 h	0.050 ± 0.006	1.35 ± 0.02	27 ± 3
	3 h	0.025 ± 0.003	1.33 ± 0.03[f]	53 ± 6
	6 h	0.027 ± 0.001	1.34 ± 0.07	50 ± 3

[a] Permeabilities are averages of duplicate or triplicate measurements with the standard error of mean. [b] The permeability was a single measurement. [c] The membranes were modified with 3 mM reagent in HFE-7100 for three hours. [d] Modification for three hours with **1**. [e] The membranes were refluxed in 3 mM **1** in HFE-7100 solution. [f]These entries are the same data.

As for the reagent concentration (all other conditions the same), the selectivity increased significantly from 1 to 3 mM **1**, and then remained constant as the reagent concentration went from 3 to 10 mM. The permeability shows the opposite trend. For all solutes, the permeability decreased and then remained constant as the concentration went from 1 – 10 mM. The decrease for solute **2** is larger than that for solute **3c**. The result further demonstrates that the modification layer influences the transport of the solutes somewhat differently. The results are consistent with incomplete filling of the pores by the fluorous solvent when the

surface coverage of the fluorous modification is not complete. Table 2-2 show that 3 mM **1** in HFE-7100 is sufficient to obtain the maximum selectivity in our system.

Based on the same reagent and concentration, the selectivity reached the maximum value after a 3-hour reflux. The selectivity slightly decreased when the reaction time increased, but the decrease is not statistically significant. The trend of the reaction time is very similar to that of the reagent concentration. This performance can be explained by the completeness of the modification reaction, as discussed above. It is interesting to note that the permeability of solute **3c** changes after one hour, while three hours is necessary to reach constant selectivity. It indicates that a small, unmodified area does not influence the transport of the target **3c** as much as it influences the transport of the organic control **2**. Hence, three hours were employed to obtain the best selectivity in the following experiments. The final, optimized conditions are: polymeric fluorous carboxylic acid **1** in 3 mM solution refluxed with the alumina membranes for three hours.

2.4.4 Influence of membrane structure on the selectivity

The pore size has been shown to play a distinct role in the membrane performances, such as permeability and selectivity[185-187]. Generally, a larger porosity will give higher permeabilities, all else being equal. Aside from the effect of porosity, the pore size may influence transport if the pore size approaches the solute size, however this is not the case here. Several groups have found that large pore size usually results in unstable SLMs[188]. The resistance to pressure-induced flow is inversely proportional to the square of the pore size, thus membranes with larger pore sizes may be more susceptible to damage caused by the presence of a pressure gradient across the membrane. The loss of the liquid incorporated into the membrane will diminish the selectivity.

To evaluate the influence of pore size on the permeability and selectivity in our system, three commercially available alumina membranes with 20 nm, 100 nm and 200 nm nominal pore sizes modified by **1** were adopted for the transport experiments. A series of homologs (**3**) was used as the set of solutes. Recall that the stated pore size describes the 'active' surface which is only about 1 μm thick. Figure 2-3A shows how the permeability changes as the pore size increases. A similar trend was achieved for all solutes when plotting the permeability against the pore size, as we expected. The porosity of these membranes increases about a factor of 2 as the pore size goes from 20 to 200 nm[189, 190]. Figure 2-3A demonstrates that, at least for solutes **3a-c**, the change in permeability reflects this increase in porosity. For solute **3d**, this magnitude of increase is not seen. The selectivity for each solute is shown in Figure 2-3B. With one exception, the selectivities do not depend on the pore size. The only exception is the most fluorous compound, **3d**, in the membrane with the smallest pore size. If the only influence of the change in porosity is geometrical, there should be no change in selectivity. That we see an effect of pore size only on the most fluorous of the solutes tells us to seek a reason for it in the fluorous makeup of the membrane. We speculate that the contribution of the modification layer to the overall process is maximized for solute **3d** and the 20 nm pore size because the modification layer is a significant fraction of the pore space for the 20 nm membranes. Recall that the partitioning into the modification layer for solute **3d** is greater than into common fluorous liquids. Further, solute **3d** will be most influenced by the presence of a significant volume fraction of Krytox, as it is the most fluorous solute.

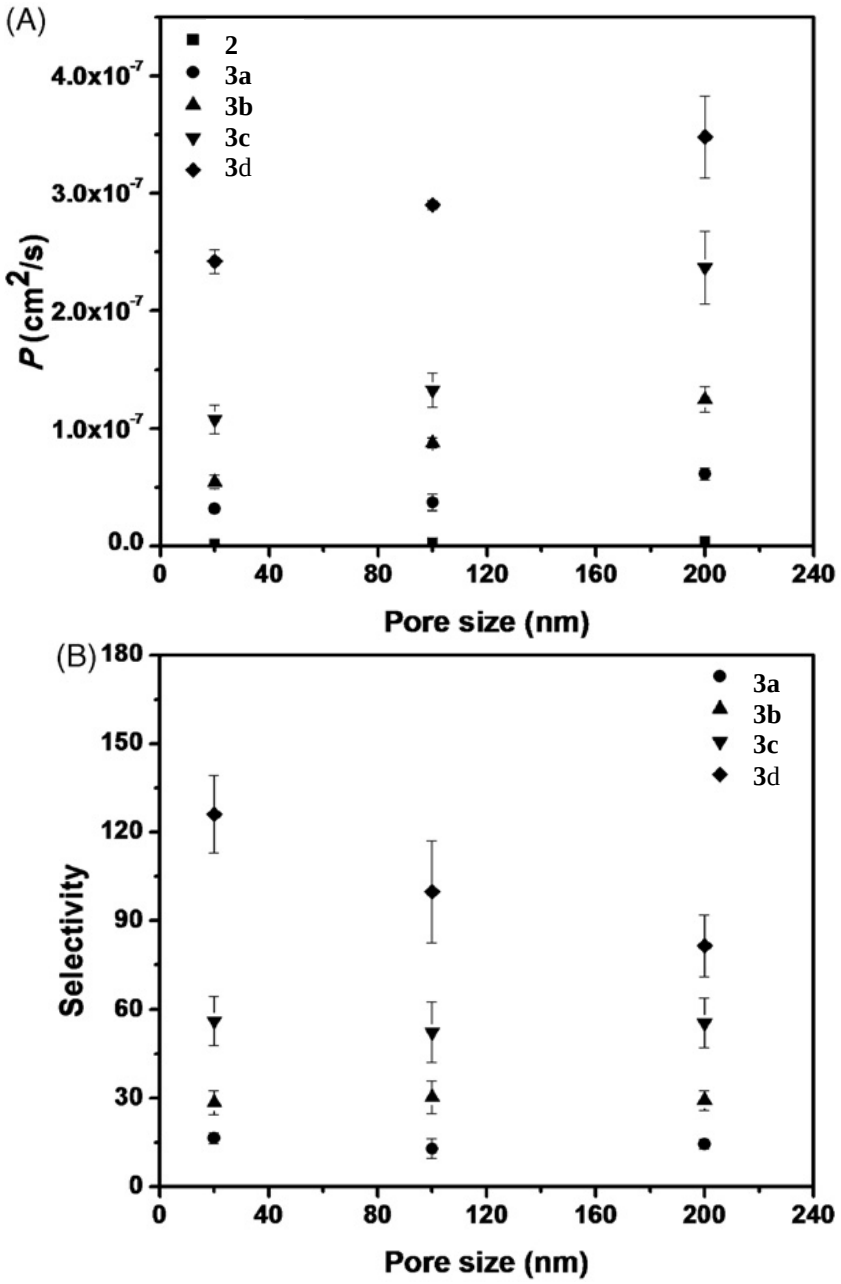

Figure 2-3. Influence of membrane pore size on the permeability (A) and selectivity (B) for different solutes **2** (■), **3a** (●), **3b** (▲), **3c** (▼), **3d** (◆). The membranes were modified by 3mM **1** in HFE-7100 for 3 h. The permeability was the average of duplicate measurements.

Stability is a concern for the applications of SLMs. Several experiments were conducted to evaluate the stability of modified SLMs. Bases such as sodium ethoxide can react with the membrane material, aluminum oxide. Hence, the transport of the organic control **2** and fluorous target **3c** through **1**-modifed membrane with PF-5080 as the fluorous liquid was observed following the introduction of sodium ethoxide into the receiving phase. The results show that there was virtually no change in the rate of transport of solutes to the receiving phase upon the addition of the base (9 mM). In addition, we established the pressure difference between the source and receiving phase required to push out the membrane solvent. The **1**-modified SLMs impregnated with PF-5080 withstood up to 13 kPa pressure difference (about 15% of an atmosphere), while the unmodified membranes leak when the pressure difference is only 430 Pa. Based on these investigations, the modified SLMs appear to be somewhat stable. Under extremes of pH and higher pressures, they would not be stable.

2.5 CONCLUSION

We have demonstrated that porous alumina membranes can be modified with fluorous carboxylic acids, and that the modified membranes imbibe fluorous solvents, becoming SLMs. The SLMs show excellent selectivity for organic compounds with a fluorous 'tag'. Even a small fluorous tag, $–CF_2–CF_3$ has a significant effect. Permeabilities are high, in the range of 10^{-7} cm^2s^{-1}.

3.0 POROUS ALUMINA-BASED FLUOROUS LIQUID MEMBRANES: DEPENDENCE OF TRANSPORT ON FLUOROUS SOLVENT

Reprinted from ***Journal of Fluorine Chemistry***, 130, Yanhong Yang, Nithya Vaidyanathan, Stephen G Weber*, Porous alumina-based fluorous liquid membranes: Dependence of transport on fluorous solvent, 1022-1027, Copyright (2009), with permission from Elsevier.

3.1 ABSTRACT

We report here the properties of supported fluorous liquid membranes based on porous alumina. The alumina is first rendered compatible with fluorous solvents by surface modification with an oligomeric perfluoropropylene oxide-based carboxylic acid, Krytox 157FSH. After modification, simply dipping the porous alumina membrane into a perfluorinated solvent results in a supported liquid membrane with high selectivity for fluorous compounds. Two homologous series of compounds differing in the number of $-CF_2-$ groups were investigated, namely esters of cinnamyl alcohol and the analogous naphthyl derivative with 2H,2H,3H,3H-perfluoroalkanoic acids ($HOOC-(CH_2)_2-(CF_2)_{n-1}CF_3$, n=2, 4, 6, 8). Four perfluorinated membrane solvents (FC-77, PF-5080, FC-3283 and FC-43) were investigated. In FC-3283, the permeabilities, which are the products of a diffusion coefficient and a partition coefficient in the solution-diffusion model, of cinnamyl alcohol derivatives are 3.62 ± 0.36 times greater than those of the analogous naphthyl

compounds for the solutes containing the same perfluorinated chain. Permeability, *P*, increases as the perfluorinated chain length increases in all of the perfluorinated solvents. Values of log(*P*) versus n are linear with a slope of 0.147 ± 0.002 but with different intercepts for the various solvents. Independent measurements of the partition coefficients of the solvents between the source/receiving phase solvent, ethanol, and the fluorous solvents reveal that the selectivity behavior is dominated by partitioning rather than diffusion. The free energy of transfer of a $-CF_2-$ group (ethanol to perfluorinated solvents) is -1.1 kJ/mol. Despite the fact that the solvents are mixtures, not pure liquids, the partition coefficients are well correlated with values calculated based on group contributions with 'mobile order and disorder' theory. The diffusion coefficients of four solutes in four membrane solvents were also determined based on the solution-diffusion model. The Stoke-Einstein equation shows satisfactory estimation of experimental results.

3.2 INTRODUCTION

A successful supported liquid membrane (SLM)[191-193] requires a proper combination of porous support and a liquid phase to achieve high selectivity, high permeability, and desirable stability. To date, organic solvents have been used widely as the supported liquid because the common application is the separation of solutes based on lipophilicity. Here, our strategy is to use perfluorocarbons or related fluorous materials to replace the commonly used organic solvents. Fluorous liquids such as perfluorinated alkanes, perfluorinated oligoethers and polyethers and perfluorinated trialkylamines are inert[165, 194], nonpolar and hydrophobic as well as oleophobic. The attraction of perfluorocarbons has been recognized by the organic synthesis community in biphasic synthesis, catalysis and extraction[146, 195, 196]. The driving force in those techniques arises

from the fact that the fluorinated compounds have weaker van der Waals interactions with solvent per molar volume than organic compounds[112]. Typically, a fluorous tag is covalently attached to the target species to give it some solubility in fluorous solvents. Other synthetic applications such as the phase-vanishing or bulk membrane techniques[197-199] use a fluorous layer but not necessarily fluorous reagents or catalysts. There is a small but growing interest in using noncovalent interactions in fluorous media for synthetic chemistry[129], selective extractions[126-128], and potentiometric sensors[163, 164]. In these applications, the permeability of the solutes (reagents, catalysts, analytes) through the fluorous medium is an important parameter in dictating the function of the fluorous phase.

We have previously worked on the transport of solutes through Teflon AF 2400 membranes, which are readily cast, thin, and mechanically strong. The preferential transport of α,α,α-trifluorotoluene over toluene was demonstrated in Krytox 157FSH (**1)**-doped polymeric Teflon AF 2400 membranes[160].

$$CF_3 - CF_2 - CF_2 - O - \left[CF\left(CF_3\right)CF_2 - O - \right]_n CF\left(CF_3\right)COOH$$

1

However, solute transport through Teflon AF 2400 membranes is slow. Also, Teflon AF imbibes the solvent from the source/receiving phase (chloroform) and as a result becomes less fluorous. We have developed fluorous SLMs[200] based on porous alumina[58, 73, 201]. In the work presented here, we have determined permeabilities and partition coefficients for two homologous series in SLMs with four different fluorous solvents. Diffusion coefficients were determined from the permeabilities and partition coefficients. We find that the transfer free energy for the –CF_2–

group (from source/receiving phase, ethanol) is the same for all four fluorous solvents investigated, however the affinity of the fluorous solvents for an organic moiety varies considerably. There are a few approaches to determine partition coefficients in fluorous systems based on empirical relationships[112, 150, 202-206]. This effort is largely focused on the perfluoro(methylcyclohexane)/toluene solvent system and the notion of 'fluorophilicity'. It is necessary to expand the range of applicability of empirical approaches. Thus, using the SLMs, we determined permeability coefficients of the solutes through four fluorous solvents. Independent measurements of the partition coefficients in the biphasic systems fluorous solvent/ethanol (where 'fluorous solvent' represents the four solvents used) allow estimation of diffusion coefficients. Partition coefficients and diffusion coefficients are well predicted by convenient approaches using group additivity methods.

3.3 EXPERIMENTAL SECTION

3.3.1 Materials

All the chemicals, unless specified otherwise, were obtained from Aldrich (Milwaukee, WI) or Sigma (St. Louis, MO). Krytox 157FSH with a carboxylic acid end group was obtained from Miller-Stephenson Chemical Co. (Morton Grove, IL). Fluorous-tagged solutes were gifts from FTI (Pittsburgh, PA). Alumina membranes (100 nm pore size, 13 mm diameter and 60 μm thickness) and polyester drain discs were obtained from Whatman (Florham Park, NJ). Hydrofluoroether-7100 (HFE-7100) (a mixture of methyl nonafluorobutyl and nonafluoroisobutyl ethers) was obtained from 3M (Minneapolis, MN). FC-3283 Fluoroinert

Electronic Liquid (a mixture of perfluorononanes), FC-43 Fluoroinert Electronic Liquid (perfluorotributylamine), FC-77 Fluoroinert Electronic Liquid (a mixture of C_8F_{18} and cyclic $C_8F_{16}O$) and PF-5080 Performance Fluid (a mixture of perfluorooctanes) were purchased from 3M (Minneapolis, MN).

3.3.2 Membrane modification

All 100 nm alumina membranes were pretreated by sequentially sonicating them in 30% H_2O_2 for 30 min, H_2O for 15 min and absolute ethanol for 30 min, and then drying at 100 °C for 30 min. Pretreated membranes were vertically mounted into a homemade Teflon rack. The rack of membranes was immersed in sixty mL of a 3 mM solution of **1** in HFE-7100 and refluxed for 3 h. After 3 hours, the modified membranes were then thoroughly rinsed with HFE-7100, absolute ethanol and dried at 80 °C for 45 min.

3.3.3 Transport experiments

Transport measurements were made using a two-compartment system at 22 ± 2°, measuring UV absorbance in the receiving phase. The membrane was dipped in a perfluorinated solvent and then mounted between two quartz cuvettes with holes in them[176]. Viton gaskets were required to prevent leaking. The transport area was defined by the holes in the gaskets/cuvettes with a diameter of 0.5 cm. A modified eight-position cuvette holder (Agilent) held four transport experiments in a rack. Each of the eight cuvettes was stirred magnetically with same stirring speed controlled by a stirring module. Typically, the four transport units were used for duplicate transport experiments conducted for two related solutes simultaneously. The source phase

containing 3 mL of 1 mM solute in ethanol (saturated with the perfluorinated solvent used in the membrane) was introduced to one of the cuvettes, while the receiving phase contained 3 mL ethanol saturated with the corresponding perfluorinated solvent. To prevent any loss of perfluorinated solvent in the membrane, the identical membrane solvent (20 μL) was added to the source and receiving phases. The concentration of solutes in the receiving phase was monitored by a Hewlett-Packard 8452A UV-Vis diode array spectrophotometer (Palo Alto, CA). The steady state flux, *J*, of a solute is given by Eq. 3-1:

$$J = \left({}^{dC_r}/_{dt} \right) \left({}^{V}/_{A} \right) (\text{mol} \cdot \text{s}^{-1} \cdot \text{cm}^{-2})$$

Equation 3-1

where *A* is the effective area of the membrane for transport, *V* is the volume of the receiving phase and dC_r/dt is the steady state accumulating rate of the solute in the receiving phase. The permeability, *P*, can be calculated from the flux using the following Eq. 3-2.

$$P = {}^{J \cdot l}/_{(C_s - C_r)} \approx {}^{J \cdot l}/_{C_{s_0}} (\text{cm}^2 \cdot \text{s}^{-1})$$

Equation 3-2

l is the thickness of the membrane. C_s and C_r are the concentrations of the solute in the source phase and the receiving phase, respectively. C_s - C_r is close to C_{so}, the initial concentration of the solute in the source phase, since C_r is negligible at the beginning of the experiment.

3.3.4 Determination of partition coefficients

Solute was dissolved in ethanol at the concentration of 1 mM. Solute/ethanol solution (70 μL) and perfluorinated solvent (140 μL) were placed in a VWR GC-autosampler vial (1.8 mL, West Chester, PA), shaken with the Bioshaker (distributed by BIONEXUS, Inc., Oakland, CA) at 1000 rpm and 25 °C for 30 minutes. The layers were physically separated and the ethanol layer was quantitatively analyzed by Jasco XLC (Easton, MD). Before injection, each sample was diluted five times with ethanol and 0.14 mM cinnamyl acetate was used as internal standard. A step gradient method was employed using Acquity UPLC^{TM} BEH C18 1.7 μm (1.0×50 mm) reversed-phase column from Waters (Milford, MA). Mobile phase was increased from 20% acetonitrile/80% H_2O (v/v) at 0.1 min to 95% acetonitrile/5% H_2O (v/v) at 0.2 min and remained at 95% acetonitrile/5% H_2O (v/v) for 8.8 more minutes. Finally, 20% acetonitrile/80% H_2O (v/v) was used to flush the column for 5 minutes in order to bring the column back to its initial state. The flow rate was maintained at 0.1 mL/min. The column temperature was kept at 40 °C. A Jasco X-LC^{TM} 2077 Plus acted as the detector at 250 nm. The peak areas were integrated by the software after manually defining the baseline. For calibration curves, we used a series of five standard solutions with concentrations ranging from 0.02 to 0.18 mM solutes plus 0.14 mM cinnamyl acetate in ethanol. These standard solutions were used to create the calibration curves for each solute by plotting the peak area ratio of solute/cinnamyl acetate versus solute concentration.

3.4 RESULTS AND DISCUSSION

3.4.1 Dependence of permeability coefficients on the solute properties

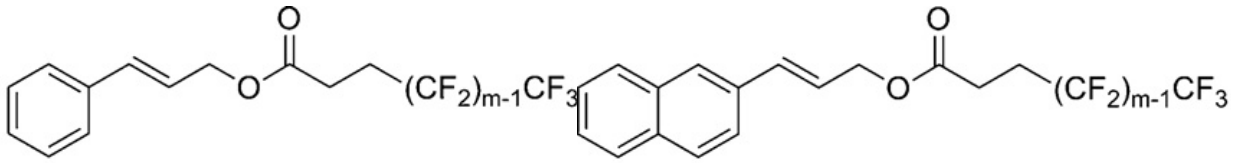

3
3a (*m* = 2)
3b (*m* = 4)
3c (*m* = 6)
3d (*m* = 8)

4
4a (*m* = 2)
4b (*m* = 4)
4c (*m* = 6)
4d (*m* = 8)

Figure 3-1. Structures of solutes studied.

Two homologous series of solutes (Figure 3-1) were used to investigate the influence of solute properties on transport through the fluorous SLMs (FSLMs). Data are listed in Table 3-1. Inspection of Table 3-1 shows that the permeability for each member of the **3**-series is about 3~4 times higher than that for the corresponding **4**-series. The average ratio of the permeabilities of members in the **3**-series over the corresponding members in the **4**-series is 3.62 ± 0.36. The insertion of an organic group is known to decrease partition coefficients in similar solvent systems[117]. Of course, the addition of an organic group leads to a larger molecular volume, and hence a lower diffusion coefficient as well. Thus, it is clear that the lower permeabilities of the **4**-series are expected. Increasing the number of $–CF_2–$ groups hastens transport through the

FSLMs, as shown in Table 3-1. Solutes with a longer perfluoroalkyl tail have a larger partition coefficient into a fluorous phase. However, the addition of a $–(CF_2)_2–$ unit no doubt increases molecular size, resulting in a decreased diffusion coefficient. Table 3-1 indicates that the permeability increases with an increasing length of perfluoroalkyl tail. In this case it is the effect of adding a $–(CF_2)_2–$ unit increases the partition coefficient more than it decreases the diffusion coefficient.

Table 3-1. Logarithmic values of *P* for **3** and **4**-series solutes.

m	Log(P /10^{-7} cm^2s^{-1}) [a]	
	4-series	**3**-series
2	-8.18 ± 0.04	-7.66 ± 0.01
4	-7.88 ± 0.06	-7.22 ± 0.02
6	-7.48 ± 0.12	-6.90 ± 0.09
8	-7.25 ± 0.02	-6.79 ± 0.02

[a] Average permeabilities based on duplicate or triplicate measurements through **1** modified 100 nm alumina membranes filled with FC-3283.

3.4.2 Dependence of permeabilities on membrane solvent

Table 3-2. Logarithmic values of P and K for the **3**-series in different membrane solvents.

m	Log(P /10^{-7} cm^2s^{-1}) [a]				Log(K) [b]			
	FC-77	PF-5080	FC-3283	FC-43	FC-77	PF-5080	FC-3283	FC-43
2	-7.31 ± 0.05	-7.43 ± 0.08	-7.66 ± 0.01	-8.09 ± 0.03	-1.57 ± 0.11	-1.63 ±0.03	-1.79 ± 0.14	-1.87 ± 0.16
4	-7.02 ± 0.04	-7.06 ± 0.02	-7.22 ± 0.02	-7.89 ± 0.02	-1.24 ± 0.10	-1.22 ± 0.06	-1.25 ± 0.04	-1.55 ± 0.11
6	-6.68 ± 0.05	-6.82 ± 0.04	-6.90 ± 0.09	-7.44 ± 0.02	-0.78 ±0.04	-0.91 ± 0.02	-0.95 ± 0.04	-1.04 ± 0.01
8	-6.41 ± 0.01	-6.54 ± 0.01	-6.79 ± 0.02	-7.27 ± 0.08	-0.44 ± 0.02	-0.51 ± 0.01	-0.62 ± 0.04	-0.74 ± 0.02

[a] The permeabilities are based on duplicate or triplicate measurements.

[b] The partition coefficients are based on triplicate measurements.

Permeabilities and partition coefficients of the **3**-series for various membrane solvents are reported in Table 3-2. The properties of these perfluorinated solvents are listed in Table 3-3. These solvents were chosen based on a compromise. Lower molecular weight solvents have lower viscosity, which increases permeabilities, however they also have lower boiling points which decreases their attractiveness. This set of solvents has on average a fairly low viscosity and a fairly high boiling point. Table 3-2 shows that similar slopes were obtained for **3**-series transport through and partitioning into the four membrane solvents when plotting the logarithmic values versus the numbers of the $–CF_2–$ group. The average slopes for the partitioning was 0.188±0.003. Thus, the free energy of the transfer of a $–CF_2–$ from ethanol to perfluorinated solvents can be calculated from such slopes as -1.1 kJ/mol. The average value of the slopes for the permeation was 0.147 ± 0.002. Thus, the addition of a $–CF_2–$ unit increases the transport rate by a factor of 1.4. The permeability shows a strong dependence on the membrane solvents in the order of FC-77>PF-5080>FC-3283>FC-43. For example, the permeability of **3d** in FC-77 is about seven times that in FC-43. The great variation in permeability goes beyond the influence of partition coefficients (Table 2) resulting from the different membrane solvents. For instance, the measured partition coefficient of **3d** in FC-77 is twice that in FC-43. Hence, we postulate that the extra variation in the permeability is caused by the effect of solvent on the solute diffusion coefficients. We defer a detailed discussion of diffusion. For now, it is sufficient to point out that the ratio of viscosities for the same two solvents (FC-77 and FC-43) is about 4. Thus, the large dependence of permeability on solvent can be rationalized.

Table 3-3. Properties of perfluorinated membrane solvents used.

Name	Boiling point (°C)	Viscosity(cP)	V_F (cm^3/mol)	δ_F ($MPa^{1/2}$)
FC-77	97	1.28	233[c]	10.5[b]
PF-5080	101	1.36	246[a]	10.5[d]
FC-3283	128	1.37	271[a]	10.6[b]
FC-43	174	5.26	356[e]	10.2[f]

[a] Increment values for the molar volume (cm^3/mol) obtained from ref [207], unless noted otherwise. [b] Increment values for the nonspecific part of the molar vaporization energy used to calculate δ_F obtained from ref [207] unless specified otherwise. [c] The molar volume of FC-77, a mixture, was determined from the molecular weight (415 g/mol) divided by the density. [d] The values of δ_F for FC-77 and PF-5080 are the same. [e] The increment value the molar volume of nitrogrn in perfluorotrialkylamines is from ref [208]. [f] The molar vaporization energy of nitrogen in triperfluoroalkyl amines from ref [208] was used to calculate the value of δ_F for FC-43.

3.4.3 Predicting solute behavior

There is a justifiable tendency to shun the use of solvent mixtures such as FC-72, FC-77, PF-5080, and FC-3283, and use solvents like perfluoromethylcyclohexane. Important quantities such as molar volume are necessarily less well defined in the former solvents compared to the latter solvent. On the other hand, in the world of applied chemistry, there is a tendency to use solvents

based on criteria other than whether a solvent is a mixture or not. We note the large difference of a factor of two in the partition coefficients mentioned above. We had not anticipated such a difference among nominally similar solvents. We therefore sought to understand whether approaches to understanding partition coefficients and diffusion coefficients based on group contribution approaches would apply to the current data. While we recognize that our data set is limited, we point out that the few computational treatments that exist focus on 'fluorophilicity' which is related to partitioning between perfluoromethylcyclohexane and toluene[202, 204, 205, 207, 209].

de Wolf *et al*. established a general relationship for the partition coefficient, *K*, based on the mobile order and disorder (MOD) theory[207].

$$\log K = 0.2171\ln(\frac{V_O}{V_F}) - 0.2171V_b(\frac{1}{V_O} - \frac{1}{V_F}) + 0.0522\frac{V_b}{T}(\delta_O^2 - \delta_F^2) - 0.1045(\frac{V_b\delta_b}{T})(\delta_O - \delta_F)$$

Equation 3-3

T is the experimental temperature (Kelvin). V_b is the molar volume of the solute. V_o and V_F are the molar volumes of the organic and the fluorous solvent, respectively. δ_b is the modified nonspecific cohesion parameter of the solute. δ_o and δ_F are the modified nonspecific cohesion parameters of the organic and the fluorous solvents. Modified nonspecific cohesion parameters account for only the non-specific force exhibited between molecules in liquids.[204] Generally, group contribution methods[207, 208] can be used to estimate the value of molar volume for solutes and solvents. Similarly, δ can be calculated from the molar volume and the molar nonspecific vaporization energy. Hence, the values of V and δ can be determined for the fluorous solutes and

the organic phase, ethanol. Table 3-4 disclosed the empirical (m.p.) and calculated properties of the fluorous esters **3**.

Table 3-4. Properties of fluorous esters **3**.

Name	Melting point (°C)	V_b (cm^3/mol)[a, c]	δ_b ($MPa^{1/2}$)[b, d]
3a	–	258	15.6
3b	–	304	15.1
3c	33	350	14.6
3d	66	396	14.3

[a] Increment values for the molar volume (cm^3/mol) obtained from ref [207]. [b] Increment values for the nonspecific part of the molar vaporization energy used to calculate δ_b obtained from ref [207]. C Increment value for the molar volume of –CH=CH_2 was used for the substitute –CH=CH–. D The calculated values of δ_b for –CH=CH_2 was employed as the values of δ_b for –CH=CH–.

For the fluorous solvents it is not so simple. Some approximations are required when using the group contribution approach for these fluorous solvents. For example, PF-5080 and FC-3283 are each mixtures; PF-5080 is a mixture of perfluorooctanes and FC-3283 is a mixture of perfluorononanes. The values of V_F were estimated based on the perfluorinated *n*-octane and *n*-nonane respectively. A comparison between the calculated values of V_F and the values determined by dividing molecular weight by density demonstrates that reasonable accuracy can

be achieved following this procedure. Therefore, the same chemical structures were used to calculate the values of δ_F for PF-5080 and FC-3283. FC-43 is not a mixture. However there is no group contribution for the nitrogen group in a perfluorotrialkylamine for estimating the value of δ_F. Considering that no specific interactions such as dipole-dipole and H-bonding exist in FC-43, the solubility parameter and the modified nonspecific cohesion parameter should be identical. Thus, we used the vaporization energy[208] to estimate the δ_F for FC-43. The most complicated case is FC-77 which is a mixture of C_8F_{18} and cyclic $C_8F_{16}O$. The molar volume can be calculated by dividing molecular weight by density. Furthermore, the δ_F for the oxygen group in perfluoroethers is small (0.03 kJ/mol), so we assumed that the incorporation of oxygen would not alter the vaporization energy significantly. Therefore, for FC-77's value of δ_F we used the value established for PF-5080. All of the values of V_F and δ_F are shown in Table 3-3.

The comparison of these calculated values from Eq. 3-3 and measured values from Table 2-2 are shown in Figure 3-2. A good linear relationship with a slope of 1.01 ± 0.06 (SEM) and an intercept value of -0.15 ± 0.06 (SEM) is achieved when experimental log(*K*) was plotted versus calculated log(*K*). The statistical analysis shows that there is no significant difference between the slope and the ideal value of unity (p = 0.870). There is a marginally significant difference between the intercept and the ideal value of zero (p = 0.027).

This good correlation demonstrates the validity and applicability of Eq. 3-3 to fluorous solvents that are mixtures as well as to a fluorous system with an associating solvent. The work published to date concerns solvents perfluoromethylcyclohexane and toluene. Thus, while the data set is of limited size it is nonetheless encouraging that established approaches to partitioning based on group contributions seem applicable to a broader set of solvents than heretofore realized.

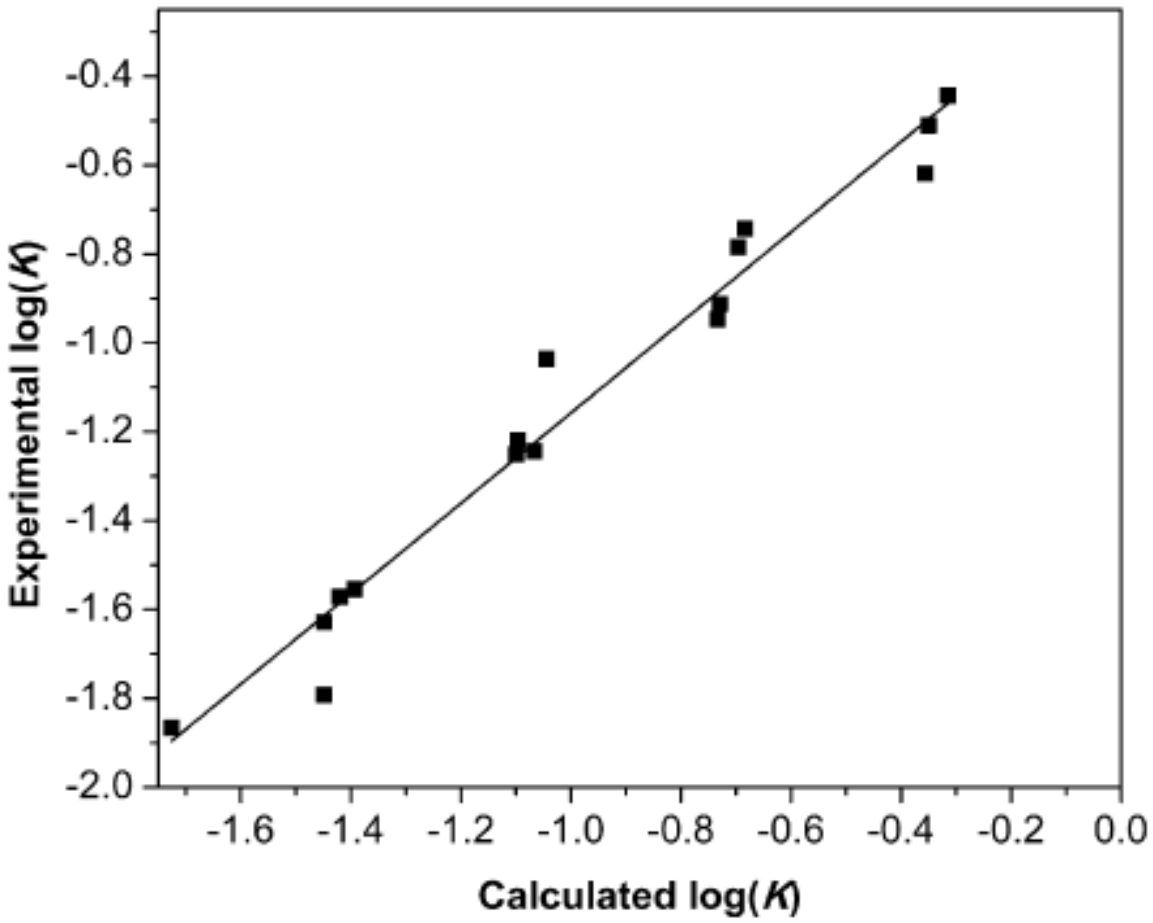

Figure 3-2. Experimental vs calculated values of log(K) for the fluorous esters **3a**–**d** partitioning from ethanol to the fluorous solvents. The points represent the averages of duplicate or triplicate measurements.

.

We are not aware of measurements of diffusion coefficients of large molecules in fluorous solvents. The diffusion coefficients of solutes in the membrane solvents can be calculated from the measured partition coefficients (K) and permeabilities (P) corrected by porosity (ϕ) as shown in Eq. 3-4.

$$D = {}^{P}/_{K\emptyset}$$

Equation 3-4

Table 3-5 shows these diffusion coefficients in the four perfluorinated solvents. We used a value for the porosity of 0.28 determined by voltammetry at the interface between two immiscible electrolyte solutions (ITIES)[190], which is a very similar system to ours. As for the partition coefficients, it would be helpful to have evidence that an established approach can predict the diffusion coefficients. We have used the Stokes-Einstein equation. The radius of each solute was calculated from the molar volume based on the group increment method[208]. The calculated diffusion coefficients are listed in Table 4, along with the experimental values. Here, we would like to point out the influence of the experimental error on our results. The average relative error for the diffusion coefficients were calculated from those for the permeability and partition coefficients. Both of the latter errors were about 10%. Therefore, the average relative error of the diffusion coefficients is about 15%. The solutes containing longer perfluoroalkyl groups gave us less relative error for permeability and partition coefficients compared to those with shorter perfluoroalkyl groups. Considering these errors, the agreement between the calculated and experimental values is satisfactory, especially for the solutes with longer perfluoroalkyl tags.

Table 3-5. Diffusion coefficients for the **1**-modified 100 nm membranes.

Solute	FC-77		PF-5080		FC-3283		FC-43	
	D_{exp}[a] (/10^{-6} cm^2/s)	D_{cal} (/10^{-6} cm^2/s)	D_{exp}[a] (/10^{-6} cm^2/s)	D_{cal} (/10^{-6} cm^2/s)	D_{exp}[a] (/10^{-6} cm^2/s)	D_{cal} (/10^{-6} cm^2/s)	D_{exp}[a] (/10^{-6} cm^2/s)	D_{cal} (/10^{-6} cm^2/s)
3a	6.6	4.4	5.7	4.1	4.8	4.1	2.2	1.1
3b	6.0	4.2	5.2	3.9	3.8	3.9	1.7	1.0
3c	4.5	4.0	3.9	3.7	3.4	3.7	1.4	1.0
3d	3.8	3.8	3.4	3.6	2.4	3.5	1.1	0.9

[a] Porosity adopted here is 0.28[190].

SLMs have been used widely for separation of ions or small organic molecules from aqueous or organic mixtures[210-214]. Hydrophobic SLMs based on organic solvents are the most common type. Carriers are typically dissolved into the membrane liquid to improve the separation selectivity. To our knowledge, there are no reports of FSLMs. We can compare range of permeabilities of the FSLMs reported here to a similar system, a mineral oil filled octadecyltrimethyoxylsilane(ODS) modified alumina membrane[215]. The investigators applied this system to the transport of small organic solutes such as phenol and its relatives. The permeabilities they achieved were in the range of ~10^{-7} cm^2/s. The permeabilities reported here for our FSLMs for larger solutes are comparable. We have previously investigated transport through films of Teflon AF2400. Permeabilities of small organic solutes were about an order of magnitude smaller than the permeabilities mentioned above in the mineral oil SLM[160]. Hence, the FSLMs appears to provide permeabilities that are greater than or at least equal to the ODS modified SLMs and the Teflon AF2400 membranes.

3.5 CONCLUSION

We have demonstrated that the modified alumina membranes impregnated with perfluorinated solvent are effective fluorous membranes. The increase of the organic domain of the solute molecules significantly decreases the permeabilities for the identical length of fluorous tag. Lengthening the perfluoroalkyl chain on the solutes shows a strong influence on the permeability and partition coefficients. The free energy of a $–CF_2–$ group from ethanol into the four perfluorinated solvents is -1.1 kJ/mol. Diffusion coefficients were calculated from the measured permeabilities and partition coefficients. The Stokes-Einstein equation was also used to estimate

the diffusion coefficients in the membrane solvents. A group contribution approach was used to determine the molar volume, and thus the effective molecular radius for the Stokes-Einstein equation. Satisfactory agreement was achieved for all solutes in each perfluorinated solvent.

4.0 PREPARATION AND ASSESSMENT OF FLUOROUS ALUMINA MEMBRANES AS SOLID REACTION SUPPORTS

4.1 ABSTRACT

We report fluorous alumina membranes as cation exchanger. Simply dipping Krytox 157FSH (**1**)-modified alumina membranes into FC-72 solution containing Krytox 157FSH results in the deposition of Krytox 157FSH due to the interactions between fluorous chains. FTIR and membrane mass measurements show that the concentration of Krytox 157FSH solution significantly influences the loading of Krytox 157FSH. The adsorption reaches equilibrium in less than 30 seconds. FTIR spectra show that the carbonyl frequency of adsorbed Krytox 157FSH decreases from 1775 cm^{-1} to 1678 cm^{-1} after the membrane was washed by water. The identical membrane was then soaked in methanol, THF, chloroform and hexanes. A constant carbonyl region is achieved which qualitatively demonstrates that there is no observed loss for adsorbed Krytox 157FSH. Preliminary study showed that the fluorous alumina membranes with adsorbed Krytox 157FSH successfully capture $Ru(bpy)_3^{2+}$ ions from aqueous solutions. The stoichiometry of the complex is that one $Ru(bpy)_3^{2+}$ ion binds to two ionic Krytox 157FSH, which indicates that all adsorbed Krytox 157FSH are reactive.

4.2 INTRODUCTION

Heterogeneous reactions based on solid supports have been widely used in catalysis, drug discovery, combinatorial and high through-put chemistry[216-228]. The basic protocol is to immobilize reagents, catalysts or scavengers onto a solid support, which facilitates easy purification and separation. Noncovalent immobilization provides high reaction efficiency since covalent attachment possible hinders reaction sites. In addition, noncovalent immobilization affords the flexibility of the choice of supporting materials and simplifies the support fabrication[229]. Perfluoroalkyl tags are readily attached to catalysts, which can be immobilized on a fluorous support. The protocol has been widely used due to easy isolation of products and catalytic recycling. For example, perfluorinated metal catalyst (palladium and rhodium) was immobilized to perfluoroalkylated silica gel for organic synthesis[230-232]. Fluorous Lewis acids were employed for Baeyer-Villiger oxidization and Diels-Alder reactions in water[233]. Schmaderer *et al.* attached perfluoroalkyl tagged flavins to fluorous silica gel for photo-oxidizing benzoyl alcohols[234]. Perfluoroalkylated polystyrene resins were fabricated as the solid supports for hydrogenation of styrene and Suzuki-Miyaura carbon-carbon bond formation[235]. Schwinn *et al.* extended the application by attaching fluorous reagent (perfluorinated benzoyl alcohol) rather than catalyst to fluorous silica gel for combinatory library synthesis without the need of perfluorinated solvents[236]. The immobilizations in those applications are based on short perfluoroalkyl chains (generally C_8F_{17} or shorter) of solid surface and tagged reagents or catalysts, which possibly results in the loss of immobilized reagents, due to the solubility in organic solvents.

Krytox 157FSH (**1**) is a perfluoropolyether (repeating unit ≈ 33) with a carboxylic acid terminal group, which have been used to modify porous alumina membranes. We initiated to

immobilize another Krytox 157FSH layer on the **1**-modified alumina membrane by the interactions between two perfluoropolyether chains. The perfluorinated chain would ensure adsorbed Krytox 157FSH (**A-1**) to stay on the **1**-modified membrane, forming **A-1**-modified membrane, as shown in Figure 4-1. Moreover, the terminal carboxyl group of Krytox 157FSH broadens the applications of the fluorous supports. O'Neal *et al.* showed that Krytox 157FSH is able to form complexes with basic pyridines and porphyrins[126-128]. Proteins and enzymes can be captured by carboxylate ion group through ion-pair interactions[130-132]. In addition, the carboxyl group enables to produce the amide bonds in the presence of 1-ethyl-3-[3-dimethylaminopropyl]carbodiimide hydrochloride (EDC) and N-hydroxysulfosuccinimide (sulfo-NHS)[237, 238]. Moreover, the ether oxygen of Krytox 157FSH provides more chain flexibility than rigid perfluoroalkanoic acids, which leads to high solubility in fluorous solvents[239]. Therefore, we can easily desorb **A-1** or related products by washing with perfluorinated solvents.

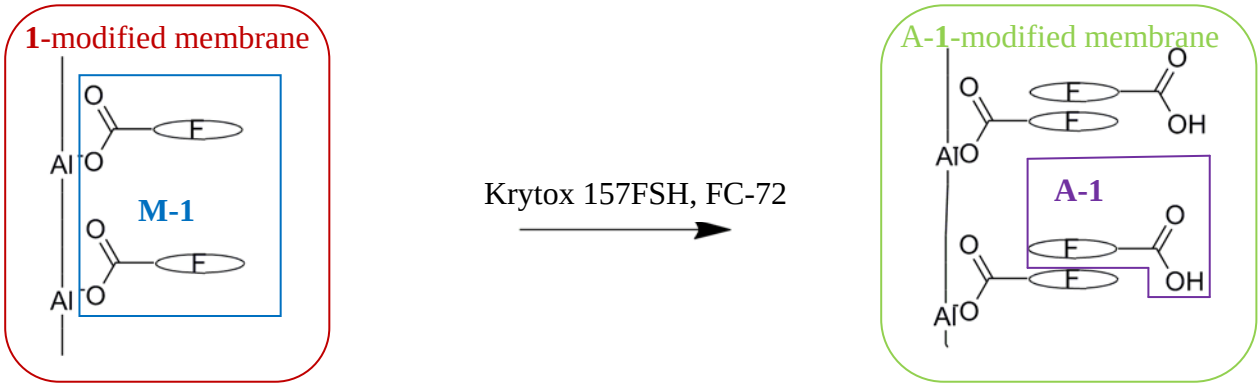

$$= CF_3 - CF_2 - CF_2 - O - \left[CF\left(CF_3\right)CF_2 - O - \right]_n CF\left(CF_3\right)$$

Figure 4-1. Schematic fabrication of **A-1**-modified membrane. Dark red square represents **1**-modified alumina membrane. Dark blue square means the modification layer from surface reaction of Krytox 157FSH with the hydroxyl groups on the alumina membrane surface. Green square represents the **1**-modifed membrane with adsorbed Krytox 157FSH that is shown as purple square.

In this chapter, we investigated the adsorption and desorption of Krytox 157FSH on **1**-modified membranes. **A-1**-modified membranes were used to capture $Ru(bpy)_3^{2+}$ ions to demonstrate the reactivity of the carboxyl groups. $Ru(bpy)_3Cl_2$ (Figure 4-2) has strong UV-Vis absorption and fluorescence, which is easily observed.

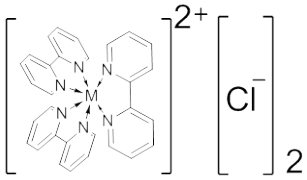

Figure 4-2. Structure of $Ru(bpy)_3Cl_2$

4.3 EXPERIMENTAL SECTION

4.3.1 Chemicals and materials

All the chemicals, unless specified otherwise, were obtained from Aldrich (Milwaukee, WI) or Sigma (St. Louis, MO). Krytox 157FSH with a carboxylic acid terminal group was obtained from Miller-Stephenson Chemical Co. (Morton Grove, IL). Alumina membranes (100 nm pore size, 13 mm diameter and 60 μm thickness) were purchased from Whatman (Florham Park, NJ). Hydrofluoroether-7100 (HFE-7100) (a mixture of methyl nonafluorobutyl and nonafluoroisobutyl ethers) was obtained from 3M (Minneapolis, MN). FC-72 Fluoroinert Electronic Liquid (a mixture of perfluorohexanes) was purchased from 3M (Minneapolis, MN). Tris(2,2'-bipyridyl)ruthenium(II) chloride hexahydrate was bought from Fluka (Milwaukee, WI).

4.3.2 A-1-modified membrane fabrication

Krytox 157FSH (**1**)-modified 100 nm porous alumina membranes were prepared as in previous studies[175, 200]. The **1**-modified membrane was submerged in different concentration of Krytox 157FSH/FC-72 solution for variable time and then air dried. Pure FC-72 solvent was used to desorb **A-1**. The membrane masses before and after soaking were measured by a XS105 DualRange analytical balance (Mettler Toledo, Columbus, OH) to calculate the loading of **A-1** on the **1**-modified membrane. FTIR (Excalibur FTS 3000, Varian, Randolph, MA) was employed to analyze **A-1**-modified membrane with the spectrum of **1**-modified membrane as reference. The peak areas were integrated by the software (Varian Resolution Pro 4.0, Varian, Randolph, MA) after manually defining the baseline.

4.3.3 Solvent stability

A piece of **A-1**-modified membrane was submerged in five mL of water for 30 minutes. The membrane was removed from water and allowed to dry in air for 20 minutes. FTIR spectra were recorded with **1**-modified membrane as reference. The same membrane was then similarly soaked in methanol, tetrahydrofuran, chloroform and hexanes, respectively and FTIR spectra were measured.

4.3.4 Ion exchange experiments

A **1**-modified 100 nm alumina membrane was submerged in 22 mM Krytox 157FSH in FC-72 solution for five minutes. After solvent evaporated, the membrane was transferred into a vial

containing 0.21 mM $Ru(bpy)_3Cl_2$ aqueous solution. The vial was put into a BioShaker (Model MBR-022 UP, made by Taitec and distributed by Bionexus, Inc., Oakland, CA) overnight at 25 °C and 350 rpm. Membrane masses were recorded at each step. A SpectraMax M2 microplate reader (Molecular Devices, Sunnyvale, CA) was employed to measure the visible absorbance (452 nm) and fluorescence (E_m = 611 nm, E_x = 452 nm) of $Ru(bpy)_3Cl_2$ solution in UV-transparent microplates. Figure 4-3 shows the visible spectrum of 0.021 mM $Ru(bpy)_3Cl_2$ solution and fluorescent spectrum excited at 452 nm. Up to four mL pure FC-72 (one mL each time) was used to desorb the complex of **A**-**1** and $Ru(bpy)_3^{2+}$ in the Bioshaker at 25 °C under 350 rpm for half an hour. The unmodified alumina membrane and **1**-modified membranes were similarly treated as control experiments.

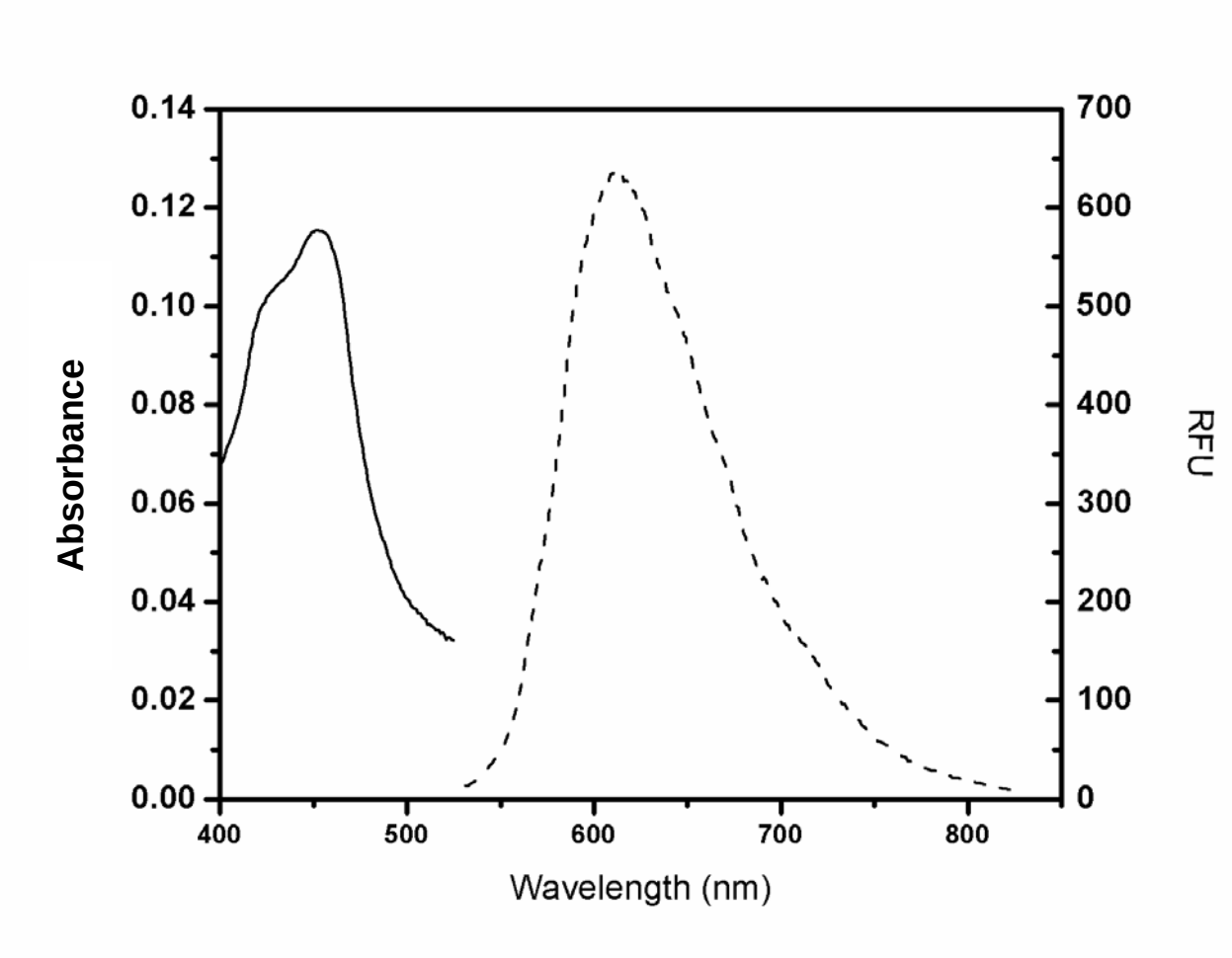

Figure 4-3. Representative UV-Vis (—, left axis) and fluorescent spectra (····, right axis, E_x = 452 nm) of 0.021 mM $Ru(bpy)_3Cl_2$ aqueous solution.

4.3.5 Derivatization of A-1-modified alumina membranes

A piece of 100 nm alumina membrane was surface modified by Krytox 157FSH (**1**), according to previous experiments[175, 200]. The **1**-modified membrane was soaked in 1 mL of a mixture of 20 mM Krytox 157FSH/FC-72 solution for five minutes. The resultant membrane was transferred into 4 mL of oxalyl chloride and stirred at 62 °C for 24 hours. Dry THF was used to wash the membrane. Excess solvent was evaporated under vacuum. The membrane was heated to reflux in

five mL of dry THF with one μL of Boc-NH($CH_2CH_2O)_2$-$CH_2CH_2NH_2$ (**6**) for 48 hours. The reactant solution was cooled to room temperature. The membrane was rinsed by dry THF as well as dioxane and dried under vacuum. Six mL of a mixture of 4M HCl/dioxane solution was stirred with the membrane at 25°C and 350 rpm by the Bioshaker for 5 hours to cleave the Boc protecting group. The product membrane was rinsed by dioxane and dried under vacuum. The amount of functional groups (-NH_2) was measured with the Kaiser test. In addition, the membrane was weighed at each step. The whole procedure is summarized in Scheme 4-1.

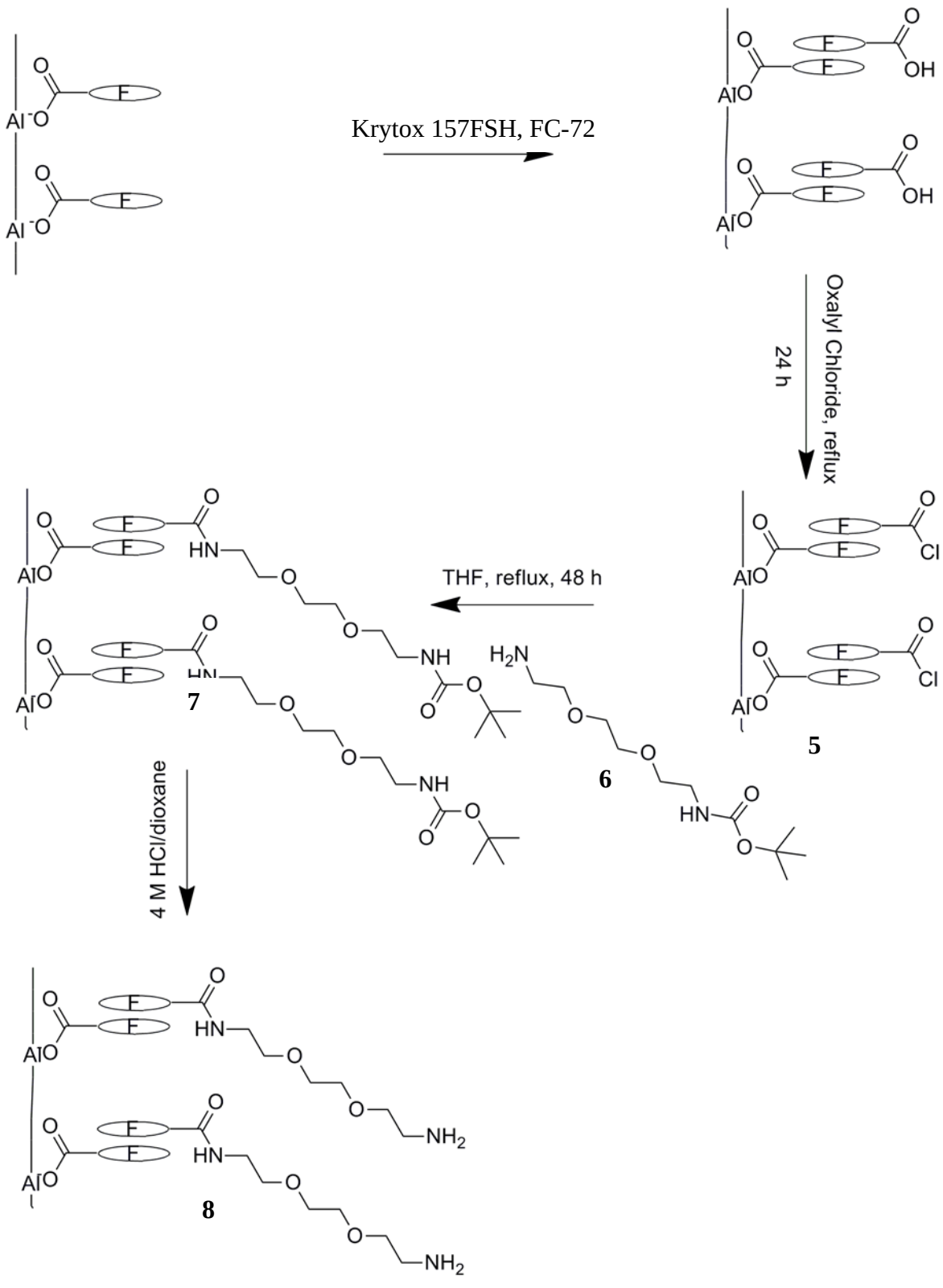

Scheme 4-1. Derivatize **A-1**-modified alumina membrane

4.4 RESULTS AND DISCUSSION

4.4.1 Validating Krytox 157FSH on 1-modified alumina membrane

Following the adsorption of Krytox 157FSH on the **1**-modified membranes, FTIR was employed to demonstrate the existence of **A-1**. Figure 4-4 shows the representative spectra of **A-1**-modified membrane (black line) with **1**-modified membrane as reference. The vibration in the range of 1200 – 1400 cm^{-1} demonstrates the appearance of the C-F stretch from the perfluoropolyether chain of **A-1**. More importantly, the vibration centered at 1774 cm^{-1} shows the characteristic stretch of carbonyl groups due to the **A-1**, which is rescaled and inserted into Figure 4-4. Specifically, Krytox 157FSH exists in dimer form[126]. The green spectrum in Figure 4-4 represents the **A-1**-membrane after soaking with pure FC-72 for five minutes. Adsorbed Krytox 157FSH dissolves into FC-72 solvent. Therefore, both vibrations at 1774 cm^{-1} and 1200 – 1400 cm^{-1} disappear, as expected. Moreover, no negative peak is observed in the range of 1200 – 1400 cm^{-1} indicating that FC-72 dissolves **A-1** on the membrane rather than the modification layer from previous chemical modification. Those observations show that the simple immobilization of the reagents (Krytox 157FSH) to the solid support and the removal of the final products are simple.

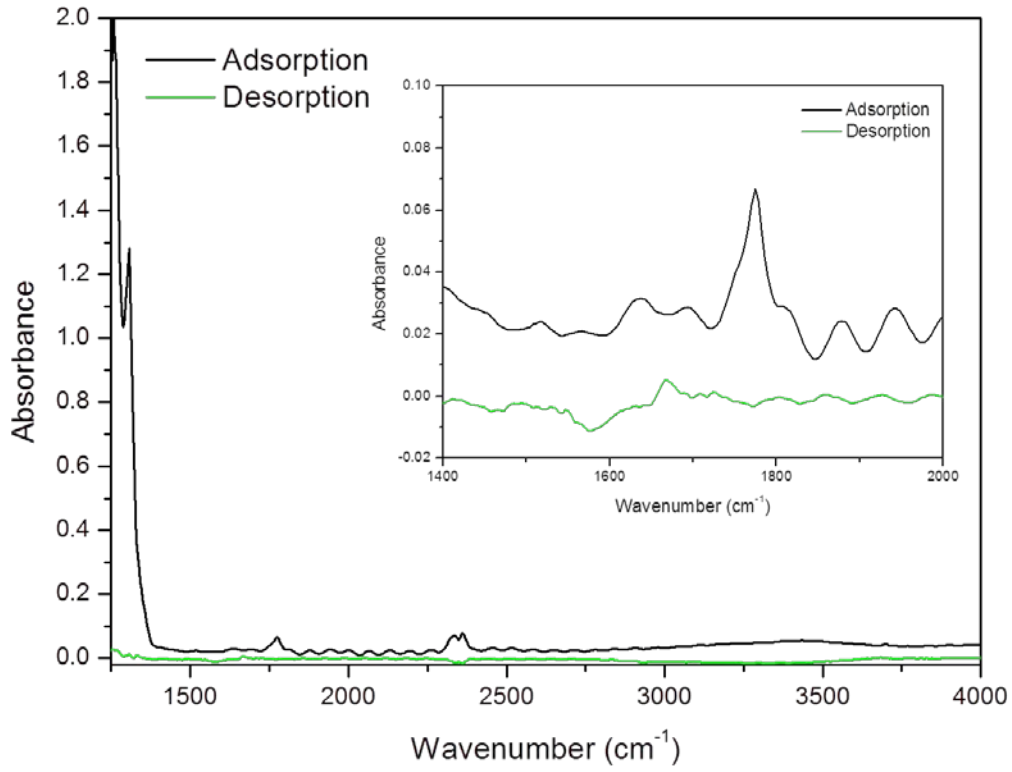

Figure 4-4. Representative FTIR spectra for **1**-modified 100 nm alumina membrane with Krytox 157FSH adsorption (—) and desorption by FC-72 (—). The **1**-modified 100 nm alumina membranes were used as reference.

4.4.2 A-1-modified membrane preparation conditions

After validating Krytox 157FSH adsorption on the **1**-modified membranes, the influences of the concentrations of Krytox157FSH solution and soaking time were investigated by FTIR. Only carbonyl vibrations are shown in Figure 4-5 for the **A-1**-modified membranes, since the adsorption in the C-F stretch is too intense to be used for quantitative analysis.

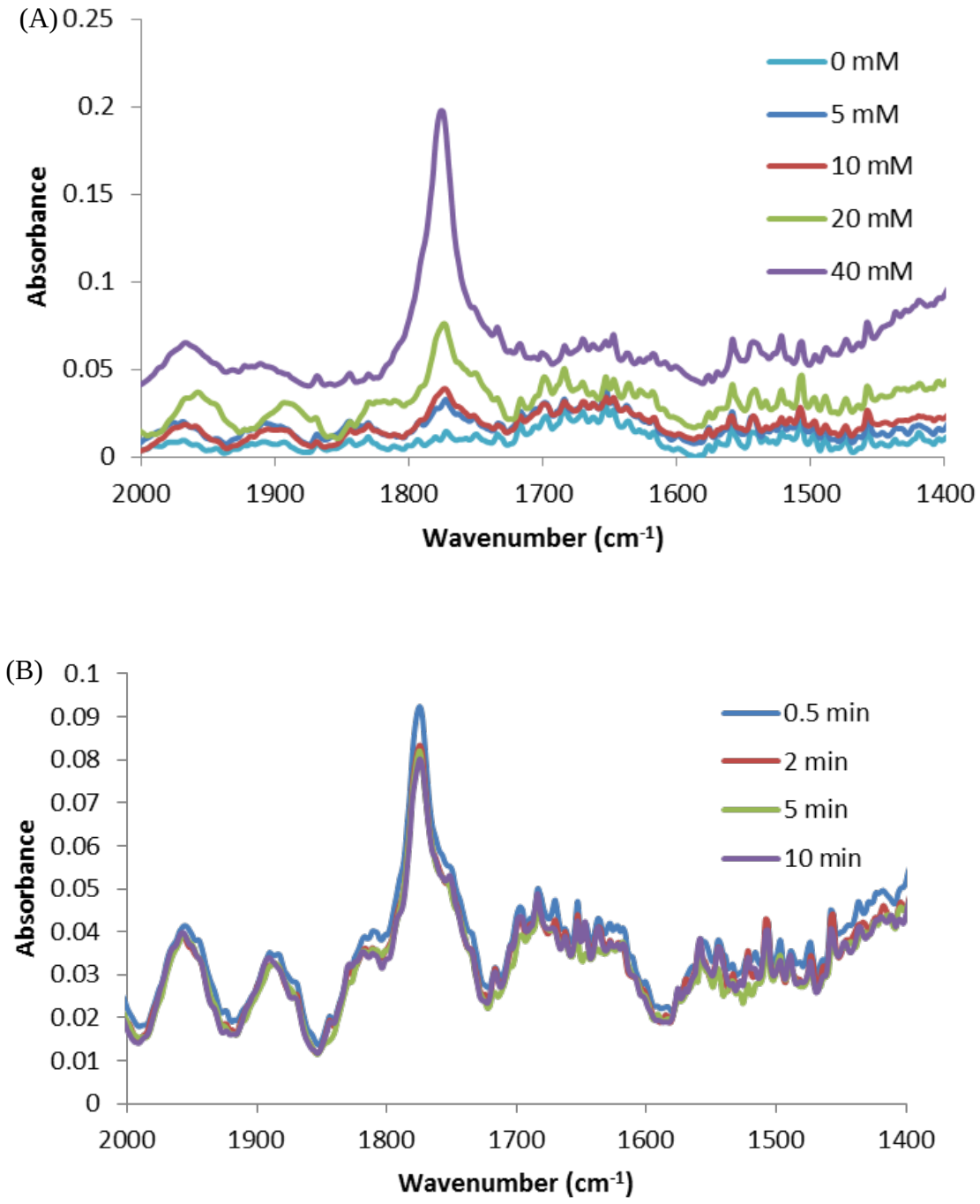

Figure 4-5. Representative FTIR spectrum for **A-1**-modified membranes under (A)variable concentration of FC-72 solutions containing Krytox 157FSH with 0 mM (—)5 mM (—), 10 mM (—), 20 mM (—) as well as 40 mM (—), and (B) at different soaking time of 0.5 min (—), 2 min (—), 5 min (—) as well as 10 min (—).Only carbonyl region is shown. **1**-modified fluorous membranes were used as reference.

Meanwhile, the loading of **A-1** on the **1**-modified membranes are measured and summarized in Table 4-1, along with the carbonyl peak areas. Figure 4-5 shows that the carbonyl stretch vibrates at 1775 cm^{-1}, indicating that Krytox 157FSH are dimers. In addition, the peak in Figure 4-5A increases while more concentrated Krytox 157FSH solution is used. Table 4-1 details the loading of Krytox 157FSH by integrating the peak areas and mass measurements. Similar increasing trend with the concentration of FC-72 solution is observed by two measurements. Moreover, the continuously increasing peak implies that adsorbed Krytox 157FSH accumulates on the membrane pore wall and surface. This observation provides a convenient way to calculate the loading of immobilized reagents. Figure 4-4B and Table 4-1shows there is no significant amount change of the loading of **A-1** down to 30 second soaking. This indicates that the adsorption of Krytox 157FSH reaches equilibrium in less than half minute. In addition, shorter submerging time is not used due to the practical issue.

Table 4-1. FTIR peak area of carbonyl stretch and adsorbed Krytox 157FSH weight[a]

Conditions		Peak area[b]	Loading amount (mol)
Concentration	5 mM	0.535	3.4×10^{-8}
	10 mM	0.835	8.9×10^{-8}
	20 mM	1.607	1.9×10^{-7}
	40 mM	4.356	4.3×10^{-7}
Soaking time	0.5 min	1.757	2.3×10^{-7}
	2 min	1.637	2.3×10^{-7}
	5 min	1.673	2.2×10^{-7}
	10 min	1.647	2.1×10^{-7}

[a] All data are from single experiment.

[b] The spectra were taken with **1**-modified membrane as reference. The peak area was integrated with manually defined baseline.

4.4.3 A-1-modified membrane stability following exposure to solvents

As a good membrane support, **A**-**1** should stay on the **1**-modified membrane under various solvent conditions. To demonstrate the solvent stability, the FTIR spectra of an **A**-**1**-modified membrane were determined following submersion in water followed by air drying. Data are shown in Figure 4-6. A second band at 1680 ~ 1700 cm^{-1} appears while the intensity at 1775 cm^{-1} decreases. This results from ionization of the carboxylic acid. Moreover, the organic solvents studied do not influence the carbonyl stretch after the **A**-**1**-modified membrane is soaked in

water. The decreased carbonyl frequency indicates that absorbed Krytox 157FSH changes from acid-acid dimer to carboxylate due to the strong acidity of Krytox 157FSH resulting from the electrophilic property of fluorine. Obviously, the organic solvents studied are poor proton sources so the carboxylate (with adventitious counterions from water) is stable. More importantly, the approximately constant carboxylate carbonyl stretch area implies that **A-1** is securely adsorbed on to the modified membranes while in contact with water, methanol, tetrahydrofuran, chloroform and hexanes. The **A-1**-modified membranes appear stable in typically used organic solvents.

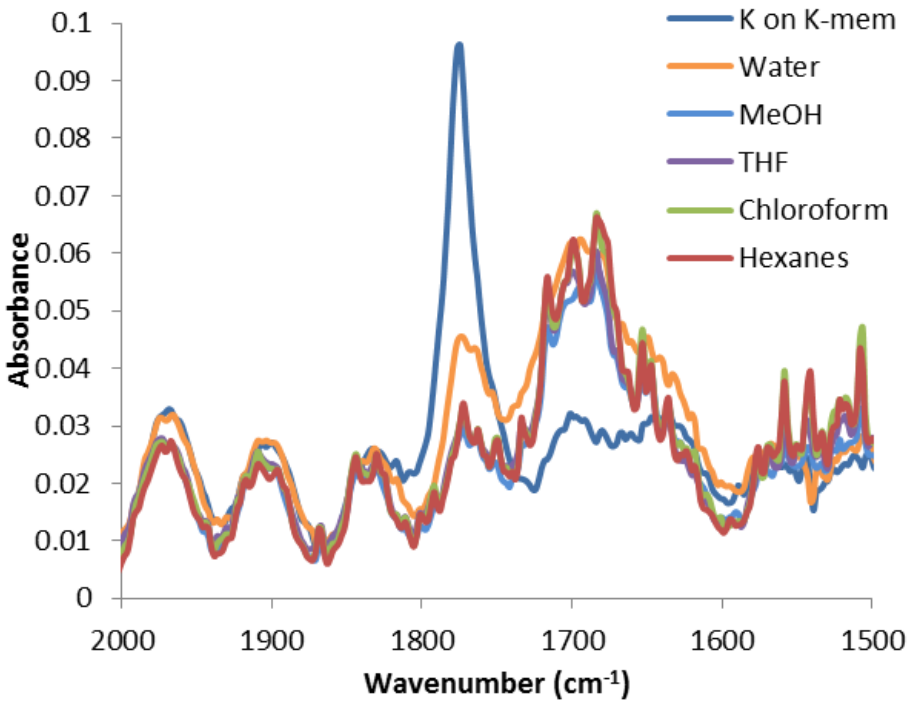

Figure 4-6. Representative FTIR spectra of Krytox 157FSH on Krytox-membrane after washing by H2O (—), methanol (—), THF (—), chloroform (—) and hexanes (—). The dark blue line (—) was Krytox 157FSH before soaking into the solvents. Only carbonyl region is shown. The Krytox-modified membrane was used as reference.

4.4.4 Ion exchange membranes: preliminary study

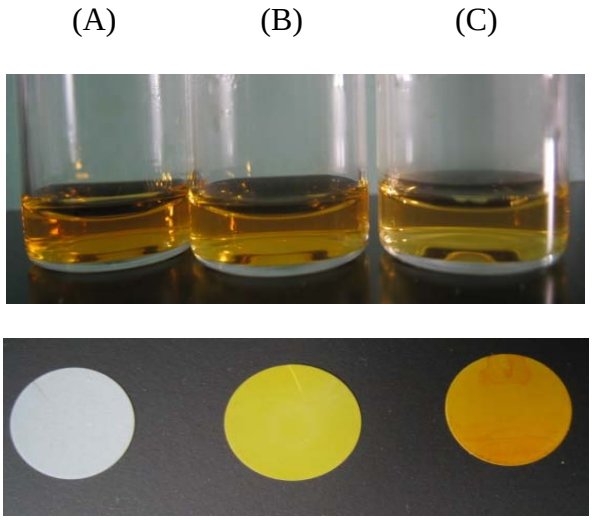

Figure 4-7. Photographs of aqueous $Ru(bpy)_3Cl_2$ solutions (upper row) after overnight soaking with unmodified alumina membrane (A, lower row), Krytox modified membrane in absence of Krytox 157FSH (B, lower row) and Krytox modified membrane in presence of Krytox 157FSH (C, lower row).

Table 4-2. A-1 and $Ru(bpy)_3^{2+}$ loading on different membranes

Membrane	Loading amount[a] (mol)	
	A-1	$Ru(bpy)_3^{2+}$
unmodified membrane	-	-
1-modified membrane	-	0.4×10^{-7}
A-1-modified membrane	2.3×10^{-7}	1.7×10^{-7}

[a] All measurements are single experiments.

We have demonstrated that **A-1** changes to ionic form while in contact with water, which indicates that the membranes are used as ion exchange membranes. Figure 4-7 represents each

membrane (lower row) and $Ru(bpy)_3Cl_2$ aqueous solutions (upper row) after the exchange experiments. The unmodified membrane has no visible color change resulting from the ion exchange. Light yellow membrane is observed for the **1**-modified membrane, while dark yellow membrane is obtained for the **A-1**-modified membrane, as shown in Figure 4-7. Correspondingly, there is no obvious color change for the solution after soaking with unmodified and **1**-modified membranes (upper row of Figure 4-7). Light yellow aqueous solution is achieved, in which the **A-1**-modified membrane was soaked. This observation shows that the unmodified and **1**-modified membranes are unable to efficiently capture $Ru(bpy)_3^{2+}$ ions from aqueous solutions. The **A-1**-modified membrane significantly exchanges $Ru(bpy)_3^{2+}$ due to the presence of **A-1**. In addition, the loading of adsorbed Krytox 157FSH on the **1**-modified membrane can be calculated from the mass gain after dipping in FC-72 solution. Table 4-2 shows that 2.3×10^{-7} moles of Krytox 157FSH are absorbed onto the **1**-modified membrane. The captured $Ru(bpy)_3^{2+}$ ions by **A-1**-modified membrane are around 1.7×10^{-7} moles, while the **1**-modified membrane adsorbs 0.4×10^{-7} moles of metal ions. Hence, 1.3×10^{-7} moles of $Ru(bpy)_3^{2+}$ ions form complexes with the **A-1**. The calculation shows that two adsorbed Krytox 157FSH captures one $Ru(bpy)_3^{2+}$ ions.

Furthermore, the spectroscopic data of those aqueous solutions are measured after exchanging with $Ru(bpy)_3^{2+}$ ions. The concentration of $Ru(bpy)_3^{2+}$ in aqueous solution is reduced due to the exchange by the ionic Krytox 157FSH on the **A-1**-modified membrane. The amount of $Ru(bpy)_3^{2+}$ ions extracted to the membranes can be calculated from the decreased concentrations. Table 4-3 summarizes the extracted $Ru(bpy)_3^{2+}$ amounts determined by the UV-Vis adsorption and fluorescence. Both measurements provide similar results. Fluorescence and absorbance experiments show that 1.2×10^{-7} moles of ions are captured from aqueous phase to the **A-1**-

modified membranes. Few amount of $Ru(bpy)_3^{2+}$ is extracted by **1**-modified membrane in both measurements. From the difference of the extracted amounts, we can obtain the number of $Ru(bpy)_3^{2+}$ that forms the complex with **A**-1 (1.0×10^{-7} mole), which approaches the theoretical stoichiometry (1.2×10^{-7} mole). Hence, the **1**-modified membrane with Krytox 157FSH loaded is successfully demonstrated as ion exchange membranes. Moreover, the preliminary quantitative analysis shows that the exchanging reaches the theoretical stoichiometry.

Table 4-3. Amounts of $Ru(bpy)_3^{2+}$ extracted to membranes from 0.21 mM $Ru(bpy)_3Cl_2$ aqueous solution [a]

Membrane	Amount extracted to membrane (mol)	
	Absorbance	Fluorescence
A-1-modified membrane	1.2×10^{-7}	1.2×10^{-7}
1-modified membrane	0.3×10^{-7}	0.2×10^{-7}
Unmodified membrane	0.0×10^{-7}	0.0×10^{-7}

[a] All measurements are single experiment.

Pure FC-72 has been demonstrated to desorb **A-1** without destroying the modification layer. Therefore, we readily dipped the membranes into FC-72 to remove the Krytox 157FSH-$Ru(bpy)_3$ complexes. Figure 4-8 shows that clear white FC-72 solution is observed for the unmodified membrane because no $Ru(bpy)_3^{2+}$ ions are exchanged. **1**-modified membrane produces clear white FC-72 solution due to the low concentration of $Ru(bpy)_3^{2+}$ ions in FC-72. The dark yellow FC-72 solution from the **A-1**-modified membrane further demonstrates the success of ion exchanging, as shown in the upper row of Figure 4-8. Meanwhile, almost similar membranes are achieved for **1**-modified and **A-1**-modified membranes (Figure 4-8B and C). Therefore, FC-72 easily removes the Krytox 157FSH or the complex with ions or other product.

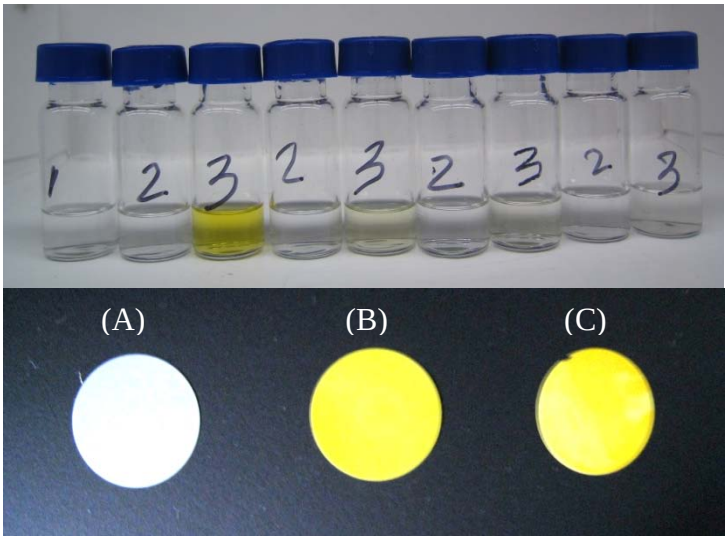

Figure 4-8. Photographs of Krytox 157FSH-Ru(bpy)$_3$ solutions (upper row) after soaking with one mL FC-72 solvent for four times. *1* represents the unmodified membrane (A); *2* indicates the Krytox modified membrane in absence of Krytox 157FSH, (B) and *3* showed the Krytox modified membrane in presence of Krytox 157FSH (C). The lower row indicated the images of the corresponding membranes soaking with four mL FC-72, except (A) the unmodified membrane, for which one mL FC-72 used.

4.4.5 Derivatizing A-1-modified membranes

Table 4-4. Measured membrane masses at each reaction step of Scheme 4-1

Membrane conditions	Membrane mass (mg)
A-1-modified membrane	11.45
5	11.37
7	10.96
8	6.53 (overnight hydrolysis) 9.24 (5 h hydrolysis)[a]

[a] The initial mass of **A-1**-modified membrane was 11.36 mg.

Oxalyl chloride is a typical reagent to improve the reactivity of carboxyl acid by forming acyl chloride. Therefore, we employed oxalyl chloride to activate the adsorbed Krytox 157FSH. After activating the carbonyl acid groups, Boc protecting amine, **6** was used to introduce nucleophilic amine groups by hydrolyzing Boc groups. The presence of amines provides diversity and flexibility to the membrane supports. However, the observed yield is around 4% determined by the Kaiser test for duplicate reactions. For simplicity, the membrane mass was measured at each step to figure out the reason to low yield. Table 4-4 lists the results throughout the reactions. No significant mass loss is observed before the hydrolysis step (**7**). However, product **8** shows less mass than the initial membrane. This indicates that the mixture of 4M HCl in dioxane destroys the membrane, and hence results in the low yield. In addition, longer hydrolysis time (overnight) brings out more membrane loss compared to five hour hydrolysis time, which confirms that the membrane is ruined by the HCl solution. The unmodified membrane fully dissolves over

weekend incubation with 4M HCl/dioxane (not shown in Table 4-4). Therefore, mild reaction conditions are required to keep the membrane stable. Aqueous solution would be a good choice as reaction solvent.

4.5 CONCLUSION

We have demonstrated the noncovalent immobilization of fluorous reagent (Krytox 157FSH) to Krytox 157FSH chemically modified alumina membranes. The membranes show good solvent stability due to the heavy perfluoropolyether chain of Krytox 157FSH. The ion exchanging with $Ru(bpy)_3^{2+}$ cations demonstrates that all Krytox 157FSH are active.

APPENDIX A

MODIFICATION SETUP

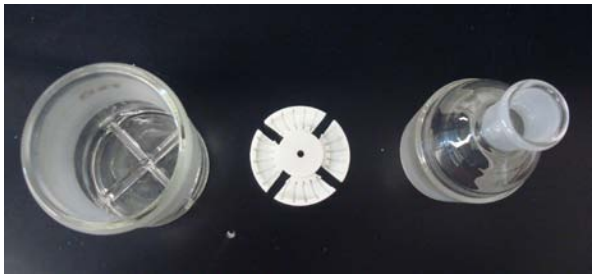

Figure A-1. Setup for modifying 13 mm alumina membranes. The left one is the flat-bottom flask to hold the Teflon rack (the middle one), which is used to vertically mount alumina membranes with the diameter of 13 mm. The right one is the adaptor connecting to the Liebig condenser.

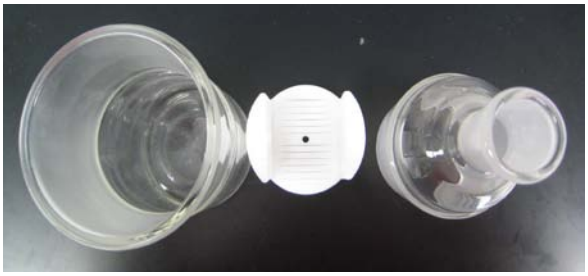

Figure A-2. Setup for modifying 47 mm alumina membranes. The left one is the flat-bottom flask to hold the Teflon rack (the middle one), which is used to vertically mount alumina membranes with the diameter of 47 mm. The right one is the adaptor connecting to the Liebig condenser.

Figure A-3. Photograph of the flat-bottom flask connecting with the Liebig condenser sitting in a heater with sand.

APPENDIX B

DEPENDENCE OF WATER CONTACT ANGLE

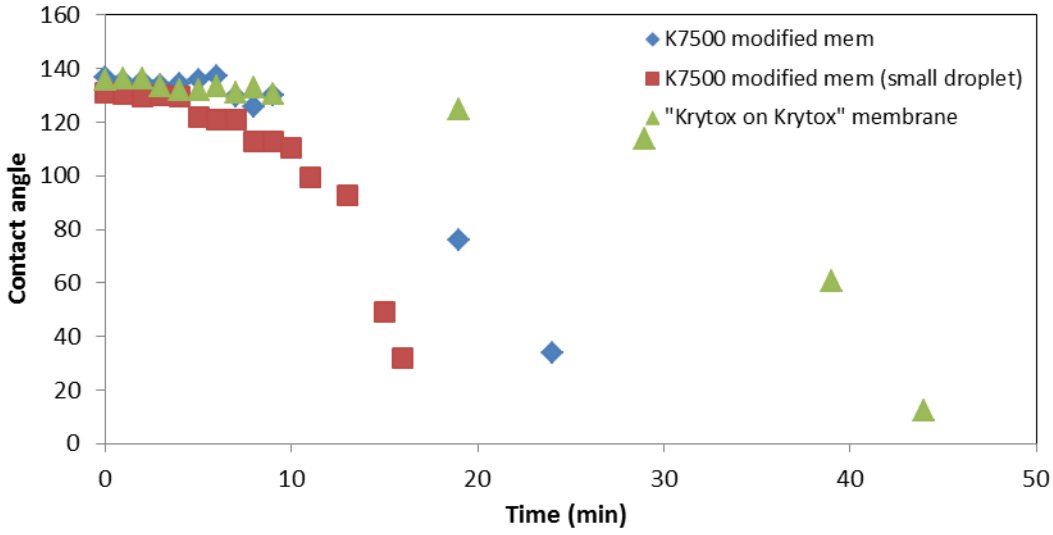

Figure B-1. Time dependence of water contact angles of "Krytox on Krytox" membrane (▲), Krytox-modified membrane (♦) and Krytox-modified membrane (■) measured with small water droplet.

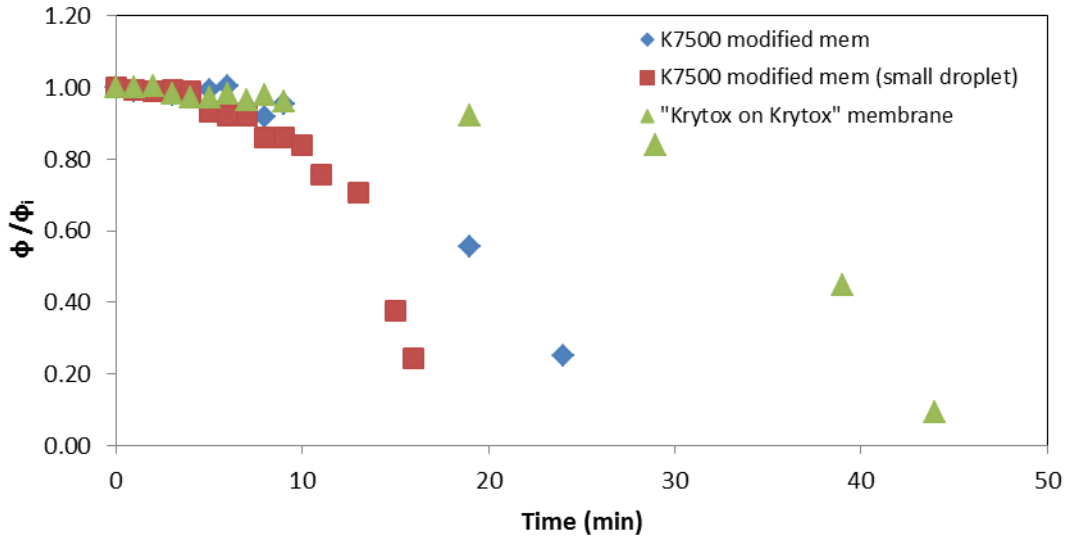

Figure B-2. Time dependence of water contact angle ratio to initial measurement of "Krytox on Krytox" membrane (▲), Krytox-modified membrane (♦) and Krytox-modified membrane (■) measured with small water droplet on time.

APPENDIX C

KINETIC STUDY OF CARBONYL STRETCH CHANGE OF KRYTOX ON KRYTOX MEMBRANE WASHED BY WATER

A piece of "Krytox on Krytox" membrane was soaked in water saturated with Krytox 157FSH overnight. FTIR measured the carbonyl stretch after slightly wiping out the water on the surface with Krytox-modified membrane as reference.

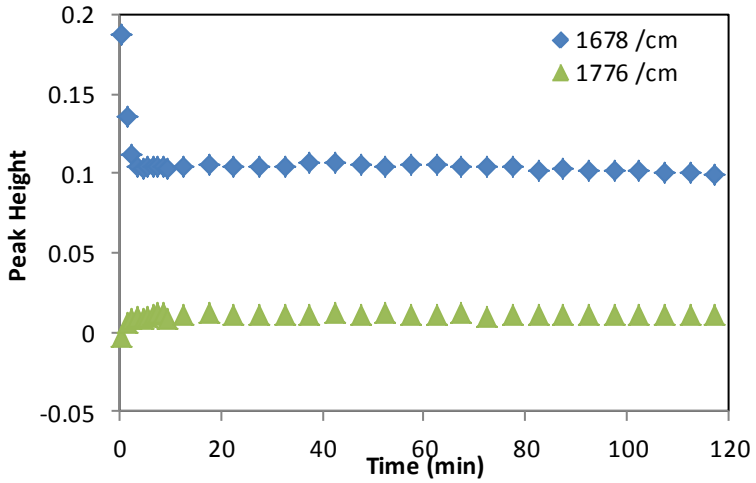

Figure C-1. Time dependence of FTIR vibrational peak height at 1678 cm^{-1} (♦) and 1776 cm^{-1} (▲). The peak height was calculated based on the left baseline (2000 cm^{-1}) and right baseline (1533 cm^{-1}). The decreased peak height at 1678 cm^{-1} and the increased peak height at 1776 cm^{-1} indicate the transfer of Krytox 157FSH from carboxylates to dimers resulting from water evaporation. The transfer reaches equilibrium in 10 minutes and results in the flatten part at both wavenumbers.

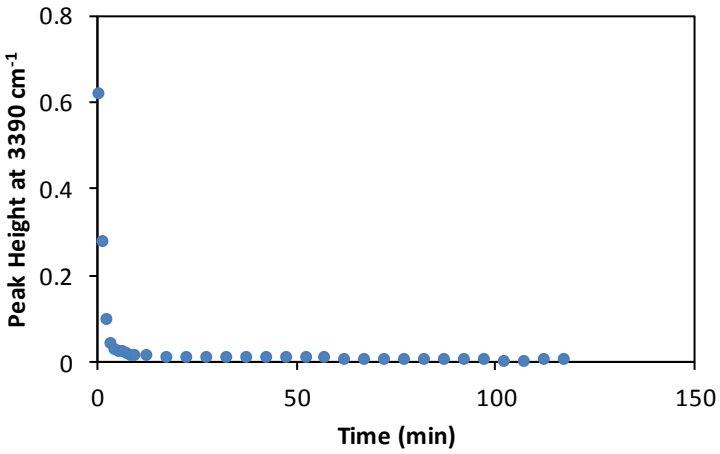

Figure C-2. Time dependence of FTIR vibrational peak height of hydroxyl stretch at 3390 cm^{-1} (●). The peak height was calculated based on the left baseline (3806 cm^{-1}) and right baseline (2605 cm^{-1}). The peak height decreases at the beginning due to water evaporation and reaches equilibrium in 10 minutes.

BIBLIOGRAPHY

1. Baker, R. W., Membrane gas-separation: applications. *Membr. Oper.* **2009**, 167-194.
2. Bernardo, P.; Drioli, E.; Golemme, G., Membrane Gas Separation: A Review/State of the Art. *Ind. Eng. Chem. Res.* **2009,** 48, (10), 4638-4663.
3. Murphy, T. M.; Offord, G. T.; Paul, D. R., Fundamentals of membrane gas separation. *Membr. Oper.* **2009**, 63-82.
4. Vorotyntsev, V. M.; Drozdov, P. N.; Vorotyntsev, I. V.; Smirnov, K. Y., Nitrous oxide high purification by membrane gas separation. *Inorg. Mater.* **2009,** 45, (11), 1263-1266.
5. Athanasekou, C. P.; Romanos, G. E.; Kordatos, K.; Kasselouri-Rigopoulou, V.; Kakizis, N. K.; Sapalidis, A. A., Grafting of alginates on UF/NF ceramic membranes for wastewater treatment. *J. Hazard. Mater.* **2010,** 182, (1-3), 611-623.
6. Cassini, A. S.; Tessaro, I. C.; Marczak, L. D. F.; Pertile, C., Ultrafiltration of wastewater from isolated soy protein production: a comparison of three UF membranes. *J. Cleaner Prod.* **2009,** 18, (3), 260-265.
7. Coskun, T.; Debik, E.; Demir, N. M., Treatment of olive mill wastewaters by nanofiltration and reverse osmosis membranes. *Desalination* **2010,** 259, (1-3), 65-70.
8. Mortaheb, H. R.; Zolfaghari, A.; Mokhtarani, B.; Amini, M. H.; Mandanipour, V., Study on removal of cadmium by hybrid liquid membrane process. *J. Hazard. Mater.* **2010,** 177, (1-3), 660-667.
9. Canselier, J. P., Surfactants in pollution removal and environmental protection. *Comun. Jorn. Com. Esp. Deterg.* **2007,** 37, 221-233.
10. Paez-Hernandez, M. E.; Ramirez-Silva, M. T.; Galan-Vidal, C. A., Environmental applications of liquid membranes. *Appl. Anal. Chem. Environ. Res.* **2005**, 189-201.
11. Parizek, T.; Bebar, L.; Stehlik, P., Persistent pollutants emission abatement in waste-to-energy systems. *Clean Technol. Environ. Policy* **2008,** 10, (2), 147-153.
12. Rahimpour, M. R.; Mazinani, S.; Vaferi, B.; Baktash, M. S., Comparison of two different flow types on CO removal along a two-stage hydrogen permselective membrane reactor for methanol synthesis. *Appl. Energy* **2011,** 88, (1), 41-51.
13. Kim, S.; Yan, J.; Schwenzer, B.; Zhang, J.; Li, L.; Liu, J.; Yang, Z.; Hickner, M. A., Cycling performance and efficiency of sulfonated poly(sulfone) membranes in vanadium redox flow batteries. *Electrochem. Commun.* **2010,** 12, (11), 1650-1653.
14. Shi, J.-L.; Yao, Z.-K.; Wang, T.; Zhu, B.-K., Membrane formation via thermally induced phase separation in HDPE/PMP/diluent system for lithium-ion battery. *Polym. Prepr. (Am. Chem. Soc., Div. Polym. Chem.)* **2010,** 51, (1), 636-637.
15. Yufit, V.; Brandon, N. P., Development and application of an actively controlled hybrid proton exchange membrane fuel cell-lithium-ion battery laboratory test-bed based on off-the-shelf components. *J. Power Sources* **2011,** 196, (2), 801-807.

16. Baroutian, S.; Aroua, M. K.; Raman, A. A. A.; Sulaiman, N. M. N., Methanol recovery during transesterification of palm oil in a TiO2/Al2O3 membrane reactor: Experimental study and neural network modeling. *Sep. Purif. Technol.* **2010,** 76, (1), 58-63.
17. Benard, S.; Giroir-Fendler, A.; Vernoux, P.; Guilhaume, N.; Fiaty, K., Comparing monolithic and membrane reactors in catalytic oxidation of propene and toluene in excess of oxygen. *Catal. Today* **2010,** 156, (3-4), 301-305.
18. Gbenedio, E.; Wu, Z.; Hatim, I.; Kingsbury, B. F. K.; Li, K., A multifunctional Pd/alumina hollow fibre membrane reactor for propane dehydrogenation. *Catal. Today* **2010,** 156, (3-4), 93-99.
19. Kingsbury, B. F. K.; Wu, Z.; Li, K., A morphological study of ceramic hollow fibre membranes: A perspective on multifunctional catalytic membrane reactors. *Catal. Today* **2010,** 156, (3-4), 306-315.
20. Fang, J.-Y.; Hung, C.-F.; Chi, C.-H.; Chen, C.-C., Transdermal permeation of selegiline from hydrogel-membrane drug delivery systems. *Int. J. Pharm.* **2009,** 380, (1-2), 33-39.
21. Gotter, B.; Faubel, W.; Neubert, R. H. H., Photothermal imaging in 3D surface analysis of membrane drug delivery. *Eur. J. Pharm. Biopharm.* **2010,** 74, (1), 26-32.
22. Kim, M. S.; Lee, D. S., Biodegradable and pH-sensitive polymersome with tuning permeable membrane for drug delivery carrier. *Chem. Commun. (Cambridge, U. K.)* **2010,** 46, (25), 4481-4483.
23. Majumder, M.; Stinchcomb, A.; Hinds, B. J., Towards mimicking natural protein channels with aligned carbon nanotube membranes for active drug delivery. *Life Sci.* **2010,** 86, (15-16), 563-568.
24. Xiang, A.; Ma, D.; McHugh, A. J., The interplay of phase inversion, polymer membrane formation, and drug release in a membrane-based delivery system. *J. Membr. Sci.* **2010,** 358, (1-2), 85-92.
25. DiFazio, F. A.; Nichols, J. B.; Pope, M. H.; Frymoyer, J. W., The use of expanded polytetrafluoroethylene as an interpositional membrane after lumbar laminectomy. *Spine (Phila Pa 1976)* **1995,** 20, (9), 986-991.
26. Greenawalt, K.; Masi, L.; Muir, C.; Burns, J., The physical properties of a hyaluronic acid based bioresorbable membrane for the prevention of post-surgical adhesions. *Mater. Res. Soc. Symp. Proc.* **1993,** 292, (Biomolecular Materials), 265-269.
27. Seibel, D. R.; McCandless, F. P., Separation of sulfur dioxide and nitrogen by permeation through a sulfolane plasticized vinyliidene fluoride film. *Ind. Eng. Chem., Process Des. Develop.* **1974,** 13, (1), 76-78.
28. Zavaleta, R.; McCandless, F. P., Selective permeation through modified polyvinylidene fluoride membranes. *J. Membr. Sci.* **1976,** 1, 333-353.
29. Liao, B. Q.; Bagley, D. M.; Kraemer, H. E.; Leppard, G. G.; Liss, S. N., A review of biofouling and its control in membrane separation bioreactors. *Water Environ. Res.* **2004,** 76, (5), 425-436.
30. Mansouri, J.; Harrisson, S.; Chen, V., Strategies for controlling biofouling in membrane filtration systems: challenges and opportunities. *J. Mater. Chem.* **2010,** 20, (22), 4567-4586.
31. Julbe, A.; Rouessac, V.; Durand, J.; Ayral, A., New approaches in the design of ceramic and hybrid membranes. *J. Membr. Sci.* **2008,** 316, (1-2), 176-185.

32. Tsuru, T.; Kondo, H.; Yoshioka, T.; Asaeda, M., Organic/inorganic nanohybrid membranes for nanofiltration of nonaqueous solutions. *Mater. Res. Soc. Symp. Proc.* **2003,** 752, (Membranes--Preparation, Properties and Applications), 97-102.
33. Kai, T.; Suma, Y.; Ono, S.; Yamaguchi, T.; Nakao, S.-I., Effect of the pore surface modification of an inorganic substrate on the plasma-grafting behavior of pore-filling-type organic/inorganic composite membranes. *J. Polym. Sci., Part A Polym. Chem.* **2005,** 44, (2), 846-856.
34. Kikukawa, T.; Kuraoka, K.; Kawabe, K.; Yamashita, M.; Fukumi, K.; Hirao, K.; Yazawa, T., Stabilities and pore size effect of proton-conducting organic-inorganic hybrid membranes prepared through surface modification of porous glasses. *J. Membr. Sci.* **2005,** 259, (1-2), 161-166.
35. Keller, F.; Hunter, M. S.; Robinson, D. L., Structural Features of Oxide Coatings on Aluminum. *J. Electrochem. Soc.* **1953,** 100, (9), 411-419.
36. Hoar, T. P.; Mott, N. F., A mechanism for the formation of porous anodic oxide films on aluminium. *J. Phys. Chem. Solids* **1959,** 9, (2), 97-99.
37. Thompson, G. E.; Furneaux, R. C.; Wood, G. C.; Richardson, J. A.; Goode, J. S., Nucleation and growth of porous anodic films on aluminium. *Nature* **1978,** 272, (5652), 433-435.
38. O'Sullivan, J. P.; Wood, G. C., The Morphology and Mechanism of Formation of Porous Anodic Films on Aluminium. *P. Roy. Soc. Lond. A. Mat.* **1970,** 317, (1531), 511-543.
39. Thormann, A.; Teuscher, N.; Pfannmöller, M.; Rothe, U.; Heilmann, A., Nanoporous Aluminum Oxide Membranes for Filtration and Biofunctionalization. *Small* **2007,** 3, (6), 1032-1040.
40. Itaya, K.; Sugawara, S.; Arai, K.; Saito, S., Properties of porous anodic aluminum oxide films as membranes. *J. Chem. Eng. Jpn.* **1984,** 17, (5), 514-520.
41. Asaeda, M.; Luong Dinh, D.; Fuji, M., Separation of alcohol/water gaseous mixtures by an improved ceramic membrane. *J. Chem. Eng. Jpn.* **1986,** 19, (1), 84-85.
42. Sano, T.; Iguchi, N.; Iida, K.; Sakamoto, T.; Baba, M.; Kawaura, H., Size-exclusion chromatography using self-organized nanopores in anodic porous alumina. *Appl. Phys. Lett.* **2003,** 83, (21), 4438-4440.
43. Ma, C.; Yeung, E. S., Entrapment of Individual DNA Molecules and Nanoparticles in Porous Alumina Membranes. *Anal. Chem. (Washington, DC, U. S.)* **2009,** 82, (2), 654-657.
44. Kuroda, K., Effect of the surface charge on the adsorption and permeation of ions to aluminum anode oxidized film. *Hyomen* **1992,** 30, (12), 1030-1041.
45. Osmanbeyoglu, H. U.; Hur, T. B.; Kim, H. K., Thin alumina nanoporous membranes for similar size biomolecule separation. *J. Membr. Sci.* **2009,** 343, (1-2), 1-6.
46. Chen, W.; Yuan, J.-H.; Xia, X.-H., Characterization and Manipulation of the Electroosmotic Flow in Porous Anodic Alumina Membranes. *Anal. Chem.* **2005,** 77, (24), 8102-8108.
47. Bluhm, E. A.; Schroeder, N. C.; Bauer, E.; Fife, J. N.; Chamberlin, R. M.; Abney, K. D.; Young, J. S.; Jarvinen, G. D., Surface effects on metal ion transport across porous alumina membranes. 2. Trivalent cations: Am, Tb, Eu, and Fe. *Langmuir* **2000,** 16, (17), 7056-7060.

48. Bluhm, E. A.; Bauer, E.; Chamberlin, R. M.; Abney, K. D.; Young, J. S.; Jarvinen, G. D., Surface Effects on Cation Transport across Porous Alumina Membranes. *Langmuir* **1999,** 15, (25), 8668-8672.
49. Yamashita, T.; Kodama, S.; Kemmei, T.; Ohto, M.; Nakayama, E.; Muramoto, T.; Yamaguchi, A.; Teramae, N.; Takayanagi, N., Separation of adenine, adenosine-5'-monophosphate and adenosine-5'-triphosphate by fluidic chip with nanometre-order diameter columns inside porous anodic alumina using an aqueous mobile phase. *Lab Chip* **2009,** 9, (10), 1337-1339.
50. Kakiage, K.; Kyomen, T.; Unno, M.; Hanaya, M., Molecular-selective adsorption property of chemically surface modified nanoporous alumina membrane by di(1-naphthyl)silanediol to anthracenes. *Appl. Organomet. Chem.* **2010,** 24, (3), 198-200.
51. Leger, C.; Lira, H. D. L.; Paterson, R., Preparation and properties of surface modified ceramic membranes. Part II. Gas and liquid permeabilities of 5 nm alumina membranes modified by a monolayer of bound polydimethylsiloxane (PDMS) silicone oil. *J. Membr. Sci.* **1996,** 120, (1), 135-146.
52. Yamaguchi, A.; Uejo, F.; Yoda, T.; Uchida, T.; Tanamura, Y.; Yamashita, T.; Teramae, N., Self-assembly of a silica-surfactant nanocomposite in a porous alumina membrane. *Nat. Mater.* **2004,** 3, (5), 337-341.
53. Yamashita, T.; Kodama, S.; Ohto, M.; Nakayama, E.; Hasegawa, S.; Takayanagi, N.; Kemmei, T.; Yamaguchi, A.; Teramae, N.; Saito, Y., Permeation flux of organic molecules through silica-surfactant nanochannels in a porous alumina membrane. *Anal. Sci.* **2006,** 22, (12), 1495-1500.
54. Yoo, S.; Ford, D. M.; Shantz, D. F., Synthesis and Characterization of Uniform Alumina-Mesoporous Silica Hybrid Membranes. *Langmuir* **2006,** 22, (4), 1839-1845.
55. Xomeritakis, G.; Liu, N. G.; Chen, Z.; Jiang, Y. B.; Koehn, R.; Johnson, P. E.; Tsai, C. Y.; Shah, P. B.; Khalil, S.; Singh, S.; Brinker, C. J., Anodic alumina supported dual-layer microporous silica membranes. *J. Membr. Sci.* **2007,** 287, (2), 157-161.
56. Yamaguchi, A.; Kajijo, T.; Teramae, N., Synthesis of mesoporous silica inside a columnar macropore. *Zeoraito* **2007,** 24, (4), 118-124.
57. Yamaguchi, A.; Mekawy, M. M.; Chen, Y.; Suzuki, S.; Morita, K.; Teramae, N., Diffusion of Metal Complexes Inside of Silica-Surfactant Nanochannels within a Porous Alumina Membrane. *J. Phys. Chem. B* **2008,** 112, (7), 2024-2030.
58. Odom, D. J.; Baker, L. A.; Martin, C. R., Solvent-Extraction and Langmuir-Adsorption-Based Transport in Chemically Functionalized Nanopore Membranes. *J. Phys. Chem. B* **2005,** 109, (44), 20887-20894.
59. Ge, D.; Shen, Y.; Shi, W.; Zhang, Q. Preparation of compatible gelatin-epoxy silane-anodic alumina composite membrane for protein separation. 2007-10009960 101254415, 20071207., **2008**.
60. Shi, W.; Shen, Y.; Ge, D.; Ma, Y.; Wu, D.; Zhang, Q. Preparation process of affinity chitosan-amino silane-anodic alumina composite membrane. 2008-10071236 101288830, 20080617., **2008**.
61. Shi, W.; Shen, Y.; Ge, D.; Zhang, Q. Preparation of compatible gelatin-amino silane-anodic alumina composite membrane for protein separation. 2007-10009962 101254416, 20071207., **2008**.

62. Wu, J. P.; Brown, I. W. M.; Bowden, M. E.; Kemmitt, T., Palladium coated porous anodic alumina membranes for gas reforming processes. *Solid State Sci.* **2010,** 12, (11), 1912-1916.
63. Itoh, N.; Tomura, N.; Tsuji, T.; Hongo, M., Deposition of palladium inside straight mesopores of anodic alumina tube and its hydrogen permeability. *Microporous Mesoporous Mater.* **2000,** 39, (1-2), 103-111.
64. Kajiwara, M.; Uemiya, S.; Kojima, T.; Kikuchi, E., Rhodium- and iridium-dispersed porous alumina membranes and their hydrogen permeation properties. *Catal. Today* **2000,** 56, (1-3), 83-87.
65. Lin, X.; Ham, A. S. W.; Villani, N. A.; Lye, W.-k.; Huang, Q.; Lawrence, M. B.; Helmke, B. P.; Reed, M. L., Fabrication of nanoscale hydrophobic regions on anodic alumina for selective adhesion of biologic molecules. *Mater. Res. Soc. Symp. Proc.* **2003,** 773, (Biomicroelectromechanical Systems (BioMEMS)), 25-30.
66. Inguanta, R.; Amodeo, M.; D'Agostino, F.; Volpe, M.; Piazza, S.; Sunseri, C., Developing a procedure to optimize electroless deposition of thin palladium layer on anodic alumina membranes. *Desalination* **2006,** 199, (1-3), 352-354.
67. Inguanta, R.; Amodeo, M.; D'Agostino, F.; Volpe, M.; Piazza, S.; Sunseri, C., Preparation of Pd-coated anodic alumina membranes for gas separation media. *J. Electrochem. Soc.* **2007,** 154, (3), D188-D194.
68. Sun, J.; Xu, R.; Zhang, Y.; Ma, M.; Gu, N., Magnetic nanoparticles separation based on nanostructures. *J. Magn. Magn. Mater.* **2007,** 312, (2), 354-358.
69. Ott, A. W.; Klaus, J. W.; Johnson, J. M.; George, S. M.; McCarley, K. C.; Way, J. D., Modification of Porous Alumina Membranes Using Al2O3 Atomic Layer Controlled Deposition. *Chem. Mater.* **1997,** 9, (3), 707-714.
70. Xiong, G.; Elam, J. W.; Feng, H.; Han, C. Y.; Wang, H.-H.; Iton, L. E.; Curtiss, L. A.; Pellin, M. J.; Kung, M.; Kung, H.; Stair, P. C., Effect of Atomic Layer Deposition Coatings on the Surface Structure of Anodic Aluminum Oxide Membranes. *J. Phys. Chem. B* **2005,** 109, (29), 14059-14063.
71. Zhang, S.; Cheng, F.; Tao, Z.; Gao, F.; Chen, J., Removal of nickel ions from wastewater by Mg(OH)2/MgO nanostructures embedded in Al2O3 membranes. *J. Alloys Compd.* **2006,** 426, (1-2), 281-285.
72. Xu, W.-H.; Kyotani, T.; Tomita, A.; Yokoyama, Y.; Inahara, J.; Touhara, H., Properties of chemically modified carbon-coated membranes prepared from anodic aluminum oxide films. *Carbon'01, Int. Conf. Carbon* **2001**, 884-885.
73. Chang, C.-S.; Suen, S.-Y., Modification of porous alumina membranes with n-alkanoic acids and their application in protein adsorption. *J. Membr. Sci.* **2006,** 275, (1-2), 70-81.
74. Brevnov, D. A.; Barela, M. J.; Brooks, M. J.; Lopez, G. P.; Atanassov, P. B., Fabrication of Anisotropic Super Hydrophobic/Hydrophilic Nanoporous Membranes by Plasma Polymerization of C4F8 on Anodic Aluminum Oxide. *J. Electrochem. Soc.* **2004,** 151, (8), B484-B489.
75. Jain, P.; Sun, L.; Dai, J.; Baker, G. L.; Bruening, M. L., High-Capacity Purification of His-tagged Proteins by Affinity Membranes Containing Functionalized Polymer Brushes. *Biomacromolecules* **2007,** 8, (10), 3102-3107.
76. Liabres i Xamena, F. X.; Teruel, L.; Alvaro, M.; Garcia, H., Donor/conductor/acceptor triads spatially organized on the micrometer-length scale: an alternative approach to photovoltaic cells. *Chem.--Eur. J.* **2007,** 13, (2), 515-519.

77. Losic, D.; Cole, M. A.; Dollmann, B.; Vasilev, K.; Griesser, H. J., Surface modification of nanoporous alumina membranes by plasma polymerization. *Nanotechnology* **2008,** 19, (24), 245704/1-245704/7.
78. Shi, W.; Shen, Y.; Ge, D.; Xue, M.; Cao, H.; Huang, S.; Wang, J.; Zhang, G.; Zhang, F., Functionalized anodic aluminum oxide (AAO) membranes for affinity protein separation. *J. Membr. Sci.* **2008,** 325, (2), 801-808.
79. Tenhaeff, W. E.; Gleason, K. K., Surface-Tethered pH-Responsive Hydrogel Thin Films as Size-Selective Layers on Nanoporous Asymmetric Membranes. *Chem. Mater.* **2009,** 21, (18), 4323-4331.
80. Vlassiouk, I.; Krasnoslobodtsev, A.; Smirnov, S.; Germann, M., "Direct" Detection and Separation of DNA Using Nanoporous Alumina Filters. *Langmuir* **2004,** 20, (23), 9913-9915.
81. Zha, F. F.; Fane, A. G.; Fell, C. J. D., Phenol removal by supported liquid membranes. *Sep. Sci. Technol.* **1994,** 29, (17), 2317-43.
82. Le, Q. T. H.; Ehler, D. S.; McCleskey, T. M.; Dye, R. C.; Pesiri, D. R.; Jarvinen, G. D.; Sauer, N. N., Ultrathin gates for the transport of phenol from supported liquid membranes to permanent surface modified membranes. *J. Membr. Sci.* **2002,** 205, (1-2), 213-222.
83. Barghi, S. H.; Adibi, M.; Rashtchian, D., An experimental study on permeability, diffusivity, and selectivity of CO2 and CH4 through [bmim][PF6] ionic liquid supported on an alumina membrane: Investigation of temperature fluctuations effects. *J. Membr. Sci.* **2010,** 362, (1-2), 346-352.
84. Kirchner, A.; MacKenzie, K. J. D.; Brown, I. W. M.; Kemmitt, T.; Bowden, M. E., Structural characterisation of heat-treated anodic alumina membranes prepared using a simplified fabrication process. *J. Membr. Sci.* **2007,** 287, (2), 264-270.
85. Lee, C.-W.; Kang, H.-S.; Chang, Y.-H.; Hahm, Y.-M., Thermotreatment and chemical resistance of porous alumina membrane prepared by anodic oxidation. *Korean J. Chem. Eng.* **2000,** 17, (3), 266-272.
86. Khan, M. I.; Wang, X.; Bozhilov, K. N.; Ozkan, C. S., Electrochemical fabrication of InSb nanowires using porous alumina membrane and their characterization. *Mater. Res. Soc. Symp. Proc.* **2008,** 1080E, (Semiconductor Nanowires), No pp given, Paper #: 1080-O08-09.
87. Brown, I. W. M.; Bowden, M. E.; Kemmitt, T.; MacKenzie, K. J. D., Structural and thermal characterisation of nanostructured alumina templates. *Curr. Appl Phys* **2006,** 6, (3), 557-561.
88. Zaman, J.; Chakma, A., Inorganic membrane reactors. *J. Membr. Sci.* **1994,** 92, (1), 1-28.
89. Kormann, H.-P.; Schmid, G.; Pelzer, K.; Philippot, K.; Chaudret, B., Gas Phase Catalysis by Metal Nanoparticles in Nanoporous Alumina Membranes. *Z. Anorg. Allg. Chem.* **2004**, 630, (12), 1913-1918 .
90. Omata, K.; Masuda, A.; Ishii, H.; Suzuki, H.; Yamada, M., Artificial neural network aided screening for membrane disc catalysts for oxidative reforming of methane. *Appl. Catal., A* **2009,** 362, (1-2), 14-19.
91. Takai, A.; Saida, T.; Sugimoto, W.; Wang, L.; Yamauchi, Y.; Kuroda, K., Preparation of mesoporous Pt-Ru alloy fibers with tunable compositions via evaporation-mediated direct templating (EDIT) method utilizing porous anodic alumina membranes. *Chem. Mater.* **2009,** 21, (14), 3414-3423.

92. Lee, H. J.; Yasukawa, T.; Suzuki, M.; Lee, S. H.; Yao, T.; Taki, Y.; Tanaka, A.; Kameyama, M.; Shiku, H.; Matsue, T., Simple and rapid preparation of vertically aligned gold nanoparticle arrays and fused nanorods in pores of alumina membrane based on positive dielectrophoresis. *Sens. Actuators, B* **2009,** B136, (2), 320-325.
93. Joo, S. W.; Banerjee, A. N., FESEM studies of densely packed aligned nickel nanopillars on silicon substrate by electrochemical deposition through porous alumina membrane. *Mater. Sci. Eng., B* **2010,** 175, (1), 36-40.
94. Li, C.; Wang, X.; Chen, G.; He, L.; Cao, H., Fabrication of Ni/Al2O3 core-shell nanowire arrays in porous alumina membranes. *Chem. Lett.* **2010,** 39, (1), 64-65.
95. Liu, C.-J.; Chen, S.-Y.; Shih, L.-J.; Huang, H.-J., Fabrication of nanotubules of thermoelectric gamma -Na0.7CoO2 using porous aluminum oxide membrane as supporting template. *Mater. Chem. Phys.* **2010,** 119, (3), 424-427.
96. Shi, G.; Mo, C. M.; Cai, W. L.; Zhang, L. D., Photoluminescence of ZnO nanoparticles in alumina membrane with ordered pore arrays. *Solid State Commun.* **2000,** 115, (5), 253-256.
97. Peng, T.; Yang, H.; Chang, G.; Dai, K.; Hirao, K., Synthesis of bamboo-shaped TiO2 nanotubes in nanochannels of porous aluminum oxide membrane. *Chem. Lett.* **2004,** 33, (3), 336-337.
98. Barreca, D.; Gasparotto, A.; Tondello, E., Gold nanotubes by template-directed synthesis. *J. Nanosci. Nanotechnol.* **2005,** 5, (6), 994-998.
99. Sommerlatte, J.; Cagnon, L.; Bourgault, D.; Goesele, U.; Nielsch, K., Ordered nanowires based on V-VI materials: from synthesis in organic electrolytes to electrical characterization. *Int. Conf. Thermoelectr.* **2008,** 26th, 5-7.
100. Wang, Y.; Shimada, S.; Kiyono, H.; Yamamoto, Y., Preparation and characterization of BN nanotubes with controllable sizes by template-aided synthesis. *Mater. Res. Soc. Symp. Proc.* **2008,** 1081E, (Carbon Nanotubes and Related Low-Dimensional Materials), No pp given.
101. Yanagishita, T.; Fujimura, R.; Nishio, K.; Masuda, H., Preparation of uniform-sized polymer nanofibers by extrusive spinning using ordered anodic porous alumina. *Chem. Lett.* **2010,** 39, (3), 188-189.
102. Zhu, S.; Li, Y.; Zhang, J.; Lue, C.; Dai, X.; Jia, F.; Gao, H.; Yang, B., Biomimetic polyimide nanotube arrays with slippery or sticky superhydrophobicity. *J. Colloid Interface Sci.* **2010,** 344, (2), 541-546.
103. Yang, Z.; Niu, Z., Binary hydrogel nanowires of invertible core/shell phases prepared in porous alumina membranes. *Chem. Commun. (Cambridge, U. K.)* **2002**, (17), 1972-1973.
104. Niu, Z.-w.; Li, D.; Yang, Z.-z., Porous membrane templated synthesis of polymer pillared layer. *Chin. J. Polym. Sci.* **2003,** 21, (3), 381-384.
105. Tchepournaya, I.; Vasilieva, S.; Logvinov, S.; Timonov, A.; Amadelli, R.; Bartak, D., Electrochemical Synthesis and Characterization of Redox Polymer Nanostructures. *Langmuir* **2003,** 19, (21), 9005-9012.
106. Cui, Y.; Tao, C.; Zheng, S.; He, Q.; Ai, S.; Li, J., Synthesis of thermosensitive PNIPAM-co-MBAA nanotubes by atom transfer radical polymerization within a porous membrane. *Macromol. Rapid Commun.* **2005,** 26, (19), 1552-1556.
107. Liu, X.; Xu, F.; Li, Z.; Zhang, W., Photoluminescence of poly(thiophene) nanowires confined in porous anodic alumina membrane. *Polymer* **2008,** 49, (9), 2197-2201.

108. Gonzalez-Rovira, L.; Sanchez-Amaya, J. M.; Lopez-Haro, M.; del Rio, E.; Hungria, A. B.; Midgley, P.; Calvino, J. J.; Bernal, S.; Botana, F. J., Single-Step Process To Prepare CeO2 Nanotubes with Improved Catalytic Activity. *Nano Lett.* **2009,** 9, (4), 1395-1400.
109. Liu, R.; Cho, S. I.; Lee, S. B., Poly(3,4-ethylenedioxythiophene) nanotubes as electrode materials for a high-powered supercapacitor. *Nanotechnology* **2008,** 19, (21), 215710/1-215710/8.
110. Tao, C.; Yang, S.; Zhang, J., Template-synthesized protein nanotubes with controlled size based on layer-by-layer method. *Chin. J. Chem.* **2010,** 28, (2), 325-328.
111. Hildebrand, J. H.; Scott, R. L., *The Solubility of Nonelectrolytes. 3rd ed*. 1950; p 475 pp.
112. Cui, S. T.; Cochran, H. D.; Cummings, P. T., Vapor-Liquid Phase Coexistence of Alkane−Carbon Dioxide and Perfluoroalkane−Carbon Dioxide Mixtures. *J. Phys. Chem. B* **1999,** 103, (21), 4485-4491.
113. Goss, K.-U.; Bronner, G., What Is So Special about the Sorption Behavior of Highly Fluorinated Compounds? *J. Phys. Chem. A* **2006,** 110, (30), 9518-9522.
114. O'Neal, K. L.; Zhang, H.; Yang, Y.; Hong, L.; Lu, D.; Weber, S. G., Fluorous media for extraction and transport. *J. Chromatogr., A* **2010,** 1217, (16), 2287-2295.
115. Horváth, I. T.; Rábai, J., Facile Catalyst Separation Without Water: Fluorous Biphase Hydroformylation of Olefins. *Science* **1994,** 266, (5182), 72-75.
116. de Wolf, E.; Ruelle, P.; van den Broeke, J.; Deelman, B.-J.; van Koten, G., Prediction of Partition Coefficients of Fluorous and Nonfluorous Solutes in Fluorous Biphasic Solvent Systems by Mobile Order and Disorder Theory. *J. Phys. Chem. B* **2004,** 108, (4), 1458-1466.
117. Hildebrand, J. H.; Prausnitz, J. M.; Scott, R. L., *Regular and Related Solutions. The Solubility of Gases, Liquids, and Solids*. 1970; p 228 pp.
118. Gladysz, J. A.; Curran, D. P.; Horvath, I. T.; Editors, *Handbook of Flurorous Chemistry*. 2004; p 594 pp.
119. Curran, D.; Lee, Z., Fluorous techniques for the synthesis and separation of organic molecules. *Green Chem.* **2001,** 3, (1), G3-G7.
120. Curran, D. P., Strategy-Level Separations in Organic Synthesis: From Planning to Practice. *Angew. Chem., Int. Ed.* **1998,** 37, (9), 1174-1196.
121. Wipf, P.; Uto, Y., Total synthesis of the putative structure of the marine metabolite trunkamide A. *Tetrahedron Lett.* **1999,** 40, (28), 5165-5169.
122. Karakhanov, E.; Maksimov, A., Biphasic catalysis in petrochemical processes. *Russ. J. Gen. Chem.* **2009,** 79, (6), 1370-1383.
123. Meng, H.; Kalsani, V.; Kumar, K., Fluorinated Amino Acids and Reagents in Protein Design and Biomolecule Separation. In *Current Fluoroorganic Chemistry*, American Chemical Society: **2007**; 949, 487-499.
124. Dolle, R. E.; Bourdonnec, B. L.; Worm, K.; Morales, G. A.; Thomas, C. J.; Zhang, W., Comprehensive Survey of Chemical Libraries for Drug Discovery and Chemical Biology: 2009. *J. Comb. Chem.* **2010,** 12, (6), 765-806.
125. Krafft, M. P.; Riess, J. G., Perfluorocarbons: life sciences and biomedical uses. Dedicated to the memory of Professor Guy Ourisson, a true RENAISSANCE man. *J. Polym. Sci., Part A Polym. Chem.* **2007,** 45, (7), 1185-1198.
126. Yoder, N. C.; Yüksel, D.; Dafik, L.; Kumar, K., Bioorthogonal noncovalent chemistry: fluorous phases in chemical biology. *Curr. Opin. Chem. Biol.* **2006,** 10, (6), 576-583.

127. O'Neal, K. L.; Weber, S. G., Molecular and Ionic Hydrogen Bond Formation in Fluorous Solvents. *J. Phys. Chem. B* **2009,** 113, (1), 149-158.
128. O'Neal, K. L.; Weber, S. G., Extraction and Metalation of Porphyrins in Fluorous Liquids with Carboxylic Acids and Metal Salts. *J. Phys. Chem. B* **2009,** 113, (21), 7449-7456.
129. Vincent, J.-M., Noncovalent associations in fluorous fluids. *J. Fluorine Chem.* **2008,** 129, (10), 903-909.
130. Hobbs, H. R.; Kirke, H. M.; Poliakoff, M.; Thomas, N. R., Homogeneous Biocatalysis in both Fluorous Biphasic and Supercritical Carbon Dioxide Systems. *Angew. Chem., Int. Ed.* **2007,** 46, (41), 7860-7863.
131. Benaissi, K.; Poliakoff, M.; Thomas, N. R., Solubilisation of alpha -chymotrypsin by hydrophobic ion pairing in fluorous systems and supercritical carbon dioxide and demonstration of efficient enzyme recycling. *Green Chem.* **2010,** 12, (1), 54-59.
132. Shipovskov, S., Homogeneous esterification by lipase from Burkholderia cepacia in the fluorinated solvent. *Biotechnol. Prog.* **2008,** 24, (6), 1262-1266.
133. Zhao, H.; Zhang, J.; Wu, N.; Zhang, X.; Crowley, K.; Weber, S. G., Transport of Organic Solutes through Amorphous Teflon AF Films. *J. Am. Chem. Soc.* **2005,** 127, (43), 15112-15119.
134. Pinnau, I.; Toy, L. G., Gas and vapor transport properties of amorphous perfluorinated copolymer membranes based on 2,2-bistrifluoromethyl-4,5-difluoro-1,3-dioxole/tetrafluoroethylene. *J. Membr. Sci.* **1996,** 109, (1), 125-33.
135. Merkel, T. C.; Bondar, V.; Nagai, K.; Freeman, B. D.; Yampolskii, Y. P., Gas Sorption, Diffusion, and Permeation in Poly(2,2-bis(trifluoromethyl)-4,5-difluoro-1,3-dioxole-co-tetrafluoroethylene). *Macromolecules* **1999,** 32, (25), 8427-8440.
136. Pinnau, I.; He, Z.; Merkel, T., Gas and vapor transport properties of amorphous perfluorinated glassy polymers. *PMSE Prepr.* **2003,** 89, 16.
137. Polyakov, A. M.; Starannikova, L. E.; Yampolskii, Y. P., Amorphous Teflons AF as organophilic pervaporation materials. Transport of individual components. *J. Membr. Sci.* **2003,** 216, (1-2), 241-256.
138. Polyakov, A. M.; Starannikova, L. E.; Yampolskii, Y. P., Amorphous Teflons AF as organophilic pervaporation materials. Separation of mixtures of chloromethanes. *J. Membr. Sci.* **2004,** 238, (1-2), 21-32.
139. Polyakov, A.; Bondarenko, G.; Tokarev, A.; Yampolskii, Y., Intermolecular interactions in target organophilic pervaporation through the films of amorphous Teflon AF2400. *J. Membr. Sci.* **2006,** 277, (1-2), 108-119.
140. Kebabian, P. L.; Freedman, A., Fluoropolymer-based capacitive carbon dioxide sensor. *Meas. Sci. Technol.* **2006,** 17, (4), 703-710.
141. Brady, F.; Luthra, S. K.; Zhao, Y. Solid-phase preparation of [18F]fluorohaloalkanes by fluorination of solid support linked haloalkyl sulfonate with [18F]-fluoride ion. 2003-GB5630 2004056726, 20031219., **2004**.
142. Zhang, H.; Hussam, A.; Weber, S. G., Properties and Transport Behavior of Perfluorotripentylamine (FC-70)-Doped Amorphous Teflon AF 2400 Films. *J. Am. Chem. Soc.* **2010**, 17867–17879.
143. Hofmann, D.; Entrialgo-Castano, M.; Lerbret, A.; Heuchel, M.; Yampolskii, Y., Molecular Modeling Investigation of Free Volume Distributions in Stiff Chain Polymers

with Conventional and Ultrahigh Free Volume Comparison between Molecular Modeling and Positron Lifetime Studies. *Macromolecules* **2003,** 36, (22), 8528-8538.
144. Nakamura, H.; Linclau, B.; Curran, D. P., Fluorous Triphasic Reactions:Transportative Deprotection of Fluorous Silyl Ethers with Concomitant Purification. *J. Am. Chem. Soc.* **2001,** 123, (41), 10119-10120.
145. Khalil, M. A. K.; Rasmussen, R. A.; Culbertson, J. A.; Prins, J. M.; Grimsrud, E. P.; Shearer, M. J., Atmospheric Perfluorocarbons. *Environ. Sci. Technol.* **2003,** 37, (19), 4358-4361.
146. Horvath, I. T.; Rabai, J., Facile catalyst separation without water: fluorous biphase hydroformylation of olefins. *Science (Washington, DC, United States)* **1994,** 266, (5182), 72-75.
147. Gladysz, J. A.; Curran, D. P., Fluorous chemistry: from biphasic catalysis to a parallel chemical universe and beyond. *Tetrahedron* **2002,** 58, (20), 3823-3825.
148. Palomo, C.; Aizpurua, J. M.; Loinaz, I.; Fernandez-Berridi, M. J.; Irusta, L., Scavenging of Fluorinated N,N'-Dialkylureas by Hydrogen Binding: A Novel Separation Method for Fluorous Synthesis. *Org. Lett.* **2001,** 3, (15), 2361-2364.
149. Curran, D. P.; Hadida, S.; Kim, S.-Y.; Luo, Z., Fluorous Tin Hydrides: A New Family of Reagents for Use and Reuse in Radical Reactions. *J. Am. Chem. Soc.* **1999,** 121, (28), 6607-6615.
150. de Wolf, E.; van Koten, G.; Deelman, B.-J., Fluorous phase separation techniques in catalysis. *Chem. Soc. Rev.* **1999,** 28, (1), 37-41.
151. Curran, D. P.; Luo, Z., Fluorous Synthesis with Fewer Fluorines (Light Fluorous Synthesis): Separation of Tagged from Untagged Products by Solid-Phase Extraction with Fluorous Reverse-Phase Silica Gel. *J. Am. Chem. Soc.* **1999,** 121, (39), 9069-9072.
152. Lindsley, C. W.; Zhao, Z.; Newton, R. C.; Leister, W. H.; Strauss, K. A., A general Staudinger protocol for solution-phase parallel synthesis. *Tetrahedron Lett.* **2002,** 43, (25), 4467-4470.
153. Vallin, K. S. A.; Zhang, Q.; Larhed, M.; Curran, D. P.; Hallberg, A., A New Regioselective Heck Vinylation with Enamides. Synthesis and Investigation of Fluorous-Tagged Bidentate Ligands for Fast Separation. *J. Org. Chem.* **2003,** 68, (17), 6639-6645.
154. Curran, D.; Fischer, K.; Moura-Letts, G., A Soluble Fluorous Palladium Complex that Promotes Heck Reactions and Can Be Recovered and Reused. *Synlett* **2004**, (8), 1379-1382.
155. Luo, Z.; Williams, J.; Read, R. W.; Curran, D. P., Fluorous Boc (FBoc) Carbamates: New Amine Protecting Groups for Use in Fluorous Synthesis. *J. Org. Chem.* **2001,** 66, (12), 4261-4266.
156. Curran, D. P.; Amatore, M.; Guthrie, D.; Campbell, M.; Go, E.; Luo, Z., Synthesis and Reactions of Fluorous Carbobenzyloxy (FCbz) Derivatives of α-Amino Acids. *J. Org. Chem.* **2003,** 68, (12), 4643-4647.
157. Curran, D. P.; Ferritto, R.; Hua, Y., Preparation of a fluorous benzyl protecting group and its use in fluorous synthesis approach to a disaccharide. *Tetrahedron Lett.* **1998,** 39, (28), 4937-4940.
158. Luo, Z.; Swaleh, S. M.; Theil, F.; Curran, D. P., Resolution of 1-(2-Naphthyl)ethanol by a Combination of an Enzyme-Catalyzed Kinetic Resolution with a Fluorous Triphasic Separative Reaction. *Org. Lett.* **2002,** 4, (15), 2585-2587.

159. Nakamura, H.; Linclau, B.; Curran, D. P., Fluorous triphasic reactions: transportative deprotection of fluorous silyl ethers with concomitant purification. *J. Am. Chem. Soc.* **2001,** 123, (41), 10119-10120.
160. Zhao, H.; Zhang, J.; Wu, N.; Zhang, X.; Crowley, K.; Weber, S. G., Transport of Organic Solutes through Amorphous Teflon AF Films. *J. Am. Chem. Soc.* **2005,** 127, (43), 15112-15119.
161. Dasgupta, P. K.; Genfa, Z.; Poruthoor, S. K.; Caldwell, S.; Dong, S.; Liu, S.-Y., High-Sensitivity Gas Sensors Based on Gas-Permeable Liquid Core Waveguides and Long-Path Absorbance Detection. *Anal. Chem.* **1998,** 70, (22), 4661-4669.
162. Larsson, H.; Dasgupta, P. K., Liquid core waveguide-based optical spectrometry for field estimation of dissolved BTEX compounds in groundwater: A feasibility study. *Anal. Chim. Acta* **2003,** 485, (2), 155-167.
163. Boswell, P. G.; Buhlmann, P., Fluorous Bulk Membranes for Potentiometric Sensors with Wide Selectivity Ranges: Observation of Exceptionally Strong Ion Pair Formation. *J. Am. Chem. Soc.* **2005,** 127, (25), 8958-8959.
164. Boswell, P. G.; Szijjarto, C.; Jurisch, M.; Gladysz, J. A.; Rabai, J.; Buhlmann, P., Fluorophilic Ionophores for Potentiometric pH Determinations with Fluorous Membranes of Exceptional Selectivity. *Anal. Chem.* **2008,** 80, (6), 2084-2090.
165. Boswell, P. G.; Lugert, E. C.; Rabai, J.; Amin, E. A.; Buhlmann, P., Coordinative Properties of Highly Fluorinated Solvents with Amino and Ether Groups. *J. Am. Chem. Soc.* **2005,** 127, (48), 16976-16984.
166. Furneaux, R. C.; Rigby, W. R.; Davidson, A. P., The formation of controlled-porosity membranes from anodically oxidized aluminum. *Nature (London, U. K.)* **1989,** 337, (6203), 147-149.
167. Mitrovic, M.; Knezic, L., Electrolytic aluminium oxide membranes -- a new kind of membrane with reverse osmotic characteristics. *Desalination* **1979,** 28, (2), 147-156.
168. Matyjaszewski, K.; Miller, P. J.; Shukla, N.; Immaraporn, B.; Gelman, A.; Luokala, B. B.; Siclovan, T. M.; Kickelbick, G.; Vallant, T.; Hoffmann, H.; Pakula, T., Polymers at Interfaces: Using Atom Transfer Radical Polymerization in the Controlled Growth of Homopolymers and Block Copolymers from Silicon Surfaces in the Absence of Untethered Sacrificial Initiatorr. *Macromolecules* **1999,** 32, (26), 8716-8724.
169. Lee, S. B.; Mitchell, D. T.; Trofin, L.; Nevanen, T. K.; Söderlund, H.; Martin, C. R., Antibody-Based Bio-Nanotube Membranes for Enantiomeric Drug Separations. *Science* **2002,** 296, (5576), 2198-2200.
170. Vlassiouk, I.; Krasnoslobodtsev, A.; Smirnov, S.; Germann, M., "Direct" Detection and Separation of DNA Using Nanoporous Alumina Filters. *Langmuir* **2004,** 20, (23), 9913-9915.
171. Gabino, F.; Belleville, M. P.; Preziosi-Belloy, L.; Dornier, M.; Sanchez, J., Evaluation of the cleaning of a new hydrophobic membrane for osmotic evaporation. *Sep. Purif. Technol.* **2007,** 55, (2), 191-197.
172. Karaman, M. E.; Antelmi, D. A.; Pashley, R. M., The production of stable hydrophobic surfaces by the adsorption of hydrocarbon and fluorocarbon carboxylic acids onto alumina substrates. *Colloids Surf., A* **2001,** 182, (1-3), 285-298.
173. Hare, E. F.; Shafrin, E. G.; Zisman, W. A., Properties of Films of Adsorbed Fluorinated Acids. *J. Phys. Chem.* **1954,** 58, (3), 236-239.

174. Ha, K.; Ahn, H.-J.; Son, C., Studies on the E7 liquid crystal orientations confined to perfluorinated carboxylic acid - treated cylindrical cavities of Anodisc membranes by FTIR sepectroscopy. *Liq. Cryst.* **2006,** 33, (8), 935-940.
175. Lee, S. B.; Mitchell, D. T.; Trofin, L.; Nevanen, T. K.; Söderlund, H.; Martin, C. R., Antibody-Based Bio-Nanotube Membranes for Enantiomeric Drug Separations. *Science* **2002,** 296, (5576), 2198-2200.
176. Zhang, X.; Zhao, H.; Chen, Z.; Nims, R.; Weber, S. G., Effect of Polymer Concentration on Partitioning and Molecular Recognition in Plasticized Poly(vinyl chloride). *Anal. Chem.* **2003,** 75, (16), 4257-4264.
177. Crawford, G. P.; Steele, L. M.; Ondris-Crawford, R.; Iannacchione, G. S.; Yeager, C. J.; Doane, J. W.; Finotello, D., Characterization of the cylindrical cavities of Anopore and Nuclepore membranes. *J. Chem. Phys.* **1992,** 96, (10), 7788-7796.
178. Hernandez, A.; Calvo, J. I.; Pradanos, P.; Palacio, L.; Rodriguez, M. L.; de Saja, J. A., Surface structure of microporous membranes by computerized SEM image analysis applied to Anopore filters. *J. Membr. Sci.* **1997,** 137, (1-2), 89-97.
179. Doan, V.; Koppe, R.; Kasai, P. H., Dimerization of Carboxylic Acids and Salts: An IR Study in Perfluoropolyether Media. *J. Am. Chem. Soc.* **1997,** 119, (41), 9810-9815.
180. Roach, P.; Shirtcliffe, N. J.; Newton, M. I., Progess in superhydrophobic surface development. *Soft Matter* **2008,** 4, (2), 224-240.
181. Cassie, A. B. D.; Baxter, S., Wettability of porous surfaces. *Trans. Faraday Soc.* **1944,** 40, 546-551.
182. Inazaki, S.; Oie, T.; Takaoka, H., Surface modification of poly(tetrafluoroethylene) with ArF excimer laser irradiation. *J. Photopolym. Sci. Technol.* **1994,** 7, (2), 389-395.
183. Lin, T.-K.; Wu, S.-J.; Peng, C.-K.; Yeh, C.-H., Surface modification of polytetrafluoroethylene films by plasma pretreatment and graft copolymerization to improve their adhesion to bismaleimide. *Polym. Int.* **2009,** 58, (1), 46-53.
184. Box, G. E. P.; Hunter, J. S.; Hunter, W. G., *Statistics for experimenters : an introduction to design, data analysis, and model building*. John Wiley & Sons: New York, **1978**.
185. Venkateswaran, P.; Palanivelu, K., Studies on recovery of hexavalent chromium from plating wastewater by supported liquid membrane using tri-n-butyl phosphate as carrier. *Hydrometallurgy* **2005,** 78, (1-2), 107-115.
186. Zhang, B.; Gozzelino, G.; Baldi, G., Membrane liquid loss of supported liquid membrane based on n-decanol. *Colloids Surf., A* **2001,** 193, (1-3), 61-70.
187. Pandey, A. K.; Gautam, M. M.; Shukla, J. P.; Iyer, R. H., Effect of pore characteristics on carrier-facilitated transport of Am(III) across track-etched membranes. *J. Membr. Sci.* **2001,** 190, (1), 9-20.
188. Yang, Q.; Chung, T.-S.; Xiao, Y.; Wang, K., The development of chemically modified P84 Co-polyimide membranes as supported liquid membrane matrix for Cu(II) removal with prolonged stability. *Chem. Eng. Sci.* **2007,** 62, (6), 1721-1729.
189. Palacio, L.; Pradanos, P.; Calvo, J. I.; Hernandez, A., Porosity measurements by a gas penetration method and other techniques applied to membrane characterization. *Thin Solid Films* **1999,** 348, (1-2), 22-29.
190. Platt, M.; Dryfe, R. A. W.; Roberts, E. P. L., Voltammetry with Liquid/Liquid Microarrays: Characterization of Membrane Materials. *Langmuir* **2003,** 19, (19), 8019-8025.

191. Fontas, C.; Salvado, V.; Hidalgo, M., Selective enrichment of palladium from spent automotive catalysts by using a liquid membrane system. *J. Membr. Sci.* **2003,** 223, (1-2), 39-48.
192. Molinari, R.; Argurio, P.; Pirillo, F., Comparison between stagnant sandwich and supported liquid membranes in copper(II) removal from aqueous solutions: flux, stability and model elaboration. *J. Membr. Sci.* **2005,** 256, (1-2), 158-168.
193. Reyes-Aguilera, J. A.; Gonzalez, M. P.; Navarro, R.; Saucedo, T. I.; Avila-Rodriguez, M., Supported liquid membranes (SLM) for recovery of bismuth from aqueous solutions. *J. Membr. Sci.* **2008,** 310, (1-2), 13-19.
194. Hildebrand, J. H.; Scott, R. L., *The solubility of nonelectrolytes*. Reinhold Pub. Corp.: New York, 1950.
195. P. Barthel-Rosa, L.; A. Gladysz, J., Chemistry in fluorous media: a user's guide to practical considerations in the application of fluorous catalysts and reagents. *Coord. Chem. Rev.* **1999,** 190-192, 587-605.
196. Cavazzini, M.; Montanari, F.; Pozzi, G.; Quici, S., Perfluorocarbon-soluble catalysts and reagents and the application of FBS (fluorous biphase system) to organic synthesis. *J. Fluorine Chem.* **1999,** 94, (2), 183-193.
197. Hobbs, H. R.; Thomas, N. R., Biocatalysis in Supercritical Fluids, in Fluorous Solvents, and under Solvent-Free Conditions. *Chem. Rev. (Washington, DC, U. S.)* **2007,** 107, (6), 2786-2820.
198. Iskra, J.; Stavber, S.; Zupan, M., Use of a fluorous bridge for diffusion controlled uptake of molecular chlorine in chlorine addition to alkenes. *Chem. Commun. (Cambridge, U. K.)* **2003**, (19), 2496-2497.
199. Ryu, I.; Matsubara, H.; Yasuda, S.; Nakamura, H.; Curran, D. P., Phase-Vanishing Reactions that Use Fluorous Media as a Phase Screen. Facile, Controlled Bromination of Alkenes by Dibromine and Dealkylation of Aromatic Ethers by Boron Tribromide. *J. Am. Chem. Soc.* **2002,** 124, (44), 12946-12947.
200. Vlassiouk, I.; Krasnoslobodtsev, A.; Smirnov, S.; Germann, M., "Direct" Detection and Separation of DNA Using Nanoporous Alumina Filters. *Langmuir* **2004,** 20, (23), 9913-9915.
201. Dalvie, S. K.; Baltus, R. E., Transport studies with porous alumina membranes. *Journal of Membrane Science* **1992,** 71, (3), 247-255.
202. Daniels, S. M.; Saunders, R. A.; Platts, J. A., Prediction of fluorophilicity of organic and transition metal compounds using molecular surface areas. *J. Fluorine Chem.* **2004,** 125, (9), 1291-1298.
203. Duchowicz, P. R.; Fernandez, F. M.; Castro, E. A., Alternative statistical and theoretical analysis of fluorophilicity. *J. Fluorine Chem.* **2004,** 125, (1), 43-48.
204. Huque, F. T. T.; Jones, K.; Saunders, R. A.; Platts, J. A., Statistical and theoretical studies of fluorophilicity. *J. Fluorine Chem.* **2002,** 115, (2), 119-128.
205. Kiss, L. E.; Kovesdi, I.; Rabai, J., An improved design of fluorophilic molecules: prediction of the ln P fluorous partition coefficient, fluorophilicity, using 3D QSAR descriptors and neural networks. *J. Fluorine Chem.* **2001,** 108, (1), 95-109.
206. Szabó, D.; Bonto, A.-M.; Kövesdi, I.; Gomory, A.; Rabai, J., Synthesis of novel lipophilic and/or fluorophilic ethers of perfluoro-tert-butyl alcohol, perfluoropinacol and hexafluoroacetone hydrate via a Mitsunobu reaction: Typical cases of ideal product separation. *J. Fluorine Chem.* **2005,** 126, (4), 639-650.

207. deWolf, E.; Ruelle, P.; vandenBroeke, J.; Deelman, B. J.; vanKoten, G., Prediction of Partition Coefficients of Fluorous and Nonfluorous Solutes in Fluorous Biphasic Solvent Systems by Mobile Order and Disorder Theory. *J. Phys. Chem. B* **2004,** 108, (4), 1458-1466.
208. Barton, A. F. M., *CRC Handbook of Solubility Parameters and Other Cohesion Parameters*. 1983; p 624 pp.
209. Mercader, A. G.; Duchowicz, P. R.; Sanservino, M. A.; Fernández, F. M.; Castro, E. A., QSPR analysis of fluorophilicity for organic compounds. *J. Fluorine Chem.* **2007,** 128, (5), 484-492.
210. Mohapatra, P. K.; Lakshmi, D. S.; Manchanda, V. K., Diluent effect on Sr(II) extraction using di-tert-butyl cyclohexano 18 crown 6 as the extractant and its correlation with transport data obtained from supported liquid membrane studies. *Desalination* **2006,** 198, (1-3), 166-172.
211. Ambe, S.; Katayama, O.; Ambe, F., Multitracer studies on the permeation of various elements through a supported liquid membrane containing TBP. *J. Radioanal. Nucl. Chem.* **2002,** 253, (3), 351-355.
212. Tbeur, N.; Rhlalou, T.; Hlaïbi, M.; Langevin, D.; Métayer, M.; Verchère, J.-F., Molecular recognition of carbohydrates by a resorcinarene. Selective transport of alditols through a supported liquid membrane. *Carbohydr. Res.* **2000,** 329, (2), 409-422.
213. Rhlalou, T.; Ferhat, M.; Frouji, M. A.; Langevin, D.; Métayer, M.; Verchère, J. F., Facilitated transport of sugars by a resorcinarene through a supported liquid membrane. *J. Membr. Sci.* **2000,** 168, (1-2), 63-73.
214. Hassoune, H.; Rhlalou, T.; Verchère, J.-F., Studies on sugars extraction across a supported liquid membrane: Complexation site of glucose and galactose with methyl cholate. *J. Membr. Sci.* **2008,** 315, (1-2), 180-186.
215. Odom, D. J.; Baker, L. A.; Martin, C. R., Solvent-Extraction and Langmuir-Adsorption-Based Transport in Chemically Functionalized Nanopore Membranes. *J. Phys. Chem. B* **2005,** 109, (44), 20887-20894.
216. Lessmann, T.; Waldmann, H., Asymmetric synthesis on the solid phase. *Asymmetric Synth. (2nd Ed.)* **2008**, 299-304.
217. Akagawa, K.; Kudo, K., Asymmetric synthesis in aqueous using highly functionalized resin-supported peptide catalyst. *Seisan Kenkyu* **2010,** 62, (3), 219-224.
218. Arisawa, M.; Hoshiya, N.; Shuto, S., Palladium materials supported on GaAs(001) or gold for drug development. *Yuki Gosei Kagaku Kyokaishi* **2010,** 68, (9), 920-929.
219. Gong, Y.-D.; Lee, T., Combinatorial Syntheses of Five-Membered Ring Heterocycles Using Carbon Disulfide and a Solid Support. *J. Comb. Chem.* **2010,** 12, (4), 393-409.
220. Jiao, J.; Huang, L.; Teng, D., Research progress of palladium catalysts supported by inorganic materials. *Huaxue Yu Shengwu Gongcheng* **2010,** 27, (3), 4-8.
221. Jing, G.; Li, J.; Yang, D.; Hao, J., Progress in the selective catalytic reduction of NOx with methane over solid super acid and metal oxides-based catalysts. *Huanjing Gongcheng Xuebao* **2010,** 4, (7), 1441-1447.
222. Kann, N., Recent applications of polymer supported organometallic catalysts in organic synthesis. *Molecules* **2010,** 15, 6306-6331.
223. Kulkarni, A.; Lobo-Lapidus, R. J.; Gates, B. C., Metal clusters on supports: synthesis, structure, reactivity, and catalytic properties. *Chem. Commun. (Cambridge, U. K.)* **2010,** 46, (33), 5997-6015.

224. Le Quement, S. T.; Petersen, R.; Meldal, M.; Nielsen, T. E., N-acyliminium intermediates in solid-phase synthesis. *Biopolymers* **2010,** 94, (2), 242-256.
225. Mandal, B.; Ghosh, P.; Basu, B., Recent approaches toward solid phase synthesis of beta -lactams. *Top. Heterocycl. Chem.* **2010,** 22, (Heterocyclic Scaffolds I), 261-311.
226. Van Doorslaer, C.; Wahlen, J.; Mertens, P.; Binnemans, K.; De Vos, D., Immobilization of molecular catalysts in supported ionic liquid phases. *Dalton Trans.* **2010,** 39, (36), 8377-8390.
227. Zhang, G.-l.; Wang, S.-p.; Huang, X.-h., Research progress in synthesis of nitrate esters over solid acid catalysts. *Huaxue Shiji* **2010,** 32, (9), 811-816.
228. Zhang, S.; Chen, J.; Lykakis, I. N.; Perchyonok, V. T., Streamlining organic free radical synthesis through modern molecular technology: from polymer supported synthesis to microreactors and beyond. *Curr. Org. Synth.* **2010,** 7, (2), 177-188.
229. Horn, J.; Michalek, F.; Tzschucke, C. C.; Bannwarth, W., Non-covalently solid-phase bound catalysts for organic synthesis. *Top. Curr. Chem.* **2004,** 242, (Immobilized Catalysts), 43-75.
230. Biffis, A.; Zecca, M.; Basato, M., A green protocol for the silylation of alcohols using bonded fluorous phase catalysis. *Green Chem.* **2003,** 5, (2), 170-173.
231. Tzschucke, C. C.; Bannwarth, W., Fluorous-silica-supported perfluoro-tagged palladium complexes catalyze Suzuki couplings in water. *Helv. Chim. Acta* **2004,** 87, (11), 2882-2889.
232. Hope, E. G.; Sherrington, J.; Stuart, A. M., Supported fluorous phase catalysis on PTFE, fluoroalkylated micro- and meso-porous silica. *Adv. Synth. Catal.* **2006,** 348, (12+13), 1635-1639.
233. Joji, N., Development and application of fluorous lewis acid catalytic reaction processes. *Fain Kemikaru* **2006,** 35, (1), 29-40.
234. Schmaderer, H.; Hilgers, P.; Lechner, R.; Koenig, B., Photooxidation of benzyl alcohols with immobilized flavins. *Adv. Synth. Catal.* **2009,** 351, (1+2), 163-174.
235. Audic, N.; Dyer, P. W.; Hope, E. G.; Stuart, A. M.; Suhard, S., Insoluble Perfluoroalkylated Polymers: new Solid Supports for Supported Fluorous Phase Catalysis. *Adv. Synth. Catal.* **2010,** 352, (13), 2241-2250.
236. Schwinn, D.; Glatz, H.; Bannwarth, W., Multistep Parallel Synthesis of Quinazoline-2,4-diones by a Fluorous Biphasic Concept without Perfluorinated Solvents. *Helv. Chim. Acta* **2003,** 86, (1), 188-195.
237. Grabarek, Z.; Gergely, J., Zero-length crosslinking procedure with the use of active esters. *Anal. Biochem.* **1990,** 185, (1), 131-135.
238. Staros, J. V.; Wright, R. W.; Swingle, D. M., Enhancement by N-hydroxysulfosuccinimide of water-soluble carbodiimide-mediated coupling reactions. *Anal. Biochem.* **1986,** 156, (1), 220-222.
239. Doan, V.; Köppe, R.; Kasai, P. H., Dimerization of Carboxylic Acids and Salts: An IR Study in Perfluoropolyether Media. *J. Am. Chem. Soc.* **1997,** 119, (41), 9810-9815.